Stony Brook University

Characterizing the role of Wnt/β-catenin antagonist, Chibby (Cby) in lung morphogenesis and function

A Dissertation Presented

by

Damon Love

to

The Graduate School

in Partial fulfillment of the

Requirements

for the Degree of

Doctor of Philosophy

in

Molecular and Cellular Pharmacology

Stony Brook University

December 2009

Stony Brook University

The Graduate School

Damon Love

We, the dissertation committee for the above candidate for the Doctor of Philosophy degree, hereby recommend acceptance of this dissertation.

Ken-Ichi Takemaru, Ph.D.
Dissertation Director
Assistant Professor, Department of Pharmacological Sciences

Holly Colognato, Ph.D.
Chairperson of Defense
Assistant Professor, Department of Pharmacological Sciences

J. Craig Cohen, Ph.D.
Director of Neonatal Research
Department of Pediatrics

Gerald H. Thomsen, Ph.D.
Associate Professor, Director
Graduate Program in Genetics
Dept. of Biochemistry and Cell Biology

Lawrence Martin
Dean of the Graduate School

Abstract of the Dissertation

Characterizing the role of Wnt/β-catenin antagonist, Chibby (Cby) in lung morphogenesis and function

by

Damon Love

Doctor of Philosophy

in

Molecular and Cellular Pharmacology

Stony Brook University

2009

The canonical Wnt/β-catenin pathway plays crucial roles in various aspects of lung morphogenesis and regeneration/repair. β-Catenin signaling is active throughout lung development and genetic manipulation of this signaling cascade in mice leads to severe defects in proliferation and differentiation of respiratory epithelial cells. This study examines the role of the Wnt/β-catenin antagonist Chibby (Cby) in lung development and homeostasis by characterizing the lung phenotype of *Cby*$^{-/-}$ mice.

Cby is expressed in embryonic and adult lungs and, similar to a phenotype observed in mice with conditional activation of β-catenin in the lung epithelium, *Cby*$^{-/-}$ mice

develop reduced alveolar complexity as early as 7 days after birth, which persists into adulthood. Cby expression in the alveolar epithelium is visualized during late embryogenesis and in neonates in a punctate manner, colocalizing with markers for centriolar proteins.

In the alveolar epithelium, expression of type II progenitor cell markers is increased, whereas that of terminally differentiated type I cell markers decreased. Strikingly, *Cby*$^{-/-}$ mice show a reduced number of ciliated cells with a marked paucity of cilia, and altered morphology of non-ciliated Clara cells in conducting airways. In good agreement with these phenotypes, Cby protein is detected at the basal bodies of cilia in multiciliated airway epithelial cells in addition to other monociliated cells, suggesting a role in ciliary development. Consistent with the finding that Cby is a negative regulator of Wnt/β-catenin signaling, expression of β-catenin target genes is elevated in the lung. As a consequence of these changes, *Cby*$^{-/-}$ mice exhibit altered pulmonary function.

Taken together, our data suggest that Cby facilitates proper maturation and function of the postnatal lung.

TABLE OF CONTENTS

List of abbreviations ix

Acknowledgements xi

Chapter 1: General Introduction 1

Lung Morphogenesis 1

Pulmonary Epithelial Cell Lineages 4

Clara Cells and Ciliated Cells of the Conducting Airways 5

Type I and Type II Alveolar Pneumocytes 6

The Wnt/β-Catenin Pathway 8

Wnt Signaling and Lung Morphogenesis 9

Chibby as a β-Catenin Antagonist 11

Chapter 2: Altered Lung Physiology In *Cby*$^{-/-}$ Mice 19

Materials and Methods 19

Results 27

Discussion 32

Chapter 3: The Role Of Cby in the Differentiation of Alveolar Pneumocytes 43

Introduction 43

Materials and Methods 44

Results 48

Discussion 51

Chapter 4: A Developmental Role for Cby in Multiciliated Epithelial Cells 57

Introduction 57

Materials and Methods 57

Results 62

Discussion 66

Chapter 5: Conclusions and Future Directions 77

Summary of thesis findings 77

Future directions 82

References 86

LIST OF FIGURES

Chapter 1

Table 1-1 Expression of cell lineage-specific markers in epithelial cell lineages in the developing mouse lung 14

Figure 1-1 Key events in lung morphogenesis 15

Figure 1-2. Respiratory Epithelial Cells 16

Figure 1-3 Canonical Wnt Pathway 17

Figure 1-4 Cby expression in multiple mouse tissues throughout development 18

Chapter 2

Figure 2-1 Cby is expressed throughout murine lung development 36

Figure 2-2 Wnt/β-catenin pathway activity is elevated in Cby null lungs 37

Figure 2-3 Gross alveolarization defects in *Cby*$^{-/-}$ lungs 38

Figure 2-4 Cby null mouse lungs exhibit morphological defects in airway epithelium 39

Figure 2-5 Morphometric analysis of structural defects in the adult mouse lung 40

Figure 2-6 Abnormal pulmonary mechanics in adult *Cby*$^{-/-}$ and *Cby*$^{+/-}$ animals 41

Figure 2-7 Reduced *cby* expression in the lungs of *cby*$^{+/-}$ mice 42

Chapter 3

Figure 3-1 Cby null mice exhibit ultrastructural defects in the alveolar epithelium 55

Figure 3-2 Cby null mouse lungs exhibit differentiation defects in alveolar pneumocytes 56

Figure 3-3 Cby expression colocalizes with centrosomal markers in alveolar progenitor cells 57

Chapter 4

Figure 4-1 Cby null mice exhibit ultrastructural defects in the airway epithelium 73

Figure 4-2 Cby null mice exhibit ultrastructural defects in the airway epithelium 74

Figure 4-3 Cby null mouse lungs exhibit differentiation defects in the airway epithelium ……..…..... 75

Figure 4-4 Cellular localization of the Cby protein in airway epithelium 76

Figure 4-5 Foxj1 is expressed in multiciliated epithelial cells in adult *cby*$^{+/+}$ and *cby*$^{-/-}$ 77

Figure 4-6 Cby localizes along the motile cilia of airway epithelia in cultured epithelial cells 78

LIST OF ABBREVIATIONS

APC:	Adenomatous polyposis coli
GSK3β:	Glycogen synthase kinase β
CK1:	Casein kinase 1
ATI:	Type I alveolar pneumocytes
ATII:	Type II alveolar pneumocytes
Dvl:	Dishevelled
CC10:	Clara cell protein (also termed CC10 or CCSP)
SpC:	Secretory protein C
Aqp5:	Aquaporin 5
PTHrP:	Parathyroid hormone receptor protein
CFTR:	Cystic fibrosis transmembrane conductance regulator
MTEC:	Mouse tracheal epithelial cell
BASC:	Bronchioalveolar stem cell
BADJ:	Bronchioalveolar duct junction
LRP:	LDL-receptor-related proteins
Cby:	Chibby
LEF:	Lymphoid enhancing factor
TCF:	T-cell factor
BAT-gal:	Beta galactosidase reporter
PNEC:	Pulmonary neuroendocrine cell
PCR:	Polymerase chain reaction
RT-PCR:	Reverse transcription PCR

qPCR:	Quantitative real-time PCR
H&E:	Hematoxylin and eosin
IHC:	Immunohistochemistry
PBS:	Phosphate buffered saline
BSA:	Bovine serum albumin
MTOC:	Microtubule organizing center
TEM:	Transmission electron microscopy
SEM:	Scanning electron microscopy

ACKNOWLEDGEMENTS

I'd like to first acknowledge God, the source of my strength and through Whom all things are made possible.

I'd like to thank my advisor and mentor, Ken-Ichi Takemaru for his guidance, patience and willingness to invest, what was at the time, limited laboratory space and uncertain funding, in my scientific growth and development. Ken, I greatly appreciate your faith in my abilities and trust in my judgment in allowing the freedom of exploration into a topic that was novel to your work. It has truly been a journey of scientific discovery.

I would also like to thank Craig Cohen for his insight, adventurous spirit and for constantly challenging my scientific development and encouraging me to approach scientific problems with openmindedness and a willingness to challenge convention. It was you who taught me the valuable lesson of trusting your data and building your theoretical model around your observations, not the other way around, even when it contradicts conventional wisdom.

I thank my beloved wife, Crystal, for allowing me the freedom to pursue what was sure to be a long and unsure path, but for loving me enough to make the necessary sacrifices to make it possible. Crystal, your support, encouragement and faith in me were often the very things that got me through some of my most difficult obstacles. Both you and our daughter, Bianca, were the motivation behind the long hours, late nights, long commute and resilience in the face of failed experiments. I love you both.

A special thanks to my parents, Andrew and Rebecca Love, two of the best friends a son can have. From an early age, you always nurtured my inquisitive nature and encouraged me to never be afraid to follow my own path and believe in myself. Dad, you are simply the greatest man I have ever known. You taught me to be a man, through your word and deed and your quiet strength. Mom, the first lady to make me smile, you have been an ever-present source of comfort, encouragement and self-belief. I am proud to call myself your son.

My brother, Jason, you have grown over the years from little brother to best friend. You're encouragement and confidence in me has been a motivating force behind my early and late success. As much as I was your role model, I drew much strength over the years from you, too. You make me proud.

To my pastors, friends and family, I am thankful for all of your support, prayers, and confidence in me. Most of you have known me throughout most of the significant stages in my personal, educational and spiritual development and your have been a most treasured component of that growth.

A special thanks to the rest of my thesis committee, Holly Colognato and Gerry Thomsen, the graduate program director, Stella Tsirka, the departmental faculty and the administrative staff of the Pharmacology Department, particularly, Beverly Campbell, all of whom have played an integral role in making my experience and evolution as a scientist be as comfortable and smooth a transition as possible.

Finally, special thanks to the W. Burghardt Turner Fellowship for funding part of my graduate research, and for the continued support of the staff and community of the Stony

Brook Alliance for Graduate Education and the Professoriate, notably Nina Maung, Kathryne Piazzola and Toni Vicari.

CHAPTER 1: GENERAL INTRODUCTION

Lung Morphogenesis

Proper lung development is critical to postnatal survival in mammals and defects in the genetic program choreographing that developmental lifecycle can result in functional defects, disease pathology and death. As such, lung development is dependent upon tightly controlled interactions between the respiratory epithelium and the surrounding lung mesenchyme, which coordinate the temporal and spatial expression of multiple regulatory factors required for proper lung formation (Mucenski et al., 2003; van Tuyl et al., 2006). Development of the mouse lung closely parallels that of the human lung, providing a powerful model for lung development (Shu et al., 2002; Warburton et al., 2005).

Murine lung development can be divided into five chronological stages: (1) the *embryonic stage*, (2) the *pseudoglandular stage*, (3) the *canalicular stage*, (4) the *saccular stage* and (5) the *alveolar stage* (**FIG. 1-1**) (Chinoy, 2003; Mucenski et al., 2003; Warburton et al., 2000).

The embryonic stage begins at the 9th day of gestation (E9.5) as a midventral groove appears in the single foregut tube. This deepens and then constricts, thereby forming a separate ventral trachea and a dorsal esophagus. As the trachea elongates, primitive lung buds emerge as protrusions from the developing trachea. These early lung buds separate ventrally and rapidly proliferate, elongating into the surrounding mesenchyme to give rise to a unilobular left lung and a quadrilobular right lung. Epithelial-mesenchymal tissue

interactions fine tune the temporal-spatial expression pattern of signaling and transcriptional molecules and dictate the branching pattern of the epithelium along the anteroposterior axis (Brody and Williams, 1992; Groenman et al., 2005).

The **pseudoglandular stage**, beginning at E11.5, marks the development of the bronchial tree. Branching of the epithelial buds is a hallmark in this period as the conductive airway tree down to the terminal bronchioles is formed (Groenman et al., 2005). Lobular development occurs by branching morphogenesis, a complex process regulated by various transcription factors, growth factors, and hormones, which forms the intrapulmonary conducting airways and peripheral lung. The pulmonary mesenchyme gives rise to several different cell types, including smooth muscle of the upper airways and the pulmonary vasculature. Epithelial cells start to differentiate with the appearance of a distinct subset of cell types lining the bronchial airways including ciliated cells, goblet cells and basal cells (Chuang and McMahon, 2003; Mucenski et al., 2005; Mucenski et al., 2003; Shu et al., 2002; Warburton et al., 2000).

By the beginning of the **canalicular stage**, E16.5, the airway branching pattern is completed and the prospective gas exchange region starts to develop. The major distinguishing features between the pseudoglandular stage and canalicular stage are the development of the pulmonary vasculature and thinning of the mesenchyme. The distal regions of the bronchial airways, the respiratory bronchioli, appear and are lined with a single layer of tall columnar cells. These structures mark the future acini, small tubular structures, and are surrounded by the mesenchyme. As the tubular structures develop, thinning of mesenchyme around it occurs and the columnar epithelial cells become short columnar and eventually cuboidal epithelial cells. This thinning of the mesenchyme is

accompanied by increased vascularization in the form of a loose network of capillaries that develops around the acini, which is followed by the differentiation of the distal cuboidal epithelium into type I and type II pneumocytes (Chinoy, 2003; Groenman et al., 2005).

At approximately the 17th day of gestation (E17.5) the mouse enters the **saccular stage** of lung development and the peripheral lung undergoes a dramatic change in architecture. This stage is characterized by the growth of the pulmonary parenchyma corresponding with the thinning of the connective tissue between the airspaces and the maturation of the surfactant system. During the saccular stage, the acinar tubules dilate into terminal alveolar sacs as type I and type II pneumocytes differentiate. Meanwhile, the lung undergoes extensive maturation of vasculture, as blood vessels form the air-blood barrier alongside the epithelium and are arranged in pocket-like three-dimensional structures around the alveolar saccules (Cardoso, 2000; Warburton et al., 2000).

Lung development continues postnatally with the **alveolar stage** (P5). Alveolarization is a process that leads to a major increase in the surface area for gas exchange through septation of the terminal saccules. This is a highly active process during which alveolarization and differentiation of the conducting airways, culminates approximately 30 days after the birth of the mouse, at which time the lung is considered to be mature. Unlike the reiterative pattern of branching morphogenesis, the expansion phase of the alveolar surface is nonstereotypic. However, this process follows a recognizable, proximal-distal pattern, further illustrating the fact that lung formation is dependent upon precise spatial and temporal control of cell proliferation, migration and

differentiation. (Chuang and McMahon, 2003; Mucenski et al., 2005; Mucenski et al., 2003; Shu et al., 2002; Warburton et al., 2000).

Pulmonary Epithelial Cell Lineages

The lung has a unique distinction from all other inner organs of the body in that it is the only such organ that is exposed directly and constantly to the external environment through inhaled air during breathing. This resulting constant exposure to environmental toxins and infectious microorganisms requires a robust pulmonary defense mechanism consisting of a balanced mixture of specialized epithelial cell types with functions ranging from air humidification, filtration of air in the nasal and bronchial passages, and biochemical defenses involving surfactant proteins in gas-exchanging regions and surfactant lipid lining. These epithelial cell lineages are arranged in a distinct proximal-distal spatial pattern in the lung which, itself, is composed of two major anatomically distinct regions: the conducting airways and gas-exchanging airspaces (Cardoso, 2000; Cardoso and Lu, 2006; Chinoy, 2003; Chuang and McMahon, 2003; Dean et al., 2005; Demayo et al., 2002).

Although there is no direct evidence of a single, pluripotent progenitor cell type in the lung, molecular markers identifying gene expression characteristics of several of the pulmonary epithelial cell lineages have enabled identification of several cell types in the lung suggested to act as progenitor cells to a subset of distinct respiratory epithelial cell types (Beers et al., 1992; Evans et al., 1986; Hong et al., 2004a, b; Kim et al., 2005; Liu et al., 2006; Mucenski et al., 2005; Reynolds et al., 2000). Basal cells, Clara cells, and to

a lesser degree, pulmonary neuroendocrine (PNE) cells have been shown to function as progenitors or stem cells in the conducting airways of mice. Alveolar epithelial type II cells (ATII) are thought to function as the progenitor of the alveolar epithelium, based on their capacity to replicate and to give rise to terminally differentiated alveolar type I cells (ATI) (**FIG. 1-2**) (Hong et al., 2004a, b; Nusse, 2008; Reynolds et al., 2000; Reynolds et al., 2008). There is growing evidence, however, that suggests a specific stem cell niche in the bronchioalveolar duct junction that contains a subset of variant Clara cells, bronchioalveolar stem cells (BASC), which has been considered to be a regional population of progenitor cells that are thought to regenerate both bronchiolar and alveolar epithelium during homeostatic turnover and in response to injury (**TABLE 1**) (Kim et al., 2005; Zhang et al., 2008).

Clara Cells and Ciliated Cells of the Conducting Airways

Clara cells are among the most morphologically and functionally diverse cell types in the mammalian lung. They are commonly recognized as columnar, nonciliated epithelial cells lining the proximal and distal conducting airways, abundant with apically enriched secretory granules (**FIG. 1-2**) (Young et al., 2006; Zhou et al., 1996). Primarily, they serve in a protective capacity as they have the ability to detoxify xenobiotics by metablolizing lipophilic pollutants through cytochrome *P*-450 (CYP)-mediated metabolism. They also secrete proteins with important biological activities, notably the 15.8-kDa Clara cell protein (CC16 or CC10), the major protein secreted by Clara cells and one of the main secretory proteins of the lung, believed to serve as an antioxidant and

anti-inflammatory agent (Broeckaert et al., 2000; Zhou et al., 1996). Clara cells are also believed to serve as progenitor cells, giving rise to ciliated cells as well as basal cells, which in turn can self-renew and contribute to other lineages. Ciliated cells, however, are terminally differentiated and do not appear to divide.

Ciliated cells are found throughout the lung as well as other parts of the body and are responsible for efficient mucociliary transport, a major defense system of the lung that removes pathogenic microbes and inhaled particles from the respiratory tract. Impairment of mucociliary function is a component of such diseases as cystic fibrosis, asthma, and primary ciliary dyskinesia, which have their beginnings in childhood while the lung is developing (Cohen and Larson, 2008; Cohen et al., 1998; Groenman et al., 2005; Ostrowski et al., 2002; Rowe et al., 2005; Toskala et al., 2005; Voronina et al., 2009). The developmental appearance of ciliated cells occurs in a proximal-to-distal gradient that initiates on E14.5 and is essentially complete by approximately E16. After this time, bronchiolar ciliated cells are maintained through proliferation and differentiation of Clara cells (Dawe et al., 2007; Park et al., 2006a; Park et al., 2006b; Toskala et al., 2005; Van Winkle et al., 1995).

Type I and Type II Alveolar Pneumocytes

The alveolar epithelium serves, in large part, to provide a large, thin surface area for gas exchange after birth. Two primary cell types populate the alveolar epithelium in normal adult lungs: alveolar epithelial type I (ATI) and alveolar epithelial type II (ATII) cells. The ATII cells, cuboidal in shape, are limited to the corners of the alveoli and

situated between ATI cells (**FIG. 1-2**). They contain prominent cytoplasmic lamellar bodies and produce a variety of proteins involved in the inflammatory response, as well as proteins that have either immunomodulary or antioxidant roles. The most specialized function of type II cells, however, is the production and secretion of surfactant to maintain the proper airway surface tension for respiration (Shu et al., 2002; Wade et al., 2006). In addition, during lung development, ATII cells are progenitor cells for ATI cells that constitute the gas exchange surface in alveoli. ATII cells also maintain the capacity for self-renewal in response to lung injury to repopulate the pulmonary epithelium. ATII cell proliferation and hyperplasia, followed by transdifferentiation into ATI cells is a hallmark of alveolar epithelial injury. This helps to restore the normal air-blood barrier (Bhaskaran et al., 2007; McElroy and Kasper, 2004).

By virtue of their squamous shape, ATI cells cover the major surface area of alveoli and thus are the main epithelial component of the thin air-blood barrier (Bhaskaran et al., 2007). ATI cells are highly specialized for the key lung function of gas exchange and make up 95% of the total surface area of the peripheral lung and they function by transporting oxygen and carbon dioxide across the alveolar space to the capillary beds that surround the alveoli. ATI cells are also important in the regulation of alveolar fluid balance and surfactant secretion by ATII cells in response to mechanical stretch (Demayo et al., 2002; Edwards, 2001; McElroy and Kasper, 2004; Sanchez-Esteban et al., 2001; Williams, 2003).

The Wnt/β-Catenin Pathway

The morphogenesis of lungs is dependent upon intricate interactions between the endodermally derived respiratory epithelium and the surrounding mesenchyme, and involves a complex network of signal transduction events initiated by several families of secreted factors (Cardoso and Lu, 2006; Warburton et al., 2000). One such signaling pathway, the canonical Wnt/β-catenin pathway, has been shown to play a crucial role in normal lung development and homeostasis (Cardoso and Lu, 2006; Morrisey, 2003; Pongracz and Stockley, 2006).

The Wnt proteins are composed of a 19-member family of cysteine-rich secreted signaling glycoproteins that have been shown to play important roles in regulating cell differentiation, proliferation, and polarity. Wnt proteins signal through three known pathways, though the most well-characterized being the canonical Wnt pathway, which utilizes β-catenin as the key component in this signaling cascade (Barker and Clevers, 2006; Brembeck et al., 2006; Moon et al., 2004; Mucenski et al., 2005; Zhurinsky et al., 2000).

β-Catenin, a 781-amino acid protein, was initially characterized for its role in mediating cell adhesion by binding to the cytoplasmic domain of cell-cell adhesion receptors of the cadherin family, linking cadherins to the actin cytoskeleton through its association with α-catenin(Brembeck et al., 2006). In the canonical Wnt signaling pathway, β-catenin functions as a transcriptional coactivator, associating with the DNA-binding proteins lymphoid enhancer factor/T-cell factor (Lef/Tcf) (Brembeck et al., 2006; Mucenski et al., 2005; Nelson and Nusse, 2004; Zhurinsky et al., 2000).

In the absence of a Wnt ligand, cytoplasmic β-catenin is engaged by a multiprotein complex consisting of glycogen synthase kinase 3 (GSK3), casein kinase I (CKI), the adenomatous polyposis coli (APC) tumor suppressor protein, and axin (**FIG. 1-3**). Then β-catenin is sequentially phosphorylated at its N-terminal serine/threonine residues CKI and GSK3. Subsequently the phosphorylated form of β-catenin is recognized by the F-box/WD-repeat ubiquitin ligase β-TrCP, and is targeted for ubiquitination-mediated proteasomal degradation (Brembeck et al., 2006; Nelson and Nusse, 2004; Zhurinsky et al., 2000). Wnts bind to the Frizzled (Fz) family of 7-pass transmembrane receptors and the LDL-receptor-related proteins 5 and 6 (LRP 5/6), and activate the cytoplasmic disheveled (Dvl) protein, which in turn inhibits GSK3 activity. In parallel, LRP 5/6 recruits axin to the plasma membrane, where it is targeted for degradation. As a result, β-catenin becomes stabilized and its cytoplasmic levels subsequently rise, followed by its translocation into the nucleus where it interacts with DNA-bound Lef/Tcf proteins to activate the transcription of downstream target genes(Brembeck et al., 2006; Moon et al., 2004; Nelson and Nusse, 2004; Zhurinsky et al., 2000). Dysregulation of the Wnt/β-catenin pathway has been linked to a number of human pathologies, most notably cancer (Moon et al., 2004).

Wnt Signaling and Lung Morphogenesis

Multiple Wnt ligands and Frizzled receptors are differentially expressed in the developing and adult lung, and gain- and loss-of-function studies in mice confirm the importance of Wnt signaling in regulating diverse aspects of lung morphogenesis. Evidence of the importance of Wnt signaling in lung morphogenesis first came from the

study by Shu *et. al.* (2002), who demonstrated that mice lacking Wnt7b exhibited hypoplasia and extensive hemorrhaging in the lung, and died perinatally due to respiratory failure (Shu et al., 2002).

Transgenic mouse studies have provided further evidence of the role of β-catenin in influencing proper respiratory epithelial cell differentiation and lung morphogenesis. Conditional deletion of β-catenin specifically in progenitor cells of the lung epithelium results in an increase in bronchial airway formation in mouse embryos (Mucenski et al., 2003). This is accompanied by the complete absence of alveolarization, resulting in respiratory failure at birth.

On the other hand, sustained activation of β-catenin signaling specifically in the developing lung disrupts epithelial cell differentiation, causing enlargement of peripheral air spaces (Mucenski et al., 2005). In addition, β-catenin activation induced the expression of surfactant protein C (SpC), an alveolar type II cell marker, as well as metaplasia of cells lining the bronchial airways. These alveolarization defects were apparent in the early postnatal period of alveolarization and in adulthood. In a similar study, constitutive β-catenin activation was induced by fusing β-catenin to Lef1 and inserting this construct downstream of the lung-endoderm-specific SpC promoter (Okubo and Hogan, 2004). Though lungs appeared grossly normal, internally, they contained highly proliferative, abnormally developed epithelium lacking fully differentiated lung cell types. Furthermore, genes associated with differentiated cell types were downregulated, while genes associated with proliferation were upregulated.

More recently, the Wnt/β-catenin pathway has been shown to control lung stem cell expansion and regeneration/repair (De Langhe and Reynolds, 2008; Zhang et al., 2008). Given the essential role of Wnt signaling in the development and maintenance of the tissue, it is not surprising that this pathway has been associated with various lung diseases including lung cancer and pulmonary fibrosis.

Chibby as a β-Catenin Antagonist

Chibby (Cby) is a 14.5-kDa protein evolutionarily conserved from fly to human, first isolated through yeast-based screening using the C-terminal activation domain of β-catenin as bait (Takemaru et al., 2003). Lef/Tcf luciferase reporter (TOPFLASH) analyses in mammalian cultured cells and RNAi studies in *Drosophila melanogaster* embryos demonstrate that Cby competitively binds to β-catenin, preventing its interaction with Lef/Tcf, and thereby repressing subsequent activation of downstream targets (Takemaru et al., 2003). Furthermore, RNAi inhibition of Cby expression in *D. melanogaster* embryos leads to the segment polarity defects that mimic the gain-of-function phenotype of the Wingless (Wg) pathway, and overexpression of the Wg target genes *engrailed* and *ultrabithorax*, confirming the biological importance of Cby's function (Takemaru et al., 2003).

Using *in vitro* cell culture systems, Cby has been shown to facilitate adipocyte and cardiomyocyte differentiation of pluripotent stem cells through inhibition of β-catenin signaling (Li et al., 2007; Singh et al., 2007). More recently, 14-3-3 adaptor proteins were isolated as novel Cby-binding partners (Li et al., 2008). Cby and 14-3-3 form a

stable trimolecular complex with β-catenin, and cooperate to promote cytoplasmic localization of β-catenin, leading to down-regulation of target gene expression. Therefore, Cby antagonizes β-catenin signaling through at least two distinct molecular mechanisms, i.e. competing with Lef/Tcf transcription factors for binding to β-catenin in the nucleus (Takemaru et al., 2003), and facilitating nuclear export of β-catenin via interaction with 14-3-3 (Li et al., 2008). However, the function of Cby in vertebrates remains largely unexplored.

In order to examine the role of Cby in vertebrates, Cby-knockout mice were generated. On the C57BL/6J background, these animals display dramatic phenotypes, including a high incidence of embryonic lethality, otitis and sinusitis due to the lack of mucociliary clearance, and runt phenotype (Voronina et al., 2009). Furthermore, these mice exhibit pancreatic degeneration, intestinal immaturity, adipocyte differentiation defects, cystic kidneys and infertility. They are growth-retarded, and most die in 2 to 3 weeks of age probably due to starvation but about 30% of them survive into adults (**FIG. 1-4**).

These mice also exhibit defects in motile cilia formation in the nasal epithelium. *Cby*$^{-/-}$ mice exhibit a paucity of cilia in the nasal passages and a complete lack of mucociliary clearance, likely attributed to the reduction of mature motile cilia. Consistent with this phenotype, Cby proteins are highly enriched at the apical basal bodies of developing cilia in the nasal epithelium, suggesting a role for Cby in ciliogenesis (Voronina et al., 2009).

In addition to these phenotypes, I found that c*by*$^{-/-}$ mice also display a lung phenotype consisting of abnormally developed peripheral airspaces and bronchial airways as well as mechanical defects. It is intriguing to note that the lung phenotypes of *cby*$^{-/-}$ mice are similar to those observed in mice with activated β-catenin in airway epithelial cells (Mucenski et al., 2005), including aberrant epithelial cell differentiation and alveolarization defects that begin postnatally. The aim of this project is to investigate the role of Cby in lung development and function, and contribute to better understanding of the complicated processes underlying lung morphogenesis and diseases.

Table 1-1. Expression of cell lineage-specific markers in epithelial cell lineages in the developing mouse lung

Gestational age	Cell lineage	Marker gene expression			
		SpA	SpC	cGRP	CC10
E12-14	Epithelium (BADJ?)	+	+	+	+
E18	ATII	+	+		+
	Clara Cell	+			+
	PNEC			+	

Adapted from Warburton (2000) and Jacks (2005)

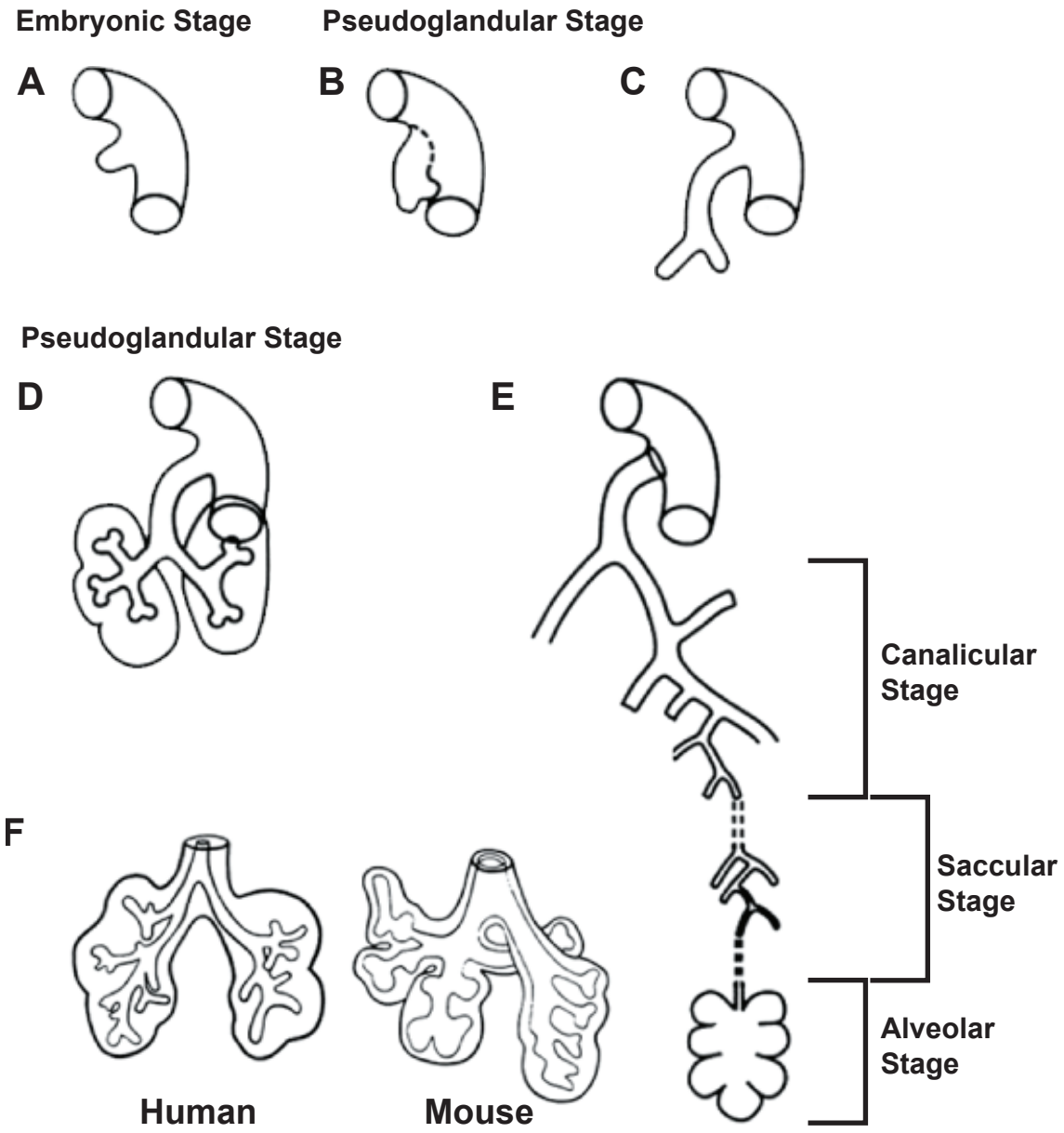

Figure 1-1. Key events in lung morphogenesis. (A) The primitive lung bud emerges as the laryngo-tracheal groove from the ventral surface of the primitive foregut. (B-D) Branching morphogenesis commences with the dorso-ventral separation of the primitive trachea from the early esophagus, followed by lobar bronchi branching from the primary bronchi. (E) The branching program is stereotypically reproducible during the canalicular stage and later, during the saccular stage, becomes more random. Alveolarization begins postnatally in the mouse and is completed by day 28-30. (F) The species differences between mouse and human pulmonary lobation is demonstrated in the diagram comparing human embryonic lungs at 7-8 weeks of gestation with that of the E12 mouse lungs. Note the trilobular left and bilobular right human lungs compared to the quadrilobular right and unilobular left muring lungs. Adapted from Warburton, et. al. (2000)

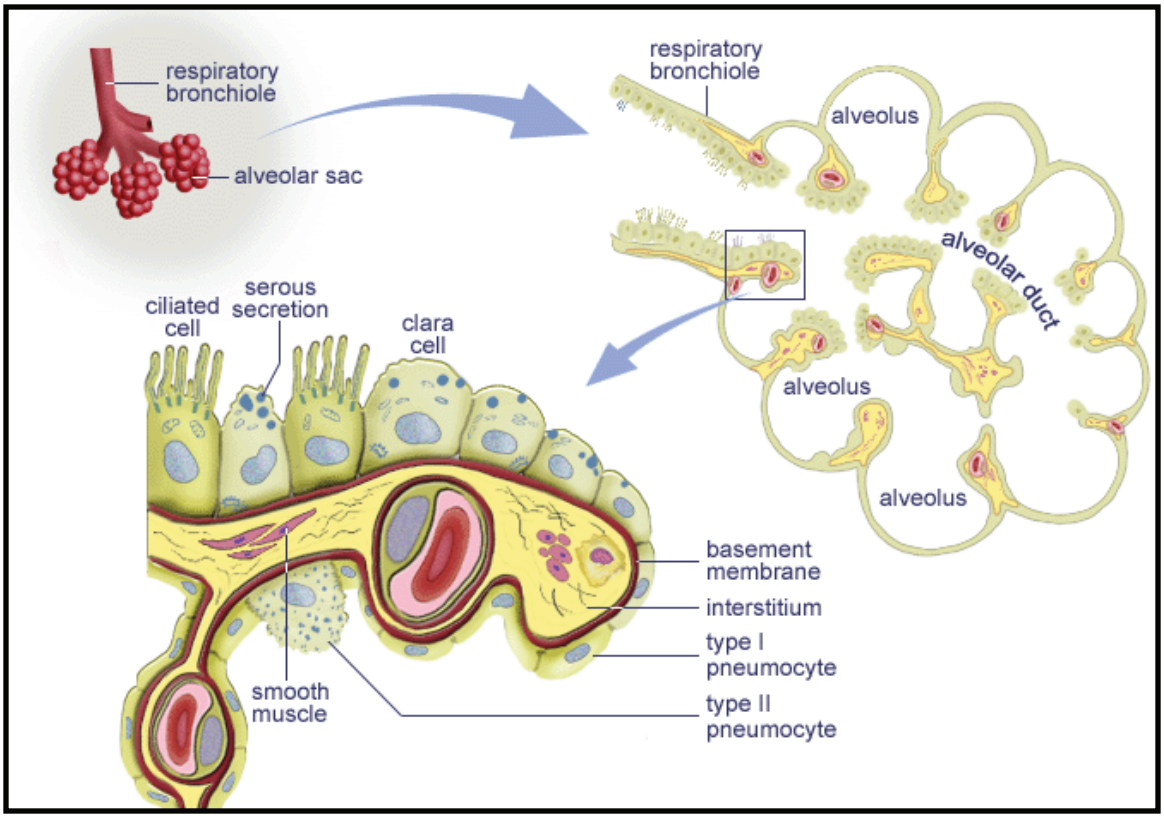

Figure 1-2. Respiratory Epithelial Cells. The respiratory epithelium is lined with a balanced mixture of specialized cell types that carry out functions that range from detoxification, air humidification and mucociliary clearance. The respiratory bronchiole epithelium consists of ciliated cuboidal cells and clara cells. Alveolar ducts are small ducts leading from the respiratory bronchioles to the alveolar sacs. The alveolae are lined with surfactant-producing ATII cells and thin, squamous ATI epithelial cells. Adapted from McKee, M. "Lecture 26: Histology of the Respiratory System" Molson Medical Informatics, 2002, <http://www.mmi.mcgill.ca/mmimediasampler2002>

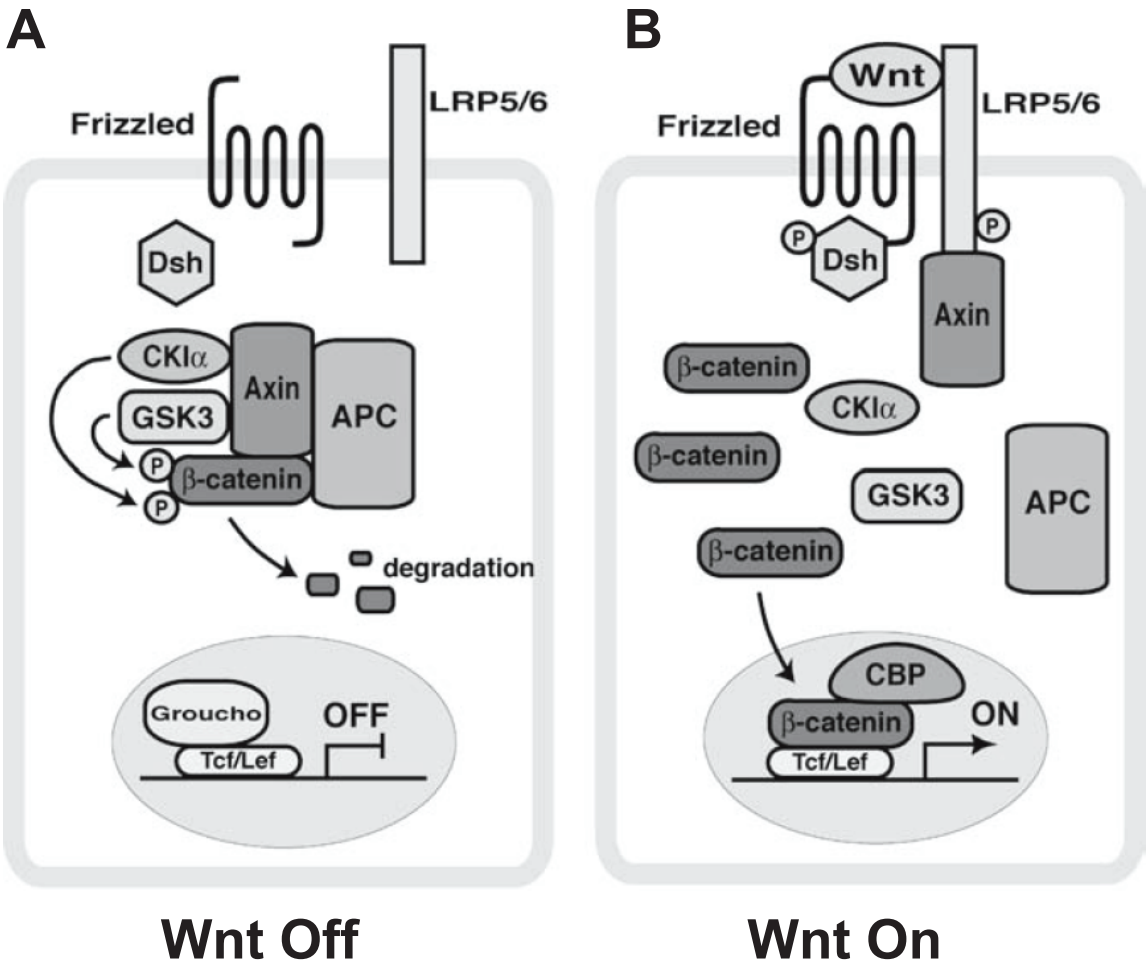

Figure 1-3. Canonical Wnt Pathway. (A) In the absence of a Wnt signal, β-catenin is held by the scaffold proteins APC and Axin in the destruction complex, and sequentially phosphorylated by the kinases CKIα and GSK3. Consequently, β-catenin is constantly degraded by the ubiquitin-proteasome pathway. In the nucleus, Tcf/Lef transcription factors actively repress target gene expression by recruiting transcriptional co-repressors, such as Gro/TLE. (B) Wnt binding to Frizzled receptors and LRP5/6 co-receptors induces Frizzled-Dsh complex formation and the sequential phosphorylation of LRP5/6 by GSK3 and CKI, promoting recruitment of Axin to the plasma membrane and inactivation of the destruction complex. Stabilized β-catenin then translocates into the nucleus and forms a complex with Tcf/Lef factors by displacing Gro/TLE proteins. β-Catenin stimulates expression of Wnt target genes by recruiting various co-activators including CBP.

K-I Takemaru et al., 2008

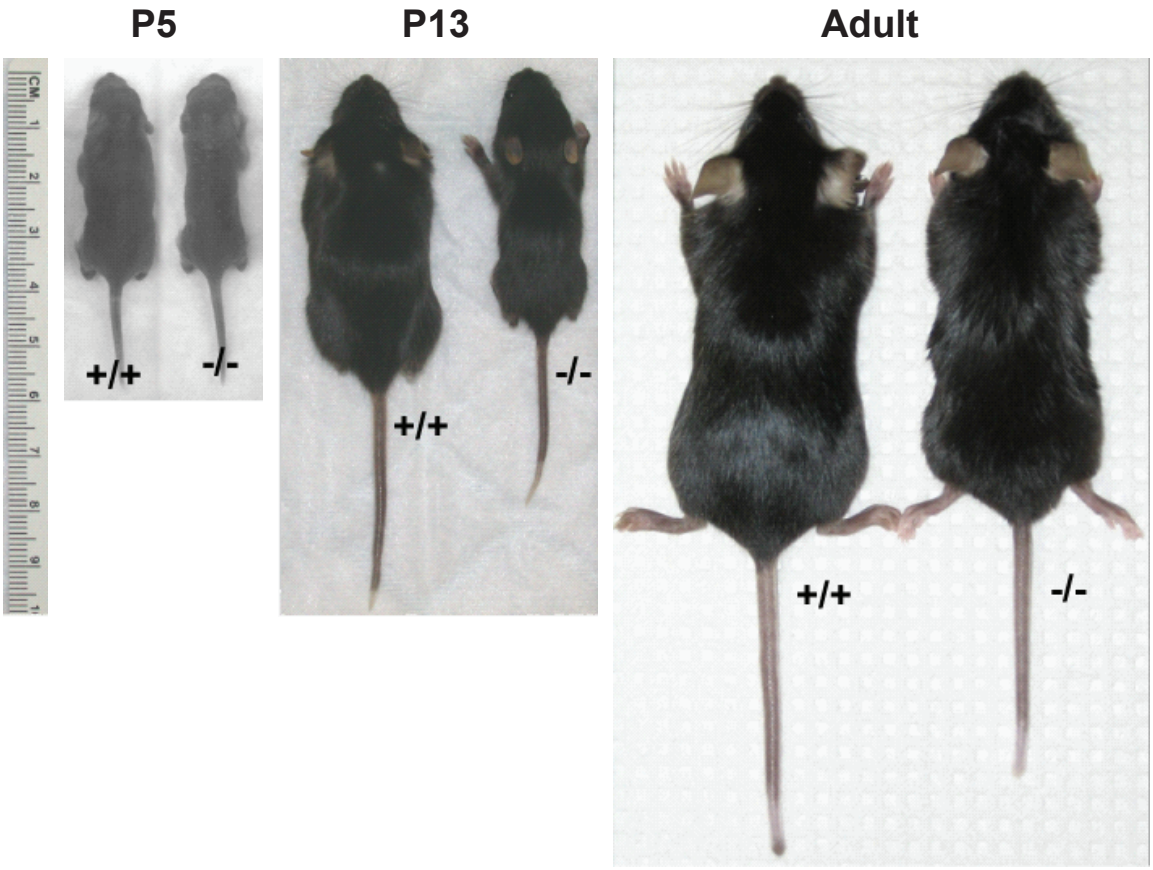

Figure 1-4. Cby expression in multiple mouse tissues throughout development. The Cby null mouse demonstrates a runted phenotype at birth and through early adolescence. By adulthood (here, appx. 3mos), the phenotype is recovered to a degree, although the Cby null mouse remains smaller.

CHAPTER 2: ALTERED LUNG PHYSIOLOGY IN *CBY*$^{-/-}$ MICE

Introduction

Cby is expressed throughout all stages of mouse embryonic development (Voronina et al., 2009). Here we demonstrate that cby is consistently expressed in the embryonic lung, from the onset of lung morphogenesis (E14.5) and into adulthood. Proper lung development has been linked to canonical Wnt signaling, such that aberrations in the signaling pathway have resulted in severe morphological as well as functional deficiencies (Liu et al., 2003; Mucenski et al., 2005; Okubo and Hogan, 2004). In support of these observations, normal ATII cell development has been linked to properly regulated Wnt pathway activity (Torday and Rehan, 2006, 2007).

In order to gain insight into the function of Cby in lung development and homeostasis, we evaluated the potential disruptions of the Wnt/β-catenin pathway caused by the loss of Cby in mouse lungs and the resulting physiological consequences in architecture and function at various developmental stages.

Materials and Methods

Animal husbandry

Cby knockout mice were created on a mixed 129/C57BL/6 background in the Transgenic Mouse Core Facility at the University of Washington, and maintained as heterozygotes. Details of gene targeting at the c*by* locus have been described previously (Voronina et al., 2009). For this study, c*by*$^{+/-}$ mice were backcrossed onto a C57BL/6 background for 7 generations. Progeny of c*by*$^{+/-}$ crosses were genotyped by PCR using

the following primers: *cby* null allele forward, 5'-CTTTCTAGAGAATAGGAACTTCGG-3'; *cby* null allele reverse, 5'-AGACACCAGTGTCAAGAGGTGAG-3' (251-bp PCR product); *cby* wild-type forward, 5'-GACAGCACTGGGACAAAGGTAAC-3'; *cby* wild-type reverse, 5'-CAAAGAGACGAGGGTCTATCATC-3' (288-bp PCR product). Animals were housed in pathogen free conditions according to protocols approved by Institutional Animal Care and Use Committee at the State University of New York at Stony Brook. All animals were maintained in a humidity- and temperature-controlled room with a 12:12-h light-dark cycle and were allowed food and water *ad libitum*.

RNA extraction and RT-PCR

Total RNA was purified from murine lungs using the RNeasy Mini Kit (Qiagen) with DNase treatment. Synthesis of cDNA was performed with oligo(dT) primers using the ThermoScript RT-PCR System (Invitrogen) according to the manufacturer's instructions. The primer sequences were as follows: Cby-1 forward, 5'-CGTTTCCTCACTGAGTTAGG-3'; Cby-1 reverse, 5'-TAGTCTGCTAATCTGACGGG-3' (506-bp PCR product); GAPDH-1 forward, 5'-ACCACAGTCCATGCCATCAC-3'; GAPDH-1 reverse, 5'-TCCACCACCCTGTTGCTGTA-3' (452-bp PCR product).

Quantitative real-time PCR analysis was performed using the iScript One-Step RT-PCR Kit with SYBR Green (BioRad) on the MiniOpticon Real-Time PCR Detection System (BioRad). The following primer pairs were used at a final concentration of 300 nM each: Cby-2 forward, 5'-TCGACTATGGAACTCCTACC-3'; Cby-2 reverse, 5'-CAGCAGAATGTCCACTTTCA-3' (185-bp PCR product); GAPDH-2 forward, 5'-

TCAACAGCAACTCCCACTCTTCCA-3'; GAPDH-2 reverse, 5'-ACCCTATTACTGTAGCCGTATTCA-3' (115-bp PCR product), CyclinD1 forward, 5′-TGTTCGTGGCCTCTAAGATGAAG-3′; CyclinD1 reverse, 5′-AGGTTCCACTTGAGCTTGTTCAC-3′; Axin2 forward, 5′-CTCCCCACCTTGAATGAAGA-3′; Axin2 reverse, 5′-ACATAGCCGGAACCTACGTG-3′; HPRT forward, 5′-TGGAAAGAATGTCTTGATTGTTGAA-3′; HPRT reverse 5′-AGCTTGCAACCTTAACCATTTTG-3′. The level of transcripts for the endogenous housekeeping genes HPRT and GAPDH were used as internal standards. The amplification steps consisted of 10 min at 50 ºC and 5 min at 95 ºC, followed by 40 cycles of denaturation for 10 sec at 95 ºC and annealing/extension for 30 sec at 58 ºC. All samples were analyzed in triplicate, and the relative Cby expression was calculated according to the comparative threshold cycle ($\Delta\Delta C_T$) method (Livak and Schmittgen, 2001).

The $\Delta\Delta C_T$ method quantifies the relative changes in gene expression of a target gene relative to a reference group using real-time PCR. The PCR amplifications are monitored using a fluorescent dye (in this case, SYBR Green) which traces the amplification cycle via fluorescent emission. The amplification plot is examined early in the reaction, at a point that represents the log phase of product accumulation. An arbitrary fluorescent emission threshold is set and an algorithm calculates the cycle at which the amplification plot crosses the threshold. This point is defined as C_T, a value that is proportional to the number of target copies present in the sample. Thus, the C_T value is a quantitative measurement of the copies of the target found in any sample (Gibson et al., 1996; Winer

et al., 1999). The data were analyzed using the following equation: $\Delta\Delta C_T = (C_{T,target} - C_{T,ref})_{TEST} - (C_{T,target} - C_{T,ref})_{CONTROL}$, where $C_{T,ref}$ corresponds to the internal control (HPRT or GAPDH). The amount of the target, normalized to an endogenous reference and relative to a control is given by the following equation: amount of target = $2^{-\Delta\Delta C_T}$ (Livak and Schmittgen, 2001).

Western blotting

Lung tissue lysates were prepared using TRIzol reagent (Invitrogen) according to the manufacturer's instructions. Equal amounts of protein samples were loaded onto a 15% SDS-PAGE, and subjected to Western blotting using rabbit polyclonal anti-Cby antibody (1:1000 dilution) (Takemaru et al., 2003).

Lung histology

Mice were sacrificed by CO_2 asphyxiation, and the trachea was exposed and cannulated. Lungs were then inflation-fixed at 20 cm WATER of pressure for 24 hr in 4% methanol-free formaldehyde (Polysciences) in 0.01M phosphate-buffered saline (PBS), pH 7.4 (Sigma). Left lung lobes were removed and dehydrated by immersion in a series of increasing ethanol washes (70%, 80%, 90% and 100%) at room temperature at 1 hr intervals. This was followed by immersion for 1 hr in Histo-Clear (National Diagnostics) at 60°C in a vacuum oven. Tissues were then immersed in a solution of 1:1 Histo-Clear in paraffin for 1 hr at 60°C in a vacuum oven. Tissues were then immersed in a solution of 100% paraffin overnight at 60°C in a vacuum oven. The next day, tissues were placed in plastic molds and embedded in paraffin.

Eight-micron tissue sections were generated, placed on slides and baked at 65°C prior to rehydration. Slides were prepared for hematoxylin and eosin (H&E) (Sigma) staining by first immersing in Histo-Clear for 5min to deparaffinize, followed by rehydration in serial ethanol washes for 2 min each from 100% ethanol to 50% ethanol. This was followed by a brief rinse in distilled water and immersion in hematoxylin for 5min at room temperature. Slides were rinsed clear in distilled water, immersed in 0.01M PBS for 1 min and rinsed again in distilled water. Slides were dehydrated serially in ethanol to 100%, immersed in eosin for 30 sec and rinsed in 100% ethanol. The sections were then mounted on coverslips with Permount (Fisher) and photographed with a Leica DM5000 microscope.

In order to examine the presence as well as distribution of collagen, Masson's trichrome stain (Sigma) was used. Slides were deparaffinized and rehydrated to distilled water. Slides were then microwaved in coplin jars at 600 watts for 25 sec in Bouin's fixative (Richard Allen Scientific) and cooled in a fume hood for 5 min. Slides were then rinsed clear in tap water followed by microwaving again for 5 sec at 800 watts. Slides were then rinsed thoroughly under running tap water and immersed for 1min in 0.01 M PBS and rinsed again in tap water. Slides were again microwaved for 20 sec at 600 watts in Biebrich Scarlet-acid Fuschin solution (Sigma), mixed and allowed to incubate for 2 min at room temperature. The slides were then rinsed quickly in several changes of deionized water and microwaved for 20 sec at 600 watts in a 1:1:2 solution of phosphotungstic acid and phosphomolybdic acid in water. Slides were immediately removed and rinsed in water and then microwaved at 600 watts for 15 sec in Aniline Blue (Sigma). After 1-min incubation, slides were rinsed in water, followed by 1-min

incubation at room temperature in a solution of 0.01 N glacial acetic acid. Slides were rinsed, dehydrated to 100% ethanol, immersed 5 min in Histo-Clear and coverslips were mounted with Permount.

BAT-gal Wnt/β-catenin reporter mice

Generation and characterization of the BAT-gal mice have been previously described (Maretto et al., 2003). The BAT-gal transgene on the *cby*$^{-/-}$ background was obtained by crossing BAT-gal with *cby*$^{+/-}$ mice. The *cby*$^{-/-}$ mutation was identified by genotyping of harvested embryos as described above. Embryonic ages were estimated from the day of the appearance of the vaginal plug (E0.5).

β-Galactosidase assay

β-Galactosidase activity was measured using AppliedBiosystems Galacto-Light Plus System (catalog # T1007). Lungs from embryos at E15.5 and E16.5 were harvested and homogenized in the supplied lysis solution. In order to lower the endogenouse LacZ activity, lung tissue lysates were heat-inactivated for 50 min at 48°C and luminosity was measured for each sample in triplicate. Measurements were made using a tube luminometer (Monolight 2010). Protein concentrations were measured using Bio-Rad Dc Protein Assay (#500–0112). Values were normalized by protein concentration derived from the Bradford assay.

Lung morphometry

Morphometric measurements were performed on inflation-fixed c*by*$^{+/+}$ and c*by*$^{-/-}$ lungs (n = 4 per group) as described previously (Broussard et al., 2006). At least five

representative sections from the left lobes of each sample were randomly chosen at 250-mm intervals and stained with H&E. Twenty images from non-overlapping parenchymal fields in each lung section were captured at a 400x final magnification. A square lattice grid of 121-test points was then superimposed on each image to evaluate the percentage of lung area represented by saccular airspace, parenchymal tissue, and airway lumen by point-counting morphometry by two investigators. Parenchyma was defined as the gas-exchanging compartment that contained the airspaces (saccule ducts and saccules). Airways consisted of conducting airways to the level of the terminal bronchioles. Alveolar complexity of the lung was assessed by counting the number of individual saccules in each field, and measuring the mean linear intercept (Lm) (distance between alveolar walls). The Lm was determined by counting the number of intercepts over a line of known length/2 at 400x final magnification.

Respiratory function tests and pressure-volume (*PV*) curve analysis

Pulmonary mechanics were assessed on adult mice using a computer-controlled ventilator flexiVent (SCIREQ, Montreal, PQ, Canada) (Broussard et al., 2006; Cohen et al., 2004). The mice were anesthetized with intra-peritoneal pentobarbital (90 mg/kg) and the trachea was dissected free of surrounding tissue and cannulated with a 20-gauge cannula. The animals were then connected to flexiVent and ventilated with a tidal volume of 10 ml/kg; inspiratory:expiratory ratio of 66.67%, respiratory rate of 150 breaths/min, and maximum pressure of 30 cm WATER, with a positive end-expiratory pressure (PEEP) of 0 and 3 cm WATER. PEEP was controlled by submerging the expiratory limb from the ventilator into a water trap. This ventilator permits measurement of lung function by using a modification of the low-frequency forced oscillation technique

(Gomes et al., 2000). Respiratory input impedance (*Zrs*), a quality which can be defined as a generalization of the changes of resistance and compliance, was measured by systematically interrupting mechanical ventilation and allowing the mouse to expire for one second (Irvin and Bates, 2003). An 8-second broadband volume perturbation signal was then applied to the lungs with the flexiVent, after which ventilation was resumed. *Zrs* was calculated from the displacement of the ventilator's piston. The following equation was used to interpreted *Zrs* in terms of the constant-phase model (Hantos et al., 1992):

$$\text{Zrs} = \text{Raw} + 12\pi f\text{Iaw} + \frac{\text{G-iH}}{(2\pi f)^{\alpha}}$$

Raw is a frequency independent Newtonian resistance reflecting that of the conducting airways, *Iaw* is airway gas inertance, *G* characterizes tissue damping, *H* characterizes tissue stiffness (elastance), *i* is the imaginary unit, α links *G* and *H*, and *f* is frequency (Tomioka et al., 2002). A quantity known as hysteresivity ($\eta = G/H$) was calculated, which is believed to increase when regional heterogeneities develop in the lung (Lutchen et al., 1996). *Raw*, *G* and *H* were all normalized by multiplication by lung volume. *Zrs* measurements at each PEEP level were obtained in triplicate.

Analysis of *PV* curves was conducted as follows. Starting at a functional residual lung capacity (FRC) defined by the PEEP, the flexiVent was programmed to apply inspiratory volume in stepwise fashion until a peak pressure of 30 cm water was reached, followed by stepwise expiration. At each step, ventilation was paused for 1 sec and plateau pressure (*P*) was recorded and related to the total volume (*V*) delivered to produce

a quasi-static *PV* curve. Static compliance (*Cst*) was calculated from the slope of each curve as described previously (Salazar and Knowles, 1964). *Zrs* and *PV* curve data were obtained in triplicate for statistical evaluation.

Statistical analysis

Unpaired Student's *t*-test was performed to determine statistically significant differences among different genotype groups. For respiratory function tests, two-way analysis of variance (ANOVA) was used for statistical analysis, followed by Bonferroni's post-test. Values for all measurements were expressed as means ± SE, and *P* values of < 0.05 were considered significant.

Results

Cby is expressed in the developing and mature lung.

To investigate a potential role of Cby in regulating lung development or/and homeostasis, we first examined its expression in fetal and postnatal lungs. RT-PCR analysis demonstrated that *cby* mRNA is constantly present during embryonic lung development as well as in adult lungs (**FIG. 2-1A**). Furthermore, Western blotting confirmed that Cby is expressed at the protein level in the adult $cby^{+/+}$ lung but absent in the $cby^{-/-}$ lung (**FIG. 2-1B**). These data suggest a physiological role for Cby in normal lung development.

Loss of the *cby* gene results in elevated Wnt/β-catenin signaling activity in mouse lung.

Proper lung development is dependent on precise spatial and temporal regulation of Wnt pathway activity (Mucenski et al., 2005; Mucenski et al., 2003; Okubo and Hogan, 2004; Shu et al., 2005; Shu et al., 2002). *In vitro* studies have shown that overexpression of Cby represses β-catenin-dependent transcriptional activation, suggesting that Cby could regulate expression of β-catenin gene targets in the mouse lung (Greaves, 2003; Takemaru et al., 2003). To test whether or not $cby^{-/-}$ lungs result in hyperactive pathway activity, we examined BAT-gal reporter mice, which express β-galactosidase under the control of Wnt/β-catenin-responsive elements (Echelard et al., 1994; Maretto et al., 2003). Embryos derived from intercrosses between BAT-gal mice heterozygous for the *cby* allele were harvested at E15.5 and E16.5 and tissue lysates were prepared from the lungs of $cby^{+/+}$ and $cby^{-/-}$ embryos (n=3 per genotype at each age). Total protein assays were performed and enzymatic activity expressed as lacZ units/μg protein (**FIG. 2-2A**). BAT-gal assays revealed low levels of Wnt/β-catenin activity at E15.5 with activity increasing at E16.5. Loss of *cby* resulted in elevated Wnt/β-catenin activity on E15.5 ($p<0.05$) and on E16.6 ($p<0.01$) compared to controls, consistent with the real-time PCR results in the adult lung. To confirm the BAT-gal data, we performed quantitative RT-PCR on RNA extracted from adult mouse lungs to examine the expression of the known Wnt target genes *cyclinD1* and *axin2* (Jho et al., 2002; Shtutman et al., 1999). There was a twofold increase in expression of *cyclinD1* and *axin2* transcripts in $cby^{-/-}$ lungs, indicating elevated canonical Wnt signaling activity (**FIG. 2-2B**). These findings support Cby's role as a negative regulator of canonical Wnt signaling in the lung.

$Cby^{-/-}$ mice exhibit morphological defects in the respiratory epithelium.

To explore a potential role of Cby during lung development, we analyzed the lung histology of *cby*$^{-/-}$ mice (**FIG. 2-3**). Lung morphology was not significantly perturbed in *cby*$^{-/-}$ embryos compared to *cby*$^{+/+}$ controls in mice as early as E18.5 (**FIG. 2-3, A-B**) and as late as postnatal day 4 (P4) (**FIG. 2-3, C-D**). In contrast, as alveologenesis continued postnatally, enlarged distal airspaces were observed in *cby*$^{-/-}$ lungs as early as P7 (**FIG. 2-3, E-F**), and persisted in adult lungs (**FIG. 2-3, G-J**). Despite marked changes in alveolar septum formation, there were no signs of inflammation or fibrosis in the lungs of *cby*$^{-/-}$ mice at all ages analyzed (data not shown).

In addition to the alveolar defects observed, *cby*$^{-/-}$ mice demonstrate morphological defects in proximal airways (**FIG. 2-4**). The most dramatic abnormality observed in *cby*$^{-/-}$ mice is a dysmorphic Clara cells with apparent hypersecretion into the airway lumen (**FIG. 2-4, B&D, WHITE ARROW**). Additionally, there is an apparent decrease in the abundance of ciliated cell types relative to non-ciliated Clara cells in the *cby*$^{-/-}$ airway as compared to controls (**FIG. 2-4, A&C, BLACK ARROW**). This seems indicative of a differentiation defect in *cby*$^{-/-}$ mice, as Clara cells are believed to be progenitors to the terminally differentiated ciliated cells (Hong et al., 2001; Mucenski et al., 2005; Van Winkle et al., 1995).

Morphometric analysis reveals structural differences in *cby*$^{-/-}$ lungs compared to *cby*$^{+/+}$ controls.

To precisely quantify changes in lung structure, we performed morphometric analysis on the lungs from *cby*$^{-/-}$ and *cby*$^{+/+}$ adult animals. *Cby*$^{+/-}$ mice show lung phenotypes indistinguishable from those of *cby*$^{+/+}$ mice at the histological level (data not

shown), and therefore omitted from the analysis. The complexity of the lung parenchymal tissue was measured by comparing the following three parameters: the number of alveolar saccules per mm^2; the relative amount of parenchymal tissue; and the inter-airspace wall distance (mean linear intercept [Lm]), which measures the distance between alveolar walls. Consistent with our histological observations, morphometric analysis revealed a 33% decrease in the number of alveolar saccules per mm^2 in $cby^{-/-}$ lungs compared to $cby^{+/+}$ controls (2.05 ± 0.077 vs. 3.04 ± 0.082; $P < 0.001$) (**FIG. 2-5, A**). Furthermore, the gas-exchange surface area was reduced in $cby^{-/-}$ lungs in comparison with $cby^{+/+}$ control lungs as observed by the increased distance between alveolar walls (0.59 ± 0.014 μm for the $cby^{-/-}$ lung vs. 0.055 ± 0.016 μm for the $cby^{+/+}$ lung; $P < 0.05$) (**FIG. 2-5,B**) as well as by the reduced percentage of lung parenchymal tissue (33.0 ± 0.57% for the $cby^{-/-}$ lung vs. 34.9 ± 0.61% for the $cby^{+/+}$ lung; $P < 0.05$) (**FIG. 2-5,C**). It is also interesting to note that the proportion of lung airway lumen to the total lung area was significantly greater in $cby^{-/-}$ mice than that in $cby^{+/+}$ mice (3.76 ± 0.79% vs. 1.24 ± 0.14%; $P < 0.001$) (**FIG. 2-5,D**).

cby$^{-/-}$ and *cby*$^{+/-}$ mice exhibit abnormal respiratory mechanics.

In order to investigate the potential effects of the observed structural alterations in $cby^{-/-}$ lungs on lung function, pulmonary function tests were performed. Static compliance (*Cst*), airway resistance (R_{aw}), tissue elastance (*H*), tissue damping (*G*) and hysteresivity (η) were all measured and normalized to total lung volumes (**FIG. 2-6**). The static compliance of the lungs, which reflects elastic recoil at a given pressure, was reduced in $cby^{-/-}$ mice compared to that in $cby^{+/+}$ controls ($P < 0.05$) (**FIG. 2-6,A**). Unexpectedly, $cby^{+/-}$ lungs showed a drastic decrease in static compliance relative to $cby^{+/+}$ lungs ($P <$

0.001). Airway resistance, a frequency-independent Newtonian resistance reflecting that of the conducting airways, was also decreased in *cby*$^{-/-}$ mice compared to *cby*$^{+/+}$ mice ($P < 0.05$) (**FIG. 2-6,B**). As with static compliance, *cby*$^{+/-}$ lungs were distinctly different from both *cby*$^{+/+}$ and *cby*$^{-/-}$ lungs, demonstrating a marked increase in airway resistance ($P < 0.001$ for both comparisons). On the other hand, tissue elastance, which reflects the energy conservation in the lung tissues, was substantially increased in *cby*$^{-/-}$ lungs in comparison with that in *cby*$^{+/+}$ lungs ($P < 0.001$), while the *cby*$^{+/-}$ value was intermediate between *cby*$^{+/+}$ and *cby*$^{-/-}$ animals ($P < 0.001$ for both comparisons) (**FIG. 2-6,C**). Tissue damping, which reflects the energy dissipation in the lung tissues, was also increased in *cby*$^{-/-}$ mice relative to that in *cby*$^{+/+}$ mice ($P < 0.001$), whereas the *cby*$^{+/-}$ value was lower than both *cby*$^{+/+}$ and *cby*$^{-/-}$ mice ($P < 0.001$ for both comparisons) (**FIG. 2-6,D**). Lastly, hysteresivity, a reflection of inhomogeneities and structural changes in the lungs, was increased in *cby*$^{-/-}$ mice compared to that in *cby*$^{+/+}$ mice ($P < 0.001$), and *cby*$^{+/-}$ mice displayed lower hysteresivity than both *cby*$^{+/+}$ ($P < 0.05$) and *cby*$^{-/-}$ ($P < 0.001$) mice (**FIG. 2-6,E**). These data clearly demonstrate that targeted disruption of the *cby* gene perturbs normal lung function.

The pressure-volume (*PV*) curves for each genotype are also presented (**FIG. 2-6,F**). The *PV* curve obtained for *cby*$^{-/-}$ mice demonstrated a statistically significant difference from that for *cby*$^{+/+}$ ($P < 0.05$) and *cby*$^{+/-}$ ($P < 0.001$) mice, whereas there was no significant difference between *cby*$^{+/+}$ and *cby*$^{+/-}$ *PV* curves. Total lung capacity was similar among all three genotypes (data not shown). As expected, *cby*$^{+/+}$ lungs exhibited normal *PV* relationships. At the onset of inspiration, *cby*$^{+/+}$ lungs distended easily showing large volume changes, accompanied by small incremental increases in applied

pressure into the lungs, while showing smaller increases in volume at higher pressures as lungs reach their full capacity. In contrast, *cby*$^{-/-}$ lungs did not distend as easily, demonstrating relatively small changes in volume with the same increments in applied transpulmonary pressure both initially and at high pressures. These results suggest that *cby*$^{-/-}$ lungs have increased stiffness and are less compliant.

Reduced Cby expression in *cby*$^{+/-}$ mice.

To verify that there is no compensatory increase in the expression of the other allele in *cby*$^{+/-}$ animals and that their distinct pulmonary mechanics are indeed attributed to a reduction in Cby expression levels, we conducted quantitative real-time PCR analysis for adult lungs. As shown in **FIG. 2-7**, expression of Cby mRNA in *cby*$^{+/-}$ lungs was reduced by 30% in comparison with that in *cby*$^{+/+}$ lungs.

Discussion

The canonical Wnt/β-catenin signaling pathway plays a critical role in controlling cell proliferation and differentiation in various organ systems. It has been shown to be a prerequisite for lung morphogenesis and regeneration/repair (De Langhe and Reynolds, 2008; Morrisey, 2003; Mucenski et al., 2003; Okubo and Hogan, 2004; Shu et al., 2002; Zhang et al., 2008). In the present study, we demonstrate that mice lacking the Wnt/β-catenin antagonist, Cby, exhibit compromised postnatal lung maturation such as alveolarization defects, resulting in alterations in the mechanical properties of the lungs. Surprisingly, we found that *cby*$^{+/-}$ mice have respiratory mechanics largely distinct from those of both *cby*$^{+/+}$ and *cby*$^{-/-}$ littermates even though their lungs are morphologically

indistinguishable from *cby*$^{+/+}$ controls. Collectively, our findings support the concept that loss of Cby inhibits alveolarization and perturbs lung function.

The architectural abnormalities of the lung parenchyma are the most predominant lung phenotype resulting from the inactivation of Cby. Prior to the onset of the alveolarization stage (Warburton et al., 2000), there are no obvious structural differences between *cby*$^{-/-}$ and *cby*$^{+/+}$ lungs (**FIG. 2-3,A-D**). However, we found that there is a progressive reduction in the complexity of the parenchymal tissue of the developing *cby*$^{-/-}$ lung during alveolarization (P5 to P30; **FIG. 2-3,E-J**). In the adult mouse lung, the number of alveoli is dramatically reduced in *cby*$^{-/-}$ mice compared to *cby*$^{+/+}$ controls (**FIG. 2-3,I-J; FIG. 2-5,A**). In agreement with these findings, we also observed an increase in the distance between alveolar walls (**FIG. 2-5,B**), coincident with a decrease in the lung parenchymal tissue (**FIG. 2-5,C**) in *cby*$^{-/-}$ mice. We also detected an increase in the proportion of the lung area attributable to airway lumen, suggesting dilation of the bronchial airways (**FIG. 2-5,D**). This observation is consistent with an earlier study by Okubo, *et al.* who demonstrated that mice expressing a constitutively active β-catenin-Lef1 fusion protein expressed in the lung epithelium developed bronchial tubes that were abnormally wide and opened directly into sacules lined with a simple cuboidal or columnar epithelium (Okubo and Hogan, 2004).

There were no clear signs of pulmonary fibrosis and inflammation in *cby*$^{-/-}$ animals up to 1 year in age (data not shown). The precise molecular mechanisms underlying the reduced complexity of *cby*$^{-/-}$ lung parenchyma remain to be elucidated. However, it is interesting to note that conditional activation of β-catenin specifically in the developing lung epithelium causes airspace enlargement in the postnatal period (Mucenski et al.,

2005), suggesting that impaired alveolarization in *cby*$^{-/-}$ mice is associated with upregulation of β-catenin signaling. Consistent with this notion, we found that the complete loss of *cby* results in elevated Wnt/β-catenin pathway activity during embryonic development as well as in adult lungs as indicated by elevated LacZ activity in BAT-gal embryos and by the elevated expression of the direct β-catenin target genes, *cyclin D1* and *axin2,* in adults (**FIG. 2-2**).

To assess pulmonary structure-function relationships, we performed respiratory function tests (**FIG. 2-6**). Static compliance (*Cst*) values were reduced in *cby*$^{-/-}$ mice in comparison with *cby*$^{-+/+}$ littermates (**FIG. 2-6,A**), most likely reflecting increased stiffness of the *cby*$^{-/-}$ lungs. Conversely, there was a 2-fold increase in the tissue elastance parameter (*H*) in *cby*$^{-/-}$ lungs (**FIG. 2-6,C**), which also points to an increase in the elastic rigidity of the lung. Tissue damping (*G*) is a parameter that is closely rated to lung parenchymal tissue resistance, which reflects energy dissipation in the lung tissues. Dissipation processes within soft tissues are dependent upon elastic stress, therefore making dissipation and elastic properties fundamentally related (Ludwig et al., 1992; Sakai et al., 2001). Hysteresivity (η) is a material property of the tissue and is defined as the energy dissipated relative to the elastic energy stored in the tissue in a cycle. Because η is dependent on the material composition of the tissue, it is therefore a reflection of structural changes in the lungs (Fredberg and Stamenovic, 1989; Sakai et al., 2001), and its relationship with between *G* and *H* is reflected in the elevated values of each parameter in the *cby*$^{-/-}$ mouse (**FIG. 2-6,C-E**). The decrease in airway resistance (R_{aw}) could be due to the increase in relative size of conducting airways in the *cby*$^{-/-}$ mouse as supported by morphometric analysis (**FIG. 2-5,D**).

Consistent with these findings, analysis of *PV* curves revealed that *cby*$^{-/-}$ lungs have a decreased rate of inflation during inspiration compared to *cby*$^{+/+}$ and *cby*$^{+/-}$ lungs as indicated by a relatively flat inspiratory curve (**FIG. 2-6,F**). This suggests that more pressure is required to inflate the *cby*$^{-/-}$ lungs due to physiological and or structural differences.

A particularly intriguing observation was the unique functional pulmonary phenotype of *cby*$^{+/-}$ mice despite the absence of any obvious morphological alterations in their lungs. Most notably, *cby*$^{+/-}$ mice exhibited markedly reduced *Cst* (**FIG. 2-6,A**) and increased *Raw* (**FIG. 2-6,B**), both of which are strikingly different from *cby*$^{+/+}$ and *cby*$^{-/-}$ phenotypes. In fact, this is attributable to the reduced Cby expression in *cby*$^{+/-}$ lungs compared with *cby*$^{+/+}$ controls (**FIG. 2-7**). Thus, both alleles of the *cby* gene are essential for normal lung function. In addition, our data indicate that ~50% gene dosage changes of a single gene can have profound influences on dynamic pulmonary physiology and function without overtly affecting lung architecture at the histological level. Worthy of note, similar gene dosage effects on lung function has been documented using mouse models of cystic fibrosis (Cohen et al., 2004). Mice heterozygous for cystic fibrosis transmembrane conductance regulator (CFTR) display lung mechanics quite distinct from those of both *Cftr*$^{+/+}$ and *Cftr*$^{-/-}$ animals.

Taken together, these observations suggest that the morphological abnormalities exhibited by the *cby*$^{-/-}$ mouse are due, in part, to deregulation of Wnt/β-catenin signaling, compromising postnatal lung alveolar development and influencing pulmonary function.

In summary, we have shown that targeted disruption of the *cby* gene encoding a Wnt/β-catenin antagonist affects postnatal lung maturation, resulting in abnormal lung function. The following chapters explore the cellular and molecular bases responsible for the lung lesions in $cby^{-/-}$ mice.

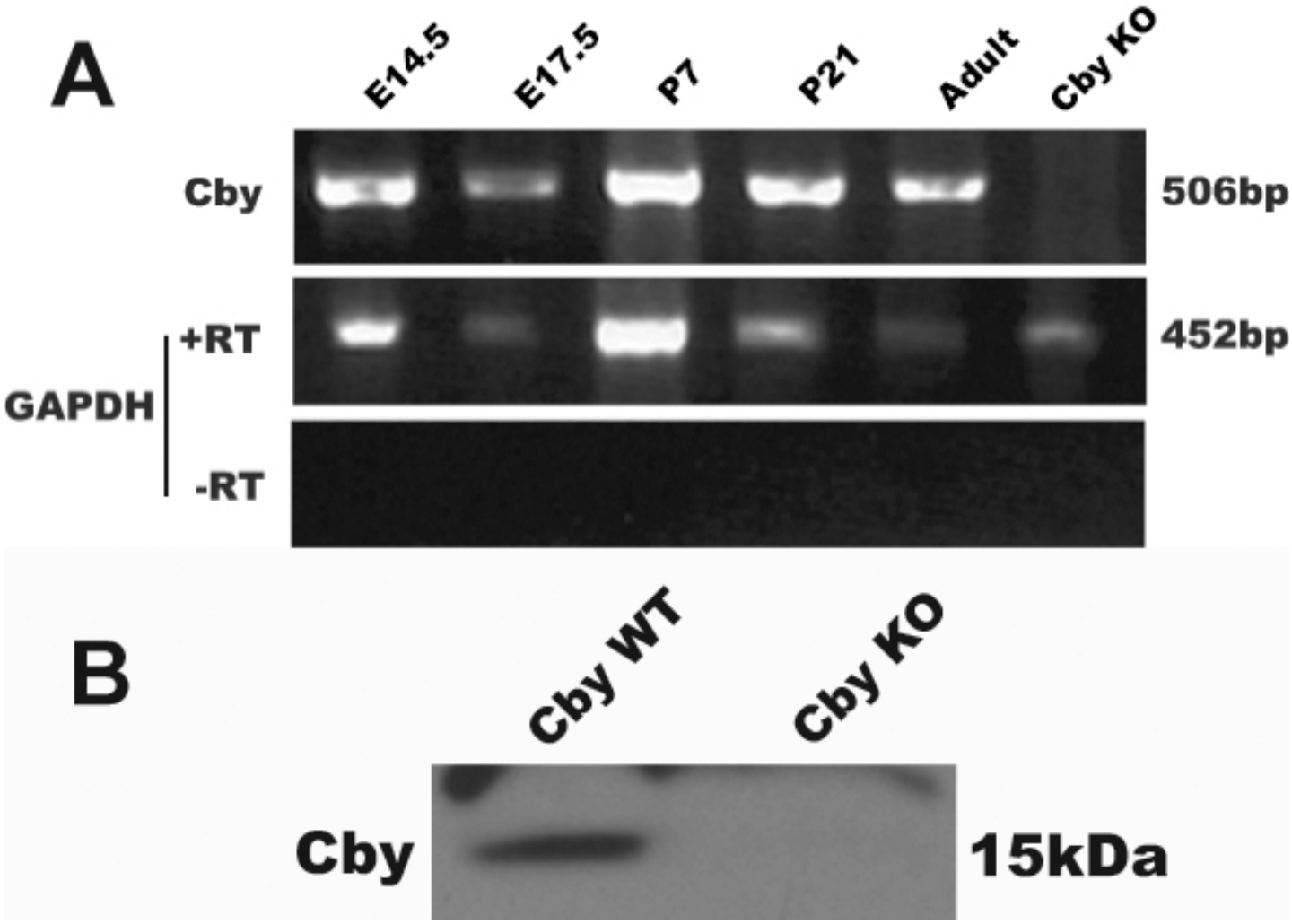

Fig. 2-1 Cby is expressed throughout murine lung development. (A) The temporal expression of Cby mRNA was analyzed by RT-PCR in lung tissue samples from embryonic day (E) 14.5, E17.5, postnatal day (P) 7, P21, adult and adult *cby*$^{-/-}$ (KO) mice. GAPDH was used as a loading control. (B) Cby protein was detected in the adult lung. Equal amounts of lung homogenates (50 µg) from *cby*$^{+/+}$ (WT) and Cby-/- (KO) adult animals were loaded onto a 15% SDS-PAGE, and subjected to Western blotting using anti-Cby antibody.

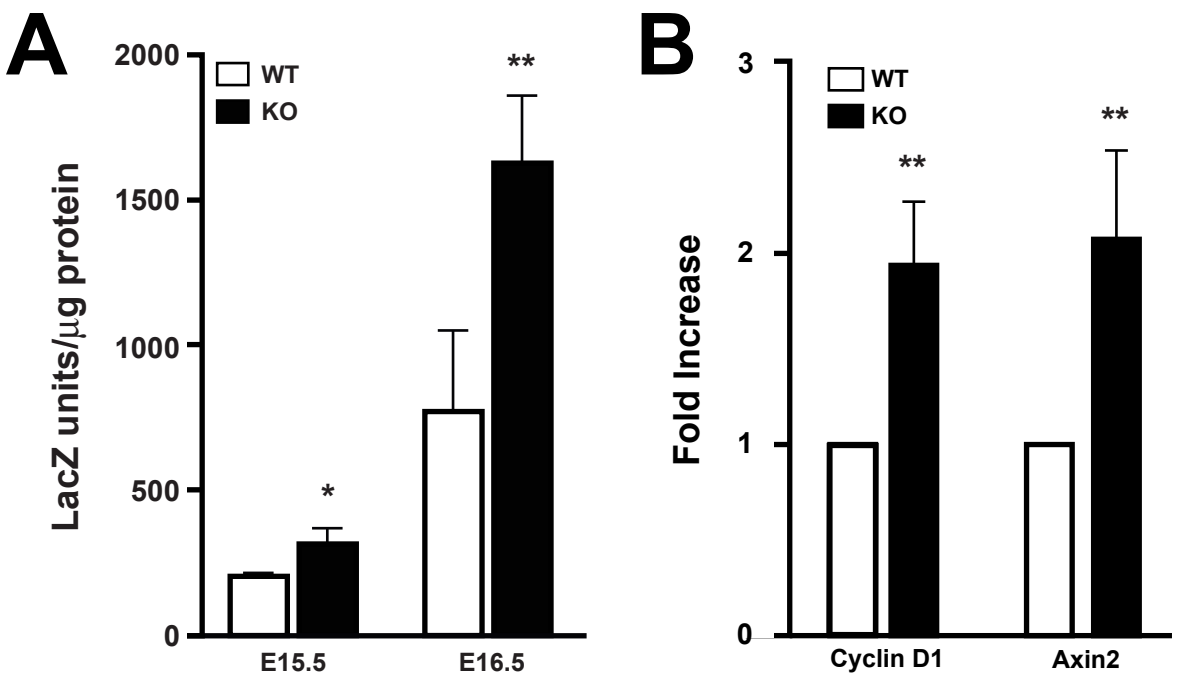

Fig. 2-2. Wnt/β-catenin pathway activity is elevated in Cby null lungs. (A) β -galactosidase enzyme assays were performed on whole lung lysates harvested from Cby+/+/BAT-gal and Cby-/-/BAT-gal embryos at E15.5 and E16.5. LacZ activity was measured as a reporter for canonical Wnt pathway activity. Values were normalized based on protein concentration. (B) Relative expression of canonical Wnt pathway target genes, Cyclin D1 and Axin 2, was measured from RNA extracted from lungs from adult mice. Values represent means ± SE. Student's t-test: *P < 0.05; **P < 0.01.

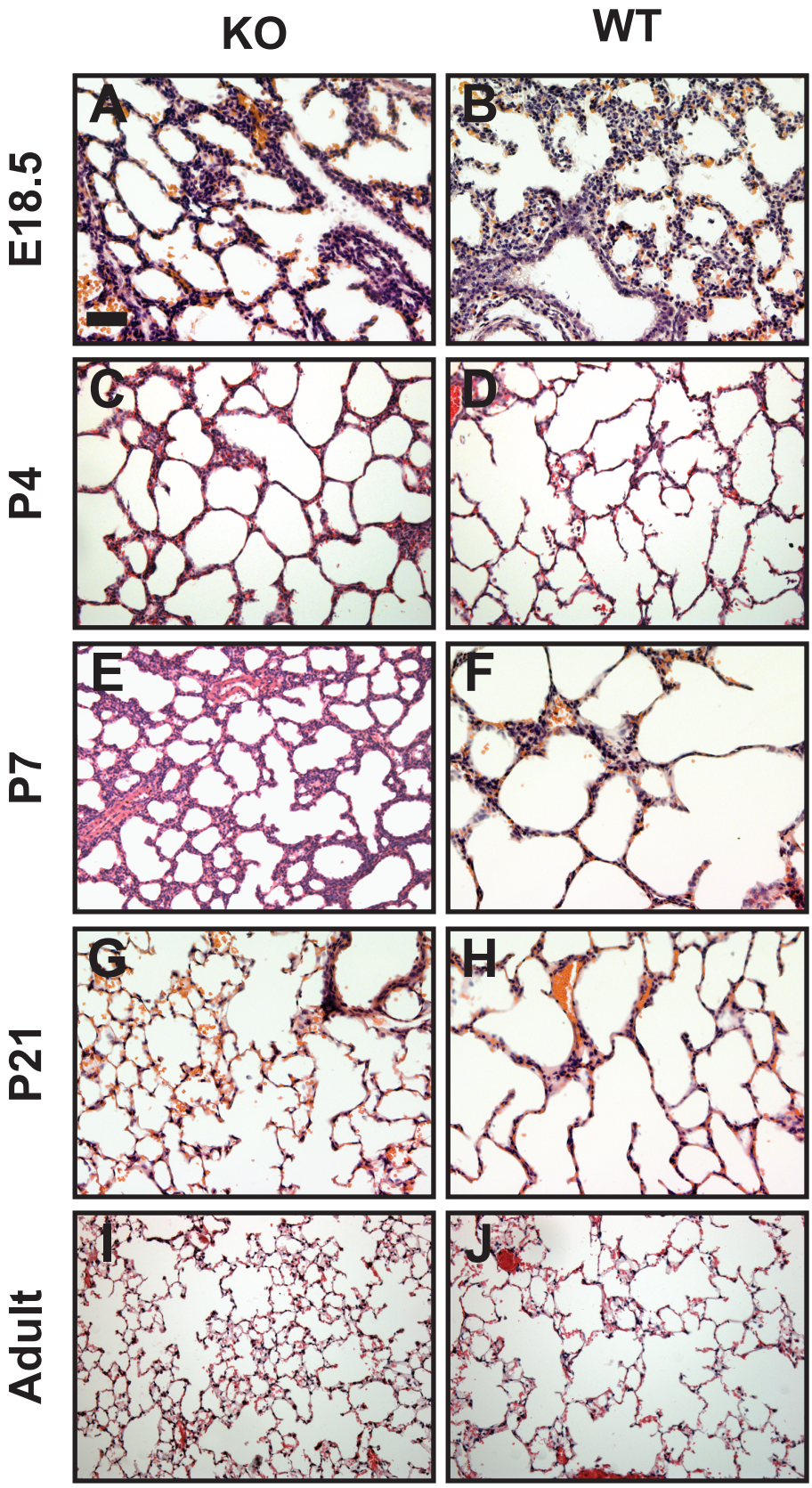
KO
WT
E18.5
P4
P7
P21
Adult
A
B
C
D
E
F
G
H
I
J

Fig. 2-3. Gross alveolarization defects in *cby*$^{-/-}$ lungs. (A) Hematoxylin and eosin (H&E)-stained lung sections were obtained from *cby*$^{+/+}$ and *cby*$^{-/-}$ mice at ages E18.5, P4, P7, P21 and adult. Late during gestation and just after birth, *cby*$^{-/-}$ lungs are morphologically indistinct from *cby*$^{+/+}$ lungs. However, the *cby*$^{+/+}$ lung complexity increases as it matures, while the *cby*$^{-/-}$ lung maintains a simplified structure with larger alveolar saccular spaces. Images presented here are representative of at least 3 animals per genotype per age. Scale bars = 100 μm.

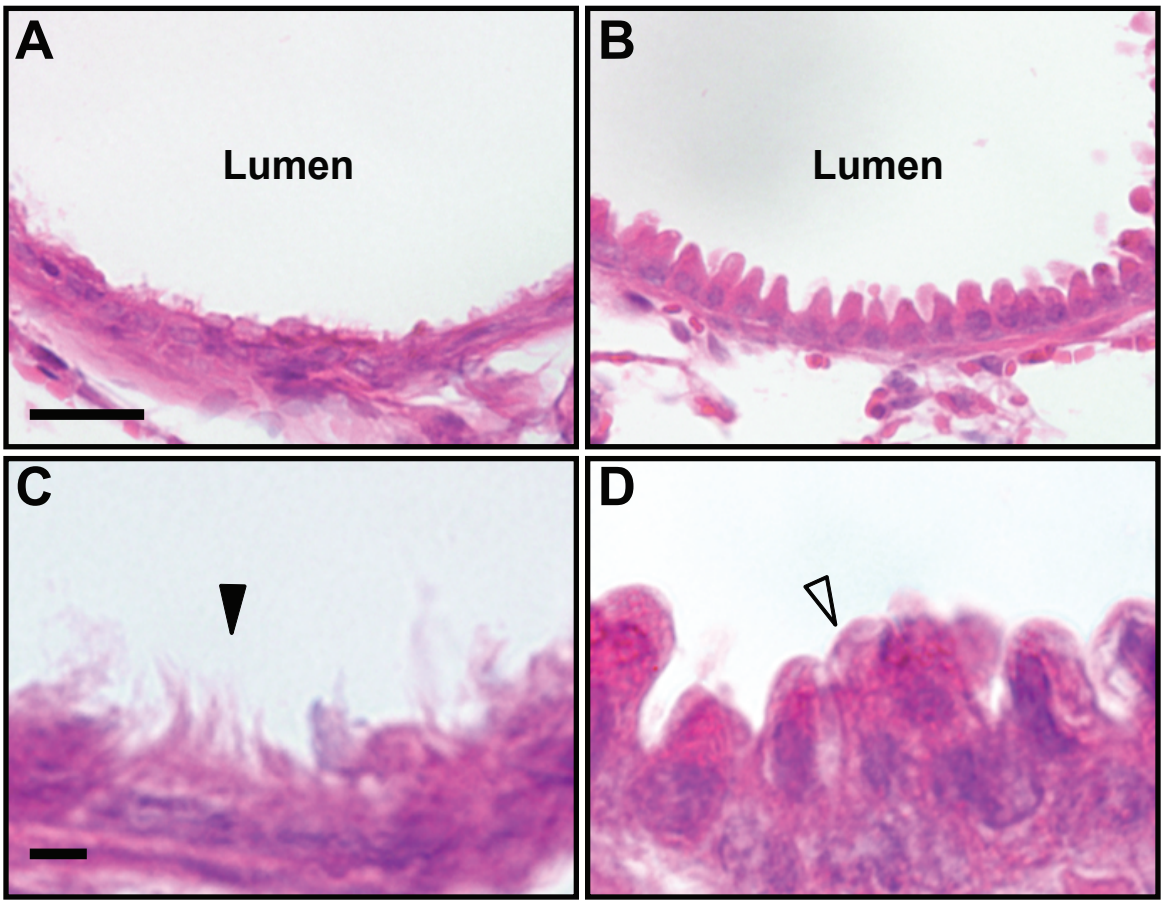

Fig. 2-4. Cby null mouse lungs exhibit morphological defects in airway epithelium. Lungs were harvested from adult wildtype (A,C) and cby null (B,D) mice at 1.5 months. H&E staining reveals abnormal Clara cell morphology in Cby-/- mice (B,D,white arrowhead) as well as the absence of ciliated cells compared to wildtype littermates (A,C, black arrowhead). Scale = 50μm (A,B) and 10μm (C,D).

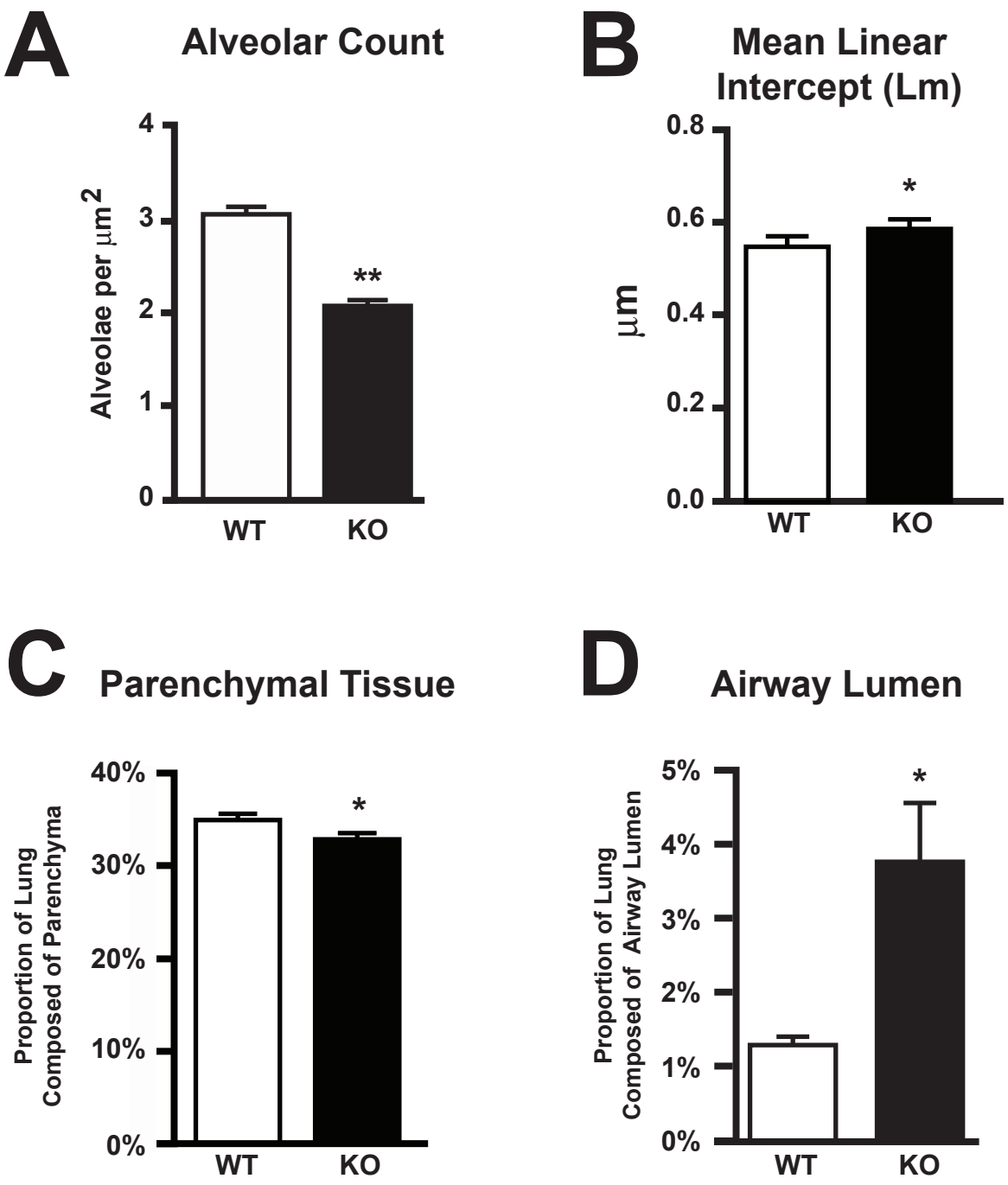

Fig. 2-5. Morphometric analysis of structural defects in the adult mouse lung. Morphometric analysis of air-exchanging parameters for adult Cby-/- lungs vs. Cby+/+ controls was performed. The alveolar saccules per μm2, inter-airspace wall distance (LM), proportion of the lung composed of parenchymal tissue, and airway luminal area relative to the total lung area were analyzed in the lungs from 10- to 13-week-old Cby-/- (KO; n = 4) and Cby+/+ (WT; n = 4) animals by two investigators blinded to genotype. Values are means ± SE. Student's t-test: **P < 0.001; *P < 0.05.

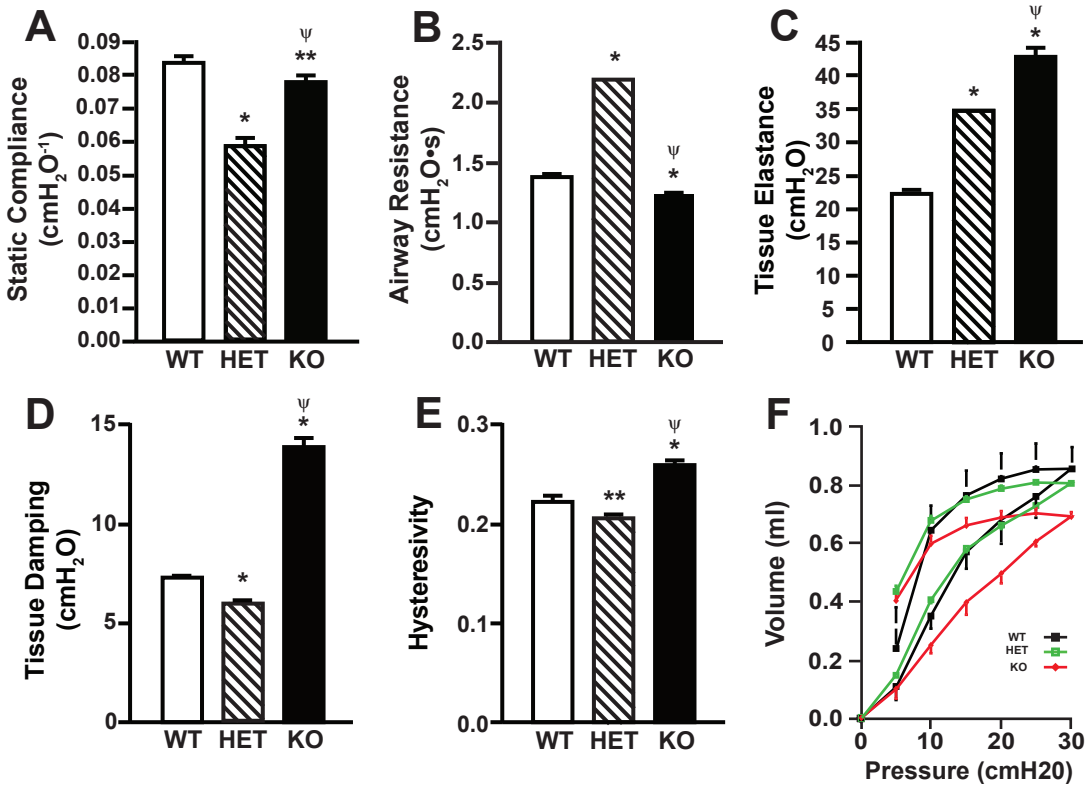

Fig. 2-6. Abnormal pulmonary mechanics in adult Cby-/- and Cby+/- animals. Static compliance (A), airway resistance (B), tissue elastance (C), tissue damping (D) and hysteresivity (E) were measured with positive end-expiratory pressure (PEEP) at 0 cm H2O in 10- to 13-week-old Cby-/- (KO; n = 5), Cby+/- (HET; n = 6) and control Cby+/+ (WT; n = 5) mice. Similar results were obtained at a PEEP of 3 cm H2O (data not shown). Values were determined by fitting the constant-phase model to measurements of respiratory input impedance (Zrs) from each genotype. All measures were normalized by multiplication by total lung capacity (TLC) except for static compliance that was normalized by division by TLC. Values are means ± SE. Bonferroni's post-test; *P < 0.001 vs. WT, **P < 0.05 vs. WT, ΨP < 0.001 vs. HET. PV curve analysis was performed with a PEEP of 0 cm H2O on adult Cby+/+ (WT; n = 5), Cby+/- (HET; n = 6) and Cby-/- (KO; n = 5) littermates (F). Similar results were obtained at a PEEP of 3 cm H2O (data not shown). All measures were normalized by division by total lung capacity (TLC). Values represent means ± SE. Student's t-test (performed on the entire data set): KO vs. HET, P < 0.001; KO vs. WT, P < 0.05; HET vs. WT, no statistically significant difference.

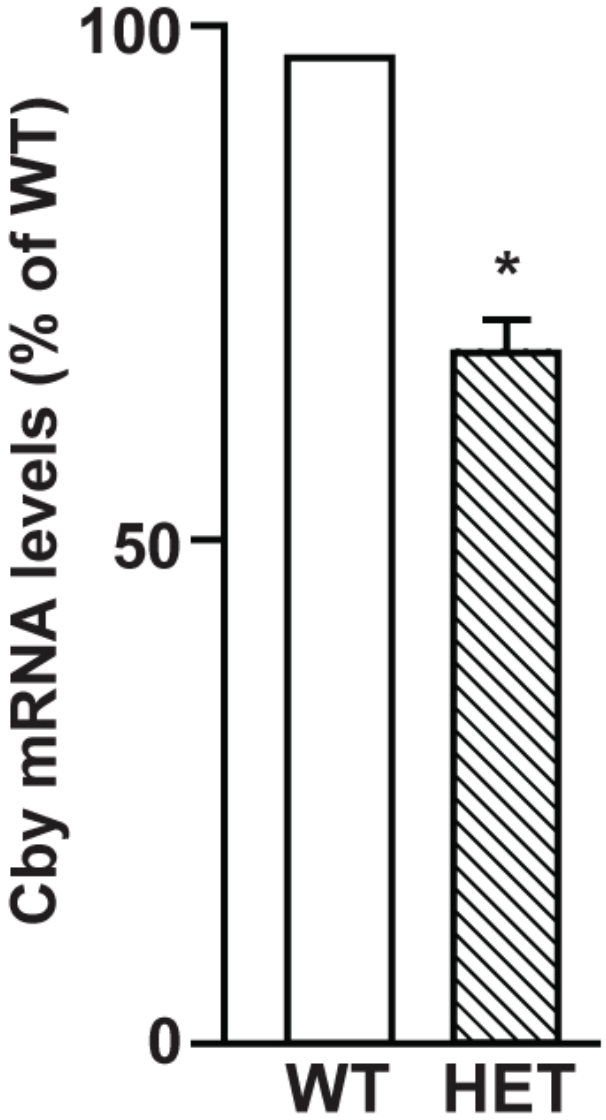

Fig. 2-7. Reduced cby expression in the lungs of cby+/- mice. Relative expression of cby mRNA in lungs was measured by quantitative real-time PCR for adult cby+/+ (WT) and cby+/- (HET) mice (n = 4 for each genotype) demonstrating a reduction of Cby expression levels in cby+/- lungs compared to cby+/+ lungs. Data are expressed as the percentage of WT controls and represent means ± SE. Student's t-test, *P < 0.001.

CHAPTER 3: THE ROLE OF CBY IN THE DIFFERENTIATION OF ALVEOLAR PNEUMOCYTES

Introduction

Canonical Wnt signaling has been shown to play an integral role in regulating the genetic choreography required for proper respiratory epithelial cell differentiation during lung development (Cohen et al., 2008; Li et al., 2009; Mucenski et al., 2003; Shu et al., 2002; Torday and Rehan, 2006, 2007; Zhang et al., 2008). More specifically, inappropriate Wnt pathway activation has been shown to result in severe defects in respiratory cell differentiation (Chilosi et al., 2003; Clevers, 2006; Moon et al., 2004; Okubo and Hogan, 2004). Data presented in the previous chapter suggest that the lung phenotype observed in *cby*$^{-/-}$ mice may be partly attributable to elevated Wnt pathway activity.

In a study by Okubo et al., investigators examined a transgenic mouse expressing a constituitively active amino-terminal deleted β-catenin-Lef1 fusion protein and demonstrated that high levels of Wnt signaling in lung epithelium inhibit the terminal differentiation of pulmonary-specific epithelial cell types as judged by cell morphology and gene expression (Okubo and Hogan, 2004). These mice exhibited no morphologically differentiated ATII cells or ATI cells as determined by electron microscopy. More recently, activation of canonical Wnt signaling has been shown to maintain lung progenitor cells, BASCs, in their undifferentiated state (Liu et al., 2006; Nusse, 2008; Reynolds et al., 2008; Zhang et al., 2008), providing further confirmation

that aberrant Wnt activity disrupts the maturation of lung cells during development. Consistent with these data, two independent *in vitro* studies demonstrated that loss of Cby results in differentiation defects in cardiomyocytes (Singh et al., 2007) and adipocytes (Li et al., 2007), suggesting that Cby promotes differentiation through inhibition of Wnt signaling.

To test the hypothesis that loss of Cby-mediated control of Wnt activity disrupts the developmental potential of respiratory epithelial cells, we examined molecular markers of differentiation in specific cell types in the airway and peripheral epithelium.

Materials and Methods

Immunohistochemistry

Immunohistochemical (IHC) staining was performed on paraffin-embedded sections. This method employed the use of the chromagen diaminobenzidine tetrahydrochloride (DAB) to detect the secondary antibody signal. Lung sections were deparaffinized and rehydrated through Histo-Clear and graded alcohol series as described above (Chapter 2). Tissues were then rinsed in tap water followed by a 20min incubation in PBST(X) (0.01M PBS, 0.5% Triton X-100) at room temperature. Because this detection method uses a horseradish peroxidase (HRP)-based system, endogenous peroxidase was quenched by incubating slides in H_2O_2 for 15min at room temperature. Slides were rinsed 2 times for 5min (2x5min) in 0.01M PBS and incubated in 0.1M sodium citrate (pH 6) in the microwave for antigen retrieval using the following format: 1 min at full power (1100watts), 2min at 20% power and a final incubation of 2min at 20% power.

Slides were allowed to cool for 20min at room temperature and were washed 2x5min in PBS.

For IHC staining with mouse monoclonal antibodies, we used the VECTOR® M.O.M.™ Immunodetection Kit (Vector Laboratories). A working solution of M.O.M.™ Mouse Ig Blocking Reagent was prepared by adding 90µl stock solution to 2.5ml PBS. Slide sections were incubated at room temperature for 1hr in working solution followed by 2x5min PBS wash. Tissue sections were incubated for 5min in a working solution of M.O.M.™ diluent prepared by adding 600µl of the manufacturer's supplied protein concentrate stock solution to 7.5ml of PBS. The primary antibody was diluted in the prepared diluents and tissue sections were incubated for 1hr at room temperature, followed by a 2x5min PBS rinse. Tissues were incubated for 1hr at room temperature in M.O.M.™ biotinylated anti-mouse IgG reagent which was prepared by adding 10µl of stock solution to 2.5ml of the M.O.M. diluent prepared above. Slides were rinsed with PBS 2x5min, followed by a 45min room temperature incubation of the tissue sections in VECTASTAIN® ABC Reagent prepared according to manufacturer's instructions (90µl Reagent A, 90µl Reagent B, 2.5ml PBS; allowed to stand 30min before use). Tissue sections were washed 2x5min in PBS and sections were incubated in ImmPACT DAB peroxidase substrate solution supplied by the manufacturer and allowed to develop until a brown substrate appeared. The reaction was terminated by immersion in water. Tissues were counterstained for 3min in a 33% solution of hematoxylin in water, rinsed and dehydrated through a series of ethanol gradations and incubated in Histo-Clear prior to mounting with permount (Fisher).

Immunofluorescence

Paraffin sections: Slides were deparaffinized and rehydrated to water as described above, followed by antigen retrieval in sodium citrate (pH 6) and triton extraction in PBST(X) also as stated. Slides were blocked for 15min at room temperature in PBST (0.5% Tween-20, 0.01M PBS) with 5% bovine serum albumin (BSA) and 5% source species serum of the secondary antibody used. For most antibodies, normal goat serum (NGS) was used. A diluent was prepared consisting of PBST and 5% BSA into which the primary antibody was diluted. Slides were incubated in the primary antibody mixture for 75min at room temperature, followed by a 2x5min rinse in PBS. Fluorescently-labeled secondary antibody was diluted into the premade diluent to a 1:500 concentration and slides were incubated for 30min at room temperature, followed by a 2x5min PBS wash. Slides were then incubated 2min at room temperature in a 1:5000 dilution of DAPI in 0.01M PBS, followed by a 1x5min PBS wash. Slides were then dried and coverslips were mounted with Fluormount-G (Southern Biotech) and stored in the dark.

Frozen sections (pre-fixed and sucrose-treated): Inflation-fixed lungs were removed and frozen sections were prepared for immunofluorescence by soaking in a solution of 30% sucrose in 0.01M PBS (pH 7.4) for 24h at 4ºC. Lungs were then embedded in freezing medium (Cryogel, Electron Microscopy Sciences) in cryomolds at -80ºC for sectioning. Tissues were sectioned, mounted on slides and allowed to air-dry for 15min. Slides were rinsed 2x5min in PBS and blocked as stated above. The remaining steps were followed as stated above.

Frozen sections (unfixed samples): Fresh, unfixed lung tissues were embedded in cryomolds with Cryogel and flash-frozen in isopentane pre-cooled in liquid nitrogen. After sectioning, tissues were mounted on slides, warmed at room temperature for 15min

and post-fixed in ice cold 4% methanol-free formalin. Slides were washed 2x5min in PBS prior to Immunostaining as stated above.

Antibodies

Primray antibodies used were: Cby (1:500, rabbit polyclonal) (Voronina et al., 2009), histone H3 (1:500, rabbit polyclonal, Sigma), pro-SpC (1:500, rabbit polyclonal, kindly provided by Avanash Chander, Stony Brook University Hospital), CCSP (1:500, goat polyclonal, kindly provided by Barry Stripp, University of Pittsburgh), aquaporin 5 (1:500, rabbit polyclonal, Sigma), acetylated α-tubulin (1:500, mouse monoclonal, Sigma), and β-catenin (1:500, mouse monoclonal, BD Transduction Laboratories). The fresh frozen method was used for the Cby and acetylated α-tubulin antibodies, while frozen, pre-fixed sections were used for all other antibodies, except for PCNA (1:1000, mouse monoclonal, Sigma) for which IHC was used. AlexaFluor 488 and 568 (Invitrogen) secondary antibodies were used at a 1:500 dilution for immunofluorescent imaging. Anti-mouse biotinylated secondary antibodies were used for IHC.

Transmission Electron Microscopy

All animals were treated strictly in accordance with NIH guidelines for the care and use of laboratory animals, and the protocols used were approved by the Institutional Animal Care and Use Committee at the State University of New York at Stony Brook. Samples used for transmission electron microscopy (TEM) were processed using standard techniques that are briefly outlined below. Mice were anesthetized intraperitoneally with 100mg/kg ketamine (Fort Dodge Animal Health, Fort Dodge, IA) and 20mg/kg xylazine (Lloyd Laboratories, Shenandoah, IA) and perfused transcardially

with 2% paraformaldehyde and 2% EM grade glutaraldehyde in 0.01M PBS buffer (pH7.4). After postfixing overnight in the perfusion fixative, samples were then placed in 2% osmium tetroxide in 0.01M PBS, dehydrated in a graded series of ethyl alcohol and embedded in Durcupan resin. Ultrathin sections of 80nm were cut with a Reichert-Jung Ultracut E Ultramicrotome and placed on formvar coated slot copper grids. Sections were then counterstained with uranyl acetate and lead citrate and viewed with a FEI Tecnai12 BioTwinG^2 electron microscope. Digital images were acquired with an AMT XR-60 CCD Digital Camera system and compiled using Adobe Photoshop.

Results

Ultrastructural analysis reveals abnormal differentiation of alveolaer pneumocytes.

The gross morphological defects observed in the peripheral lung at the light microscopic level suggest differentiation defects in alveolar pneumocytes. Furthermore, as these defects correspond to elevated Wnt activity, we predicted ATII development to be disrupted, accompanied by subsequent ATI developmental defects. In order to examine this, we analyzed the subcellular architecture of the alveolae using transmission electron microscopy.

At the ultrastructural level, although cuboidal ATII cells were observed throughout the peripheral lung epithelium in both genotypes (**FIG. 3-1, A-D**), *cby*$^{-/-}$ cells contain an abnormal abundance of lamellar bodies, the subcellular compartments in which surfactant proteins are incorporated (**FIG. 3-1, B,D**) (Baritussio et al., 1992). While it is difficult to draw solid conclusions from this particular observation, it does suggest elevated production of a differentiation marker – the surfactant protein – that is characteristic of

the ATII cell. There appears to be a slight elevation in the number of interstitial fibroblasts in the *cby*$^{-/-}$ alveolar pneumocytes, which could suggest delays in differentiation due to Wnt elevation, as Wnt pathway elevation has been associated with idiopathic pulmonary fibrosis (Moon et al., 2004; Morrisey, 2003; Selman and Pardo, 2006). It is important to note, however, that there is no evidence of fibrosis in *cby*$^{-/-}$ lungs, so the increase in interstitial fibroblasts may too mild to lead to a fibrotic phenotype, though it may suggest developmental immaturity.

In the *cby*$^{+/+}$ lung, ATI cells, unlike the cuboidal ATII cells, are composed of a thin, squamous structure, encompassing a large surface area. By contrast, ATI cells of the *cby*$^{-/-}$ lung exhibit a thick, disorganized morphology. While not cuboidal, these cells are thicker than typical ATI cells, suggesting a transient state of differentiation between that of the ATII progenitor and the ATI terminally differentiated state. A similar transient cell type was observed by Evans et al. in response to NO2 induced lung injury models in which they observed the transient expression of pneumocytes expressing characteristics of both ATI and ATII cells (Evans et al., 1975; McElroy and Kasper, 2004).

Cby$^{-/-}$ mice exhibit differentiation defects in the alveolar epithelium.

To examine whether the morphological abnormalities exhibited in alveolar pneumocytes were due to differentiation defects, adult lungs were stained for immunofluorescent differentiation markers for ATI and ATII cells (**FIG. 3-2**). Immunostaining revealed abnormal expression of the type II cell (ATII) marker, Pro-SpC, compared to controls. Conversely, expression for the terminally differentiated type I cell (ATI) marker, aquaporin 5 (Aqp5), was reduced in *cby*$^{-/-}$ mice compared to controls,

also suggesting a differentiation defect, since ATI cells make up approximately 95% of the surface area of the normal adult lung and are believed to be the terminally differentiated cell type arising from its ATII progenitor (Kaplan, 2000; McElroy and Kasper, 2004; Williams, 2003). Quantitative evaluation of SpC by pixel counts of immunofluorescent images showed significant differences between control (1,437 ± 477) and *cby*$^{-/-}$ lungs (47,660 ± 4796). Evaluation of Aqp5 also showed significant differences between control (34,320 ± 8715) and *cby*$^{-/-}$ lungs (4,454 ± 2,066).

Punctate localization of Cby is evident in alveolar progenitor cell types during development.

One of the most dramatic phenotypes observed in *cby*$^{-/-}$ lungs thus far, appears related to disruptions in the differentiation of ATII progenitor cells. We, therefore, examined the subcellular localization in mouse lungs using a polyclonal anti-Cby antibody generated in our laboratory (Voronina et al., 2009). Immunostaining revealed punctate extra-nuclear Cby localization in the parenchyma of developing lungs (**FIG. 3-3, A-L**). The expression pattern revealed more abundant staining in embryos (E15.5 and E17.5) (**FIG. 3-3, D-F, J-L**) and neonates (P0) (**FIG. 3-3, G-I**), though no punctate foci of Cby protein were evident in the peripheral lung of adult mice (data not shown). It is difficult to determine the exact cell type in which Cby is detected given the complexity of the developing parenchyma, although it appears that Cby is expressed in alveolar progenitor cells, most likely ATII.

The punctate nature of Cby distribution suggests that Cby could be localized at the centrosomes in the developing lung. This is supported by recent findings by Voronina, et

al. that show that Cby localizes to the base of monocilia and centrosomes in cultured MDCK2 cells (Voronina et al., 2009). The centrosome is the major microtubule organizing center (MTOC) and is responsible for nucleating and organizing the microtubule cytoskeleton (Steffen et al., 1994; Vinogradova et al., 2005). The centrosome usually consists of a pair of mother and daughter centrioles which are organized as short cylinders of nine triplet microtubules. The building block of a microtubule is the tubulin subunit, a heterodimer of α- and β-tubulin. Both of these monomers are found in all eukaryotes, and their sequences are highly conserved. Acetylated α-tubulin is present in various microtubule structures and plays a role in stabilizing the structures of all microtubules ((Nogales, 2000; Piperno et al., 1987)Ref).

Immunostaining with the anti-acetylated α-tubulin antibody revealed a punctate expression pattern in the developing ATII alveolar pneumocytes which colocalized with Cby, suggesting that Cby is associated with centrosomes (**FIG. 3-3, D-L**). *Cby*$^{-/-}$ mice, however, did not show an obvious aberrant pattern for acetylated α-tubulin (**FIG. 3-3, B-C**).

Discussion

Immunostaining results revealed deficiencies in cytodifferentiation as *cby*$^{-/-}$ mice exhibit abnormal expression of epithelial cell differentiation markers in the alveolar pneumocytes. The terminally differentiated, squamous ATI cell makes up approximately 95% of the surface area of a normal adult mouse lung, while its progenitor, the ATII cell, while more abundant in number, are cuboidal in shape and represent a much smaller proportion of the surface area (Kaplan, 2000; McElroy and Kasper, 2004; Williams,

2003). *Cby*$^{-/-}$ mice abnormally express the ATII marker, Pro-SpC, which is consistent with the abnormal abundance of lamellar bodies incorporating surfactant protein C (**FIG. 3-2**). This observation is in good agreement with earlier findings correlating elevated Wnt pathway activity with abnormal ATII morphology (Okubo and Hogan, 2004). Conversely, there is a reduced expression of the terminally differentiated ATI cell marker, Aqp5, also consistent with ultrastructural analysis which exhibits abnormal ATI and ATII morphology (**FIG. 3-2**).

Cby immunostaining in the developing peripheral lung reveals colocalization with subsets of cytoplasmic microtubules in ATII cells as indicated by acetylated-α-tubulin localization. The acetylated-α-tubulin expression pattern likely corresponds to centrioles, a major component of the MTOC. Microtubules are required for many well characterized functions in eukaryotic cells, including the movement of chromosomes in mitosis and meiosis, intracellular transport, establishment and maintenance of cellular morphology, cell growth, cell migration and morphogenesis in multicellular organisms (Nogales, 2000). Acetylated α-tubulin is present in various microtubule structures and plays a role in stabilizing the structures of all microtubules (Piperno et al., 1987). Taken together, these data suggest that Cby may play a role in regulation of the microtubule cytoskeleton, as indicated by the structural defects in lung architecture and cell structure in *cby*$^{-/-}$ mice, suggesting an additional role for Cby during alveologenesis.

Based on this evidence, it is apparent that the phenotype observed is not solely a consequence of loss of Cby-mediated Wnt regulation, as Cby may play a role at centrosomes, for example in the maintenance of cytoskeletal structure. On the other hand, Wnt is also known to regulate microtubules with some components localizing to

centrosomes and basal bodies. We, therefore, cannot exclude the possibility that centrosomal Cby controls beta-catenin signaling.

Though the role of cby during alveolarization remains ambiguous, what appears abundantly clear is the fact that the defect resulting from loss of cby is a consequence of an early developmental deficiency. More specifically, the *cby*$^{-/-}$ phenotype seems to result from the discontinuity between stages in the developmental cascade, resulting in an alteration of alveolar cell types (Cohen and Larson, 2008). During lung organogenesis, the lungs contain transit amplifying (TA) cells, which are intermediate progenitor cell types between dedicated stem cells and their final differentiated progeny, and capable of self-renewal over the short term and give rise to one or more differentiated cell types (Rawlins and Hogan, 2006). Alveolar TA cells, such as ATII cells, are progressing through temporal states that, when disrupted – whether through Wnt-mediated delays or loss of a cell-cycle mediated role for cby, for example – the terminal differentiation state cannot be reached. Because of the limited differentiation window of the alveolar stage, it is possible that the delay in progression doesn't allow normal lung organogenesis to proceed beyond a defined developmental timeline. In other words, all or part of the lung remains in a fetal temporal state, significantly different from that of the terminally differentiated tissue (Cohen and Larson, 2008). This is supported by the delayed alveolar development observed histologically (**FIG. 2-3**) and the altered distribution of differentiation markers in the adult lung (**FIG. 3-2**) suggesting a developmentally immature adult lung.

The next chapter examines the phenotype of the bronchial respiratory epithelium and the possible roles Cby may play in other microtubule-related structures in the lung.

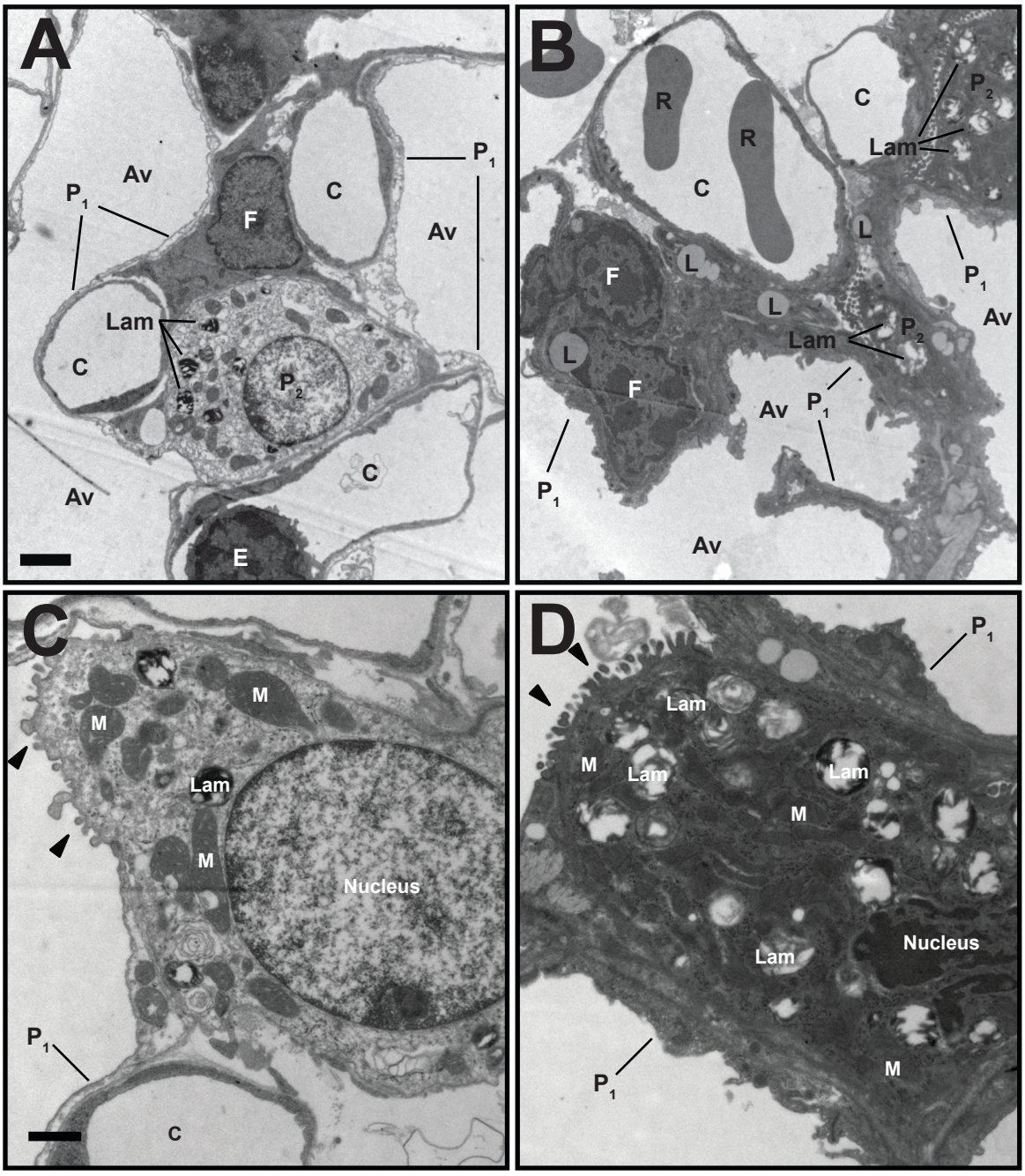

Figure 3-1. Cby null mice exhibit ultrastructural defects in the alveolar epithelium. Electron microscopy was performed on adult lung tissue from Cby-/- (B,D) and control (A,C) mice. Alveolar pneumocytes were compared in cby null mice (B,D) to controls (A,C), demonstrating morphological differences in type I (P1) and type II (P2) pneumocytes. Arrowheads denote microvilli associated with surfactant secretion. P1=Type I pneumocytes, P2=Type II pneumocytes, Lam=Lamellar bodies, C=Capillaries, R=Red blood cells, Av=Alveolar airspace, M=Mitochondria, L=Lipids, F=Interstitial Fibroblast, E=Endothelial cell. Scale = 5µm (A,B), 2µm (C,D), 4µm (E,F), and 500nm (G,H).

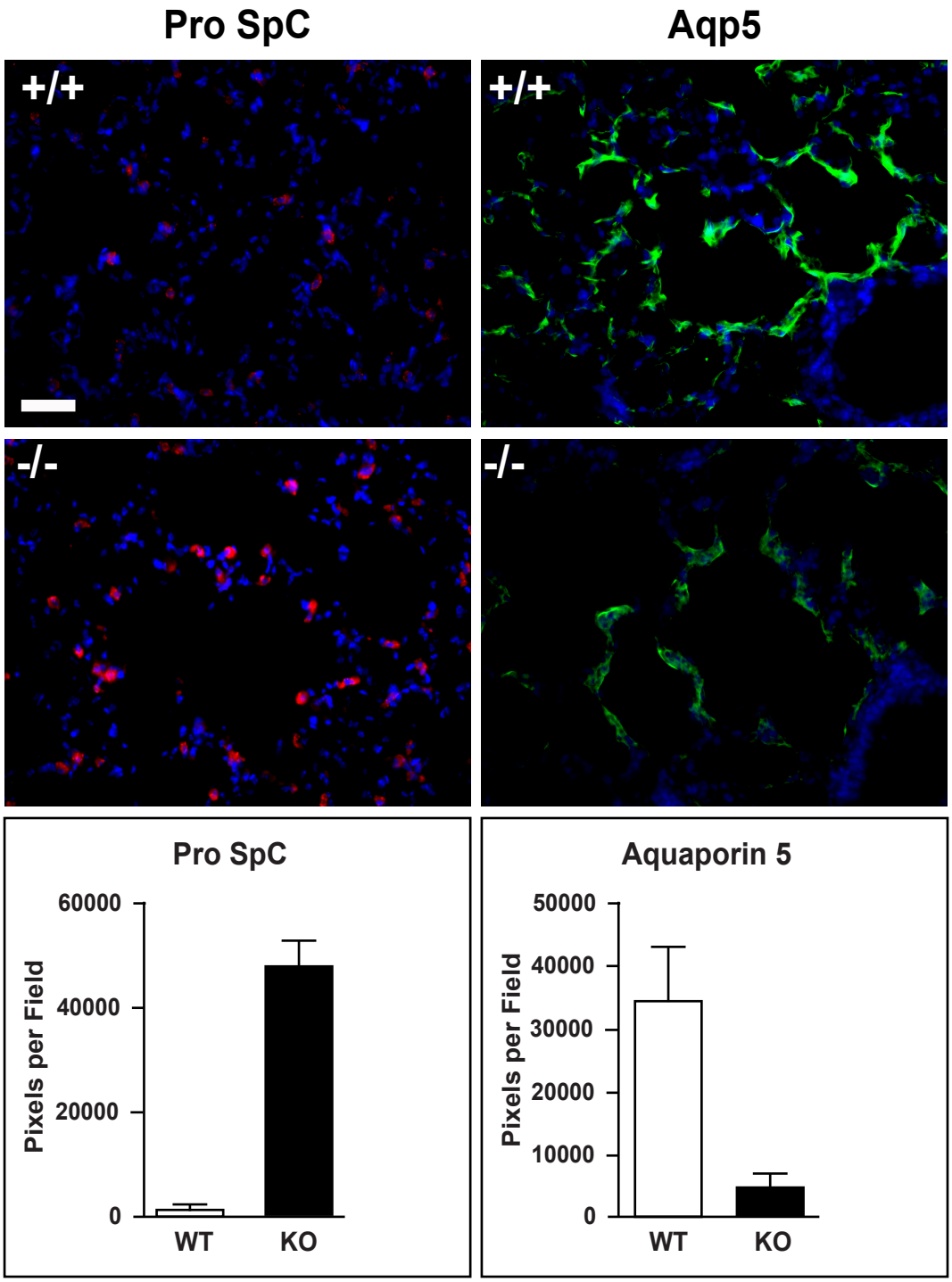

Figure 3-2. Cby null mouse lungs exhibit differentiation defects in alveolar pneumocytes. Lungs were harvested from adult WT and KO mice at 1.5 months. Peripheral lung sections were labeled with antibodies against Pro-SpC (red) and Aqp5 (green). Slidebook software was used for pixel counting of Pro-SpC and Aqp5 in a series of slides. Values represent means ± SE. Student's t-test: *P < 0.001; **P < 0.05. Scale = 50μm.

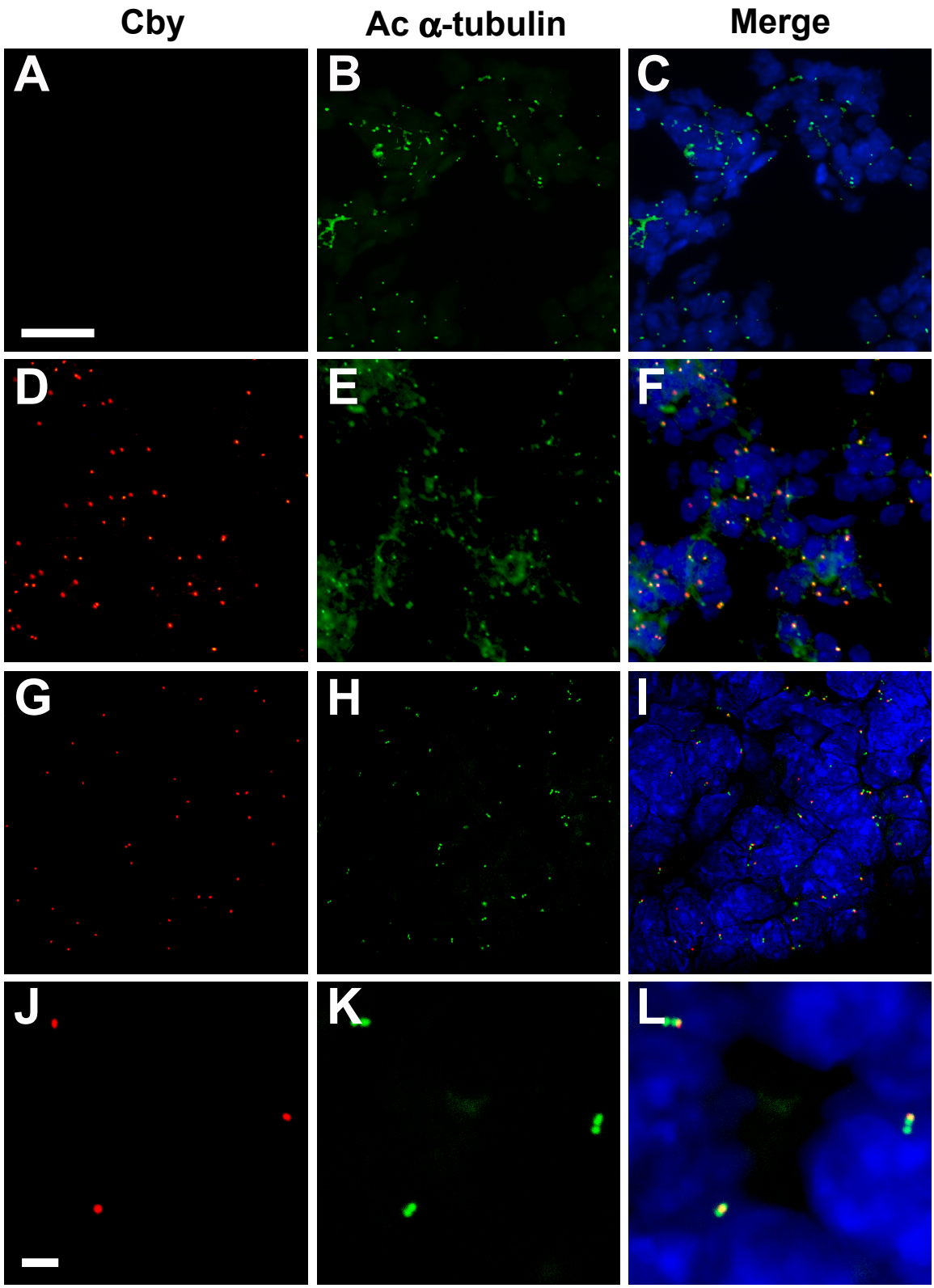
Cby
Ac α-tubulin
Merge
A
B
C
D
E
F
G
H
I
J
K
L

Figure 3-3. Cby expression colocalizes with centrosomal markers in alveolar progenitor cells. Peripheral lung sections from *cby*$^{-/-}$ (A-C) and *cby*$^{+/+}$ (D-F, J-L) embryonic mice and neonates (G-I) were double stained with antibodies against acetylated α-tubulin (green; B,E,H,K) and Cby (red, A,D,G,J), and the merged images of acetylated α-tubulin and cby are shown (C,F,I,L). *Cby*$^{-/-}$ E17.5 embryos are shown (A-C) and compared to age matched wildtype controls (D-F) to show specificity of cby antibody staining. P0 pups are shown (G-I) revealing the same punctate staining colocalizing with centrosomal markers. Enlarged images of E15.5 embryos (J-L) show detailed colocalization. Scale: A-F, 10μm; J-L, 2μm.

CHAPTER 4: A DEVELOPMENTAL ROLE FOR CBY IN MULTICILIATED EPITHELIAL CELLS

Introduction

The developmental defects observed in the alveolar epithelium of *cby*$^{-/-}$ mice suggested impairment in the differentiation pathway, leading to immature alveolae. Evidence of elevated Wnt activity suggests that this is due in part to the loss of Cby-mediated regulatory control. However, immunofluorescent expression data indicate another potential role for Cby that exists outside the signaling pathway, whereby Cby is associated with centrosomes in the microtubule-organizing center.

Histological analysis of *cby*$^{-/-}$ airways shows morphological defects in airway epithelial cell types, one of the most striking is that of the paucity of cilia, a physiological marker of terminally-differentiated cell types. Furthermore, centrioles are a major component of basal bodies, the source from which cilia grow (Dawe et al., 2007). Cby has been shown to localize to basal bodies of developing primary cilia in MDCK2 cultured cells and to the base of cilia in the nasal epithelium in mice (Voronina et al., 2009), suggesting a similar role in the epithelium of multiciliated cells in conducting airways in the mouse lung. In the following chapter, the role of Cby in the development of airway epithelial cells is analyzed.

Materials and Methods

Scanning Electron Microscopy

For scanning electron microscopy (SEM) studies, adult lungs were inflation-fixed

with 4% methanol-free formalin as described above (Chapter 2), and proximal lung tissue was removed. The tissue was then dehydrated using a graded ethanol series to 100%. Samples were then transferred to a fume hood where they were incubated for 15min each through a graded series of ethanol-hexamethyldisilazane (HMDS; Electron Microscopy Sciences) mixtures to 100% HMDS. The specimens were air-dried, mounted on scanning EM stubs, and sputter coated with gold before examination with a scanning electron microscope (LEO1550; Carl Zeiss, Inc.) at 10 kV using a back scatter detector (Robinson). Images were processed using Photoshop.

Harvesting mouse tracheal epithelial cells (MTECs)

Culture media and supplements. Supplements were from Sigma-Aldrich unless indicated. "Hams F-12 pen-strep" is Ham's F-12 media with 100 U/ml penicillin and 100 μg/ml streptomycin. "MTEC basic media" is DMEM-Ham's F-12 (1:1 vol/vol), 15 mM HEPES, 3.6 mM sodium bicarbonate, 4 mM L-glutamine, 100 U/ml penicillin, and 100 μg/ml streptomycin. "MTEC/Plus" is MTEC basic media supplemented with 10 μg/ml insulin, 5 μg/ml transferrin, 0.1 μg/ml cholera toxin, 25 ng/ml epidermal growth factor (Becton-Dickinson), 30 μg/ml bovine pituitary extract, 5% FBS, and freshly added 0.01 μM retinoic acid. "MTEC/NS" is MTEC basic media supplemented with 2% NuSerum (Becton- Dickinson) and freshly added 0.01 μM retinoic acid.

MTEC isolation. Tracheal cells from *cby*$^{+/-}$ C57BL/6 adult mice were used. Mice were euthanized and then briefly immersed in 70% ethanol (avoiding airway submersion). With the use of a sterile technique, tracheas were resected from the larynx to the bronchial main branches and collected in ice-cold Ham's F-12 pen-strep. In a

tissue culture hood, muscle and vascular tissues were dissected from tracheas in cold media. Tracheas were washed with media, opened longitudinally, and then incubated in Ham's F-12 pen-strep containing 1.5 mg/ml pronase (Roche Molecular Biochemicals) for 18 h at 4°C. The tube was inverted several times, then put on ice, and FBS was added to a final concentration of 10%. The tracheas were inverted 12 times, transferred to another tube of Ham's F-12 pen-strep with 10% FBS, inverted again, placed in one-third tube of media, inverted to further release cells, and then discarded. Contents of the three tubes were pooled and collected by centrifugation at 400 *g* for 10 min at 4°C. Cells were resuspended in 200 μl/trachea of Ham's F-12 pen-strep containing 0.5 mg/ml crude pancreatic DNase I (Sigma) and 10 mg/ml BSA. The cells were then incubated on ice for 5 min, centrifuged at 400 *g* for 5 min at 4°C, and resuspended in MTEC basic media with 10% FBS. After incubation in tissue culture plates for 3–4 h in 5% CO2 at 37°C to adhere fibroblasts, nonadherent cells were collected by centrifugation, resuspended in 100–200 μl MTEC/Plus per trachea, and counted. No attempt was made to achieve a single cell suspension from cell clumps. Cell viability was determined by trypan blue exclusion.

In vitro culture of MTECs. Supported polycarbonate and polyester porous (0.4 μM pores) membranes (Transwell and Transwell Clear; Corning-Costar) were coated with filter-sterilized 50 μg/ml type I rat tail collagen (Becton-Dickinson) in 0.02 N acetic acid using 1.0 ml/cm^2 membrane for 18 h at 25°C. Membranes were seeded to a final plating density of 1.00 x 10^5 cells/cm^2 and incubated with MTEC/Plus filling upper and lower chambers in 5% CO_2 at 37°C. Media were changed every 2 days until the cells reached confluence. Media were then removed from the upper chamber to establish an air-liquid

interface (ALI), and lower chambers only were provided fresh MTEC/NS media every 2 days. Cells on Transwell Clear membranes were monitored by inverted-phase microscopy.

Immunofluorescence

Mouse tissues were harvested and frozen fresh followed by postfixing in 4% methanol-free formalin and prepared for immunofluorescent staining as previously described (Chapter 3). Membranes in the transwells were fixed with 4% methanol-free formalin for 10min followed by 3x5min rinses with PBS. Wells that were not immediately prepared for immunostaining were stored in PBS at 4°C.

Membranes were cut away from the transwells and cut into quadrants. Each membrane section was placed in a separate well in a 96-well plate for immunostaining. Sections were rinsed 3x5min in PBST(X) and blocked for 60min at room temperature in PBST(X) with 5% BSA and 5% normal goat serum (NGS). Primary antibodies were diluted in a solution of 5% BSA and PBST(X) and incubated with membrane sections for 60 min at 37°C. Sections were rinsed 3x5min with PBST(X) and incubated with fluorescent secondary antibodies (diluted as stated above) for 30 min in the dark at room temperature. Sections were rinsed 2x5min in PBS and incubated 1:5000 in DAPI in the dark for 2 min at room temperature. Sections were rinsed once more for 5 min in PBS, mounted on slides with Fluoromount-G (Southern Biotech), covered with coverslips and stored in the dark.

Immunohistochemistry

For immunohistochemistry with anti-Foxj1 antibody (generated using amino acids 1-117; kindly provided by Steve Brody of Washington University School of Medicine), the Vectastain "Elite" Kit for Mouse IgG (Vector Laboratories) with secondary antibody and ABC complex was used. Paraffin sections were prepared as previously described (Chapter 2). Nuclear unmasking was performed in 50mM Tris buffer (pH 9.5) as follows. Slides contained in coplin jars were boiled in the microwave for 3min at 100% power (1100W). Slides were then boiled intermittently for 30sec at a time with 30sec intervals for 5min at 20% power. Slides were then boiled at 20% power continuously for an additional 5min. Solution was allowed to cool to room temperature before immersion in 4.5% hydrogen peroxide in PBS for 5min to block endogenous peroxidase activity. Slides were then washed 2x5min in PBS. Non-specific binding was blocked with 2% NGS in PBS for 30min at room temperature in a humidified chamber. Foxj1 antibody was diluted 1:100 in the prepared blocking solution and added to sections. Slides were incubated 60min at room temperature in a humidified chamber. Slides were rinsed 2x5min in PBS.

Biotinylated secondary antibody against mouse IgG provided by the manufacturer was used at a dilution of 1:200 in the NGS blocking solution. Slides were incubated 30 min at room temperature in a humidified chamber. ABC reagent was prepared according to the manufacturer's instructions and allowed to stand 30min prior to incubating on the slides for 30 min (minutes be consistent) at room temperature. Slides were washed 2x5min in PBS. DAB substrate solution was added to sections as previously stated and development was monitored for brown color (1-3 minutes). Slides were counterstained with hematoxylin, dehydrated to Histo-Clear and mounted on coverslips with Permount.

Antibodies

Antibodies used were: Cby (1:500, rabbit polyclonal) (Voronina et al., 2009), acetylated α-tubulin (dilution, mouse monoclonal, Sigma), CC10 (1:500, rabbit polyclonal; Santa Cruz) and Foxj1 (described above). The fresh frozen method was used for the Cby and acetylated α-tubulin antibodies, while frozen, pre-fixed sections were used for all other antibodies, except for Foxj1 for which IHC was used.

Results

Ultrastructural analysis reveals abnormal differentiation of proximal airway epithelium.

The gross morphological defects observed in the peripheral lung at the light microscopic level suggest differentiation defects in the respiratory epithelium. Of particular interest is the marked reduction of motile cilia in *cby*$^{-/-}$ lung accompanied by the dysmorphic Clara cell phenotype. In order to further explore this, we analyzed the subcellular architecture of conducting airways using transmission electron microscopy.

Examination of the proximal airways reveals ultrastructural abnormalities in epithelial cell types (**FIG. 4-1, A-F**). In the *cby*$^{+/+}$ airways, ciliated cells are clearly distinguished from the non-ciliated cells with normally developed cilia at the apical surface of ciliated cells (**FIG. 4-1, A,C**). The *cby*$^{-/-}$ cells are less easily distinguished, however, as the ciliated cell types have sparse and stunted ciliary projections (**FIG. 4-1, B,D**). Underdeveloped cilia appear along the apical surface of these cells, suggesting a cell type that lacks terminal differentiation compared to the wildtype control. Although, the structural integrity of the cilia themselves, however, does not appear to be disrupted,

as the axoneme retains its 9+2 configuration (**FIG. 4-1, E**), there appear to be abnormalities in basal body localization, consistent with observations previously noted in the nasal epithelium of *cby*$^{-/-}$ mice (**FIG. 4-1, D)** (Voronina et al., 2009). The *cby*$^{-/-}$ Clara cell morphology is less distinguishable from its wildtype counterpart, but there are notable morphological dissimilarities. The *cby*$^{+/+}$ Clara cell is columnar in shape and its nucleus is located basally, with an orderly distribution among ciliated cell types. In contrast, *cby*$^{-/-}$ Clara cell morphology, while columnar, is less organized structurally. The location of the nucleus appears to vary from the medial to basal portion of the cell, while the boundaries separating the neighboring ciliated cells appears less distinct. While the hypersecretory phenotype is not as prominent as in the airway histological images presented earlier, there appear to be several secretory granules in the process of secretion in the *cby*$^{-/-}$ airway (**FIG. 4-1, F; arrowheads**) supporting the observation of hypersecretory activity.

In order to analyze epithelial cell surface disruptions and to visualize differences in clara and ciliated cell topography, we observed the proximal airways from adult *cby*$^{-/-}$ and *cby*$^{+/+}$ mice by scanning EM (**FIG. 4-2, A-C**). We found that the number of cilia is dramatically decreased in the *cby*$^{-/-}$ large airway when compared with that from *cby*$^{+/+}$ controls, suggesting poor differentiation of ciliated cell types in *cby*$^{-/-}$ airways compared to their wildtype counterparts. Here, the dramatic morphology observed in airway histological sections (**FIG. 2-3**) is recapitulated in the *cby*$^{-/-}$ Clara cell (**FIG. 4-2, B,D)**. The Clara cells appear more prominent than those of the *cby*$^{+/+}$ controls, exhibiting the hypersecretory phenotype noted earlier as demonstrated by their dome-shaped phenotype.

***Cby*$^{-/-}$ mice exhibit differentiation defects in airway epithelial cells.**

To examine whether the morphological abnormalities exhibited are due to differentiation defects, adult lungs were immunostained for differentiation markers for ciliated and non-ciliated cell types in proximal airways of adult mouse lungs (**FIG. 4-3**). As previously stated, acetylated α-tubulin is a reliable marker for stabilized microtubules, a primary component of cilia (Piperno et al., 1987; Steffen et al., 1994). Staining for the ciliary cell marker acetylated α-tubulin was less abundant in *cby*$^{-/-}$ airways than in controls. Conversely, co-labeling with anti-CC10 antibody, a Clara cell marker, revealed increased marker expression in *cby*$^{-/-}$ airways, suggesting a poorly differentiated bronchial epithelium.

***Cby* localizes to the base of cilia in airway ciliated cells.**

Immunofluorescence data reveals that Cby is expressed in the cytoplasm of airway epithelial cells during development and in adulthood (**FIG. 4-4, A-I**). Co-labeling with acetylated α-tubulin revealed a colocalization pattern consistent with the results found in ATII cell staining. All cilia are extended from basal bodies, which are analogous to the mitotic centrioles, and migrate to the apical cell surface where acquisition of accessory structures follows (Dawe et al., 2007; You et al., 2004). At E15.5, Cby appears in the airway epithelial cells and co-localizes with mitotic centrioles prior to ciliary growth (**FIG. 4-4, A-C**). As airway development progresses, it is evident that Cby is associated with the basal bodies of developing cilia in the multiciliated cells of the airway epithelium. Cby is more abundantly expressed at the apical membrane of adult airway epithelial cells, specifically at the base of the cilia, an observation that is consistent with previous data demonstrating Cby expression at the base of cilia in the nasal epithelium

(Voronina et al., 2009). Similarly, cby is expressed in the trachea of adult mice (data not shown).

Normal expression of Foxj1 in *cby*$^{-/-}$ airways.

Examination of differentiation markers suggested that airway epithelial cells do not properly differentiate from non-ciliated progenitor cells to the differentiated multiciliated cell types (**FIG. 4-3**). Given the extra-nuclear localization of Cby and its association with ciliary basal bodies, it is likely that the morphological features of the *cby*$^{-/-}$ airway epithelium are attributable to a function for Cby that is not limited to its role as nuclear β-catenin inhibitor of the Wnt pathway. The presence of Cby at ciliary basal bodies, coupled with the disruptions in basal body positioning observed in *cby*$^{-/-}$ mice prompted us to examine regulators of genes involved in ciliogenesis. We therefore decided to examine the expression of the forkhead transcription factor, Foxj1 (formerly known as HFH-4), a major regulator of the ciliogenic program in multiciliated epithelial cells (You et al., 2004; Yu et al., 2008).

Foxj1 plays a key role in determining the ciliated cell fate in airway epithelial cells by promoting differentiation during late-stage ciliogenesis in airway cells when the cell is already committed to the ciliated cell phenotype. Thus, rather than directing commitment to the ciliated cell phenotye, Foxj1 appears to establish mechanisms for docking of basal bodies at the apical membrane and induction of program(s) of axoneme assembly (You et al., 2004).

In the lung, Foxj1 expression is restricted to the bronchial and bronchiolar epithelial cells and is initially detected in mice during the late pseudoglandular stage at E14.5. This

expression immediately precedes the appearance of cilia in Foxj1-positive cells (Brody and Williams, 1992; Brody et al., 1997). We therefore examined Foxj1 expression in developing (E15.5) and adult airways (**FIG. 4-5, A-D**). Immunostaining analysis revealed no difference in Foxj1 expression between the *cby*$^{-/-}$ or *cby*$^{+/+}$ airways at either stage of development, suggesting that Cby either functions downstream of Foxj1 during ciliogenesis, or is totally independent of FoxJ1.

Endogenous Cby is detected at the ciliary base of cultured mouse tracheal epithelial cells (MTECs).

Previously, Steve Brody et al. defined conditions for primary culture of MTECs that result in rapid proliferation and generation of a highly differentiated epithelium that nicely models native mouse tracheal epithelial cells (You et al., 2002). We therefore examined cultured MTECs at day 14 after conversion to air-liquid interface (ALI day 14) for their expression of endogenous Cby. Immunostaining analysis revealed that the Cby expression pattern is recapitulated in multiciliated airway epithelial cells and it is localized apically in multiciliated cells to the base of cilia. Z-axis reconstructed images of Cby and acetylated α-tubulin co-labeling show Cby as a dense band at the apical membrane beneath thick clumps of cilia (**FIG. 4-6, A-C**).

Discussion

Immunostaining results revealed deficiencies in cytodifferentiation as *cby*$^{-/-}$ mice exhibit abnormal expression of epithelial cell differentiation markers in the bronchial airways. Similar to the phenotype observed in the peripheral lung, histological and morphological defects of *cby*$^{-/-}$ mice correlated with altered expression of known markers

of airway epithelial cell differentiation. Immunostaining data revealed abnormal expression of CC10, a marker for non-ciliated Clara cells, progenitors to the terminally differentiated ciliated cell type. Conversely, these mice exhibit a significant reduction in the ciliary marker, acetylated α–tubulin.

However, ultrastructural analysis reveals structural defects that suggest deficiencies that are not solely related to cby's role as a nuclear Wnt pathway antagonist. In other words, Wnt activity has been involved in maintaining cells in an undifferentiated state, suggesting that elevated activity would disrupt the differentiation cascade, effectively impeding the switch from the Clara cell progenitor cell to the terminally-differentiated ciliated cell. Although histological and immunostaining data suggests an abnormal distribution of non-ciliated, Clara cells relative to ciliated cell types, transmission EM analysis reveals a distinct ciliated cell population, albeit, bearing a reduction in the number and size of the cilia themselves. While differentiation of the airway epithelium may be delayed due to Wnt hyperactivity, cby also appears to play a more direct role in ciliary development.

Immunostaining data shows that the Cby protein is located apically in airway epithelial cells in the trachea and in the proximal airways of the lung, localized specifically at the base of the cilia. This is also recapitulated in primary cultures of mouse tracheal epithelial cells. These data are consistent with previous findings that endogenous Cby was detected both at the base of ciliated cells in the nasal epithelium. Combined with cilia-related pathology associated with *cby*$^{-/-}$ mice, these data support the notion that Cby plays an integral role in ciliogenesis.

During ciliogenesis, mitotic centrioles migrate to the apical cell surface and dock with the cell membrane to form basal bodies, from which the cilia extend (Dawe et al., 2007; Sorokin, 1968). During the pseudoglandular stage, Cby expression is diffuse at the apical region of the cytoplasm of airway epithelial cells of ciliary lineage, colocalizing with centriolar proteins. As development proceeds, Cby is present as a dense band at the apical membrane beneath thick clumps of cilia (Figs). The apical expression of Cby in airway epithelial cells increases with developmental maturity, consistent with continued differentiation towards the ciliated cell phenotype.

Foxj1, a member of the forkhead/winged helix family of transcription factors, is implicated in centriole migration and/or docking and is expressed in ciliated epithelia. *Foxj1*-null mice have impaired ciliogenesis such that, although centriologenesis appears unimpaired, centriole migration fails (You et al., 2004). The *cby*$^{-/-}$ airway respiratory epithelium exhibits a similar, albeit less dramatic phenotype, whereby basal body polarity appears disrupted in the bronchial epithelium (**FIG. 4-1D**). This phenotype is also exhibited in *cby*$^{-/-}$ nasal epithelial cells (Voronina et al., 2009). Taken together, these data suggest that Cby most likely plays a post-centriologenic role in ciliogenesis in motile cilia, at the basal body docking level.

It is interesting to note that there are a number of studies that link the Wnt pathway and pathway components to ciliary function. The most well-characterized association between Wnt/β-catenin signaling and cilia is that of non-motile monocilia, which is best exemplified by the flow-based model of Wnt signaling in the monociliated cells of the kidney (Germino, 2005; Simons et al., 2005). In this model proposed by Simons, et al., Wnt/β-catenin signaling occurs in the absence of fluid flow. Stimulation of the primary

cilium by fluid flow is believed to result in the degradation of Dvl, thereby allowing assembly of the destruction complex and targeted degradation of cytoplasmic β-catenin.

In motile, multiciliated cells in the respiratory epithelium, however, the association with Wnt/β-catenin signaling is not as clearly defined. The only established connection to the canonical Wnt signaling appears to be through the pathway component Dvl, which has been shown to localize in punctate fashion to the apical surface of multiciliated cells and play a critical role in regulating actin assembly and basal body docking during ciliogenesis (Park et al., 2008; Vladar and Axelrod, 2008). However, this is governed through the non-canonical, planar cell polarity (PCP) pathway. Nonetheless, the because of the dual function of Dvl in both the PCP and Wnt/β-catenin pathways, it is important to know which signaling mechanism regulates docking. Further support that canonical Wnt signaling may be involved during ciliogenesis is provided by Ross, et al., in which temporal expression profiles of cultured human bronchial epithelial cells during differentiation showed elevated levels of pathway genes *ctnb1* (β-catenin), *wnt4*, and *axin2* (Ross et al., 2007). More in-depth analysis, however, must be performed in order to better understand the precise function of this pathway during development.

In each case, these studies provide interesting insights into the possible roles cby could play in ciliogenesis and ciliary-mediated cell development. For example, a number of disorders, including Bardet-Biedl syndrome (BBS), nephronophthisis (NPHP), Joubert syndrome (JBTS), Oral-facial-digital Type I (OFD 1), and Leber congenital amaurosis (LCA) are severe pathological conditions, termed ciliopathies, that result from defects in ciliary components, often resulting in disruption of Wnt signaling. Because some of the phenotypes, such as kidney cysts, are recapitulated in the *cby*$^{-/-}$ mouse, it is possible that

cby plays a role in regulating homeostasis and development of monociliated cells at both the basal body level and the transcriptional level in the nucleus. Though less clear in multiciliated, motile cell function, there exists the possibility that cby could serve in both the canonical and non-canonical Wnt pathways in similar fashion to Dvl, a key component of both pathways, which also colocalizes to basal bodies in punctate fashion and regulates docking and polarity.

The Clara cell phenotype is more difficult to interpret. However, the developmental complexity of lung organogenesis is such that it is dependent upon a number of intrinsic and extrinsic factors – humoral, biochemical, mechanical and genetic in nature – acting in concert in such an intricate fashion that it is often difficult to isolate a single cell type to determine the causative factor. It is highly likely that many of the observed effects are systemic and their causes are not immediately obvious. In the case of the disrupted Clara cell morphology, it is possible that the differentiation defects result directly from hyperactive Wnt signaling in the bronchial epithelium, as evidence suggests that bronchial epithelial development is sensitive to disruptions in canonical Wnt signaling (Mucenski et al., 2005; Mucenski et al., 2003; Shu et al., 2002). The apparent hypersecretory phenotype could also be related to the endogenous function of Clara cells. One characteristic of premature neonatal lungs is a high succeptibility to infection. It is possible that the developmentally immature *cby*$^{-/-}$ lung may be similarly sensitive and the elevated Clara cell's protective response is observed. While immunostaining for antibodies against macrophages in adult *cby*$^{-/-}$ and cby$^{+/+}$ lungs yielded inconclusive results, this could be examined further to confirm or rule out this possible explanation.

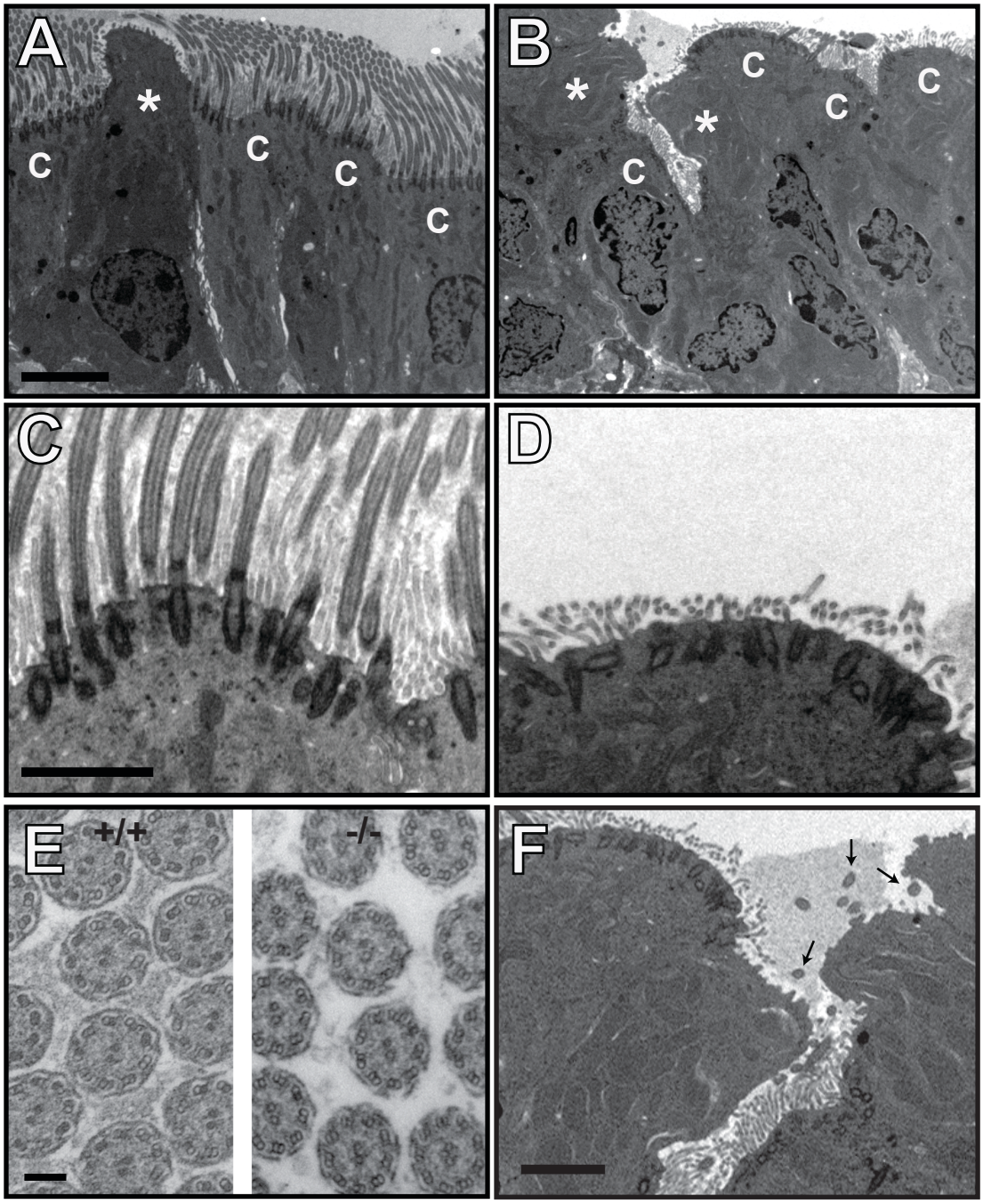

Figure 4-1. Cby null mice exhibit ultrastructural defects in the airway epithelium. Electron microscopy was performed on adult lung tissue from Cby-/- (B,D,E,F) and control (A,C,E) mice. Ciliated cell types lining the bronchial airways are compared in cby null mice (B,D) to wildtype controls (A,C). Cilia from cby-/- mice (-/-) exhibit apparently normal ciliary ultrastructure compared to wildtype (+/+), exhibited by the characteristic 9+2 axoneme and the presence of outer dynein arms (E). Arrowheads denote secretions of Clara cell secretory protein (F). **C**: Clara cell, asterisks denote ciliated cells. Scale = 5µm (A,B), 2µm (C,D), 4µm (F), and 100nm (E).

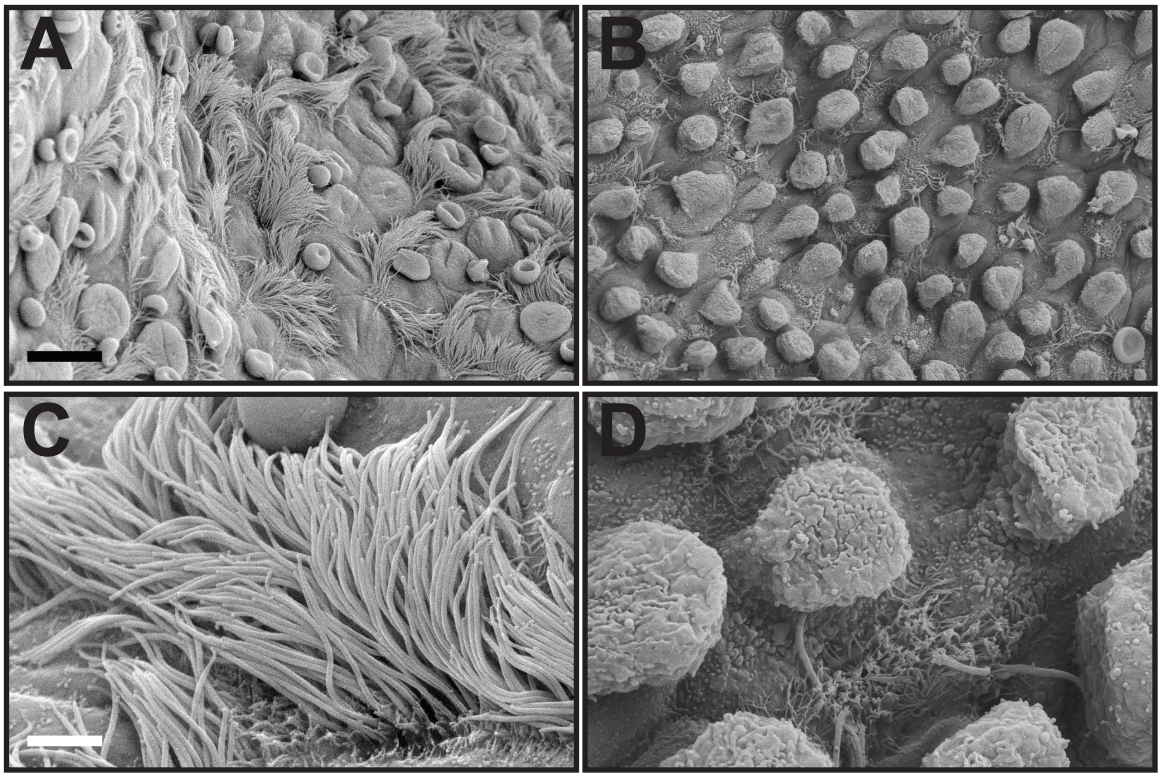

Figure 4-2. Cby null mice exhibit ultrastructural defects in the airway epithelium. Scanning Electron microscopy was performed on ciliated cells in the large proximal airways of adult Cby-/- (B,D) and control (A,C) mice. Scale: 10μm (A-B) and 2μm (C-D).

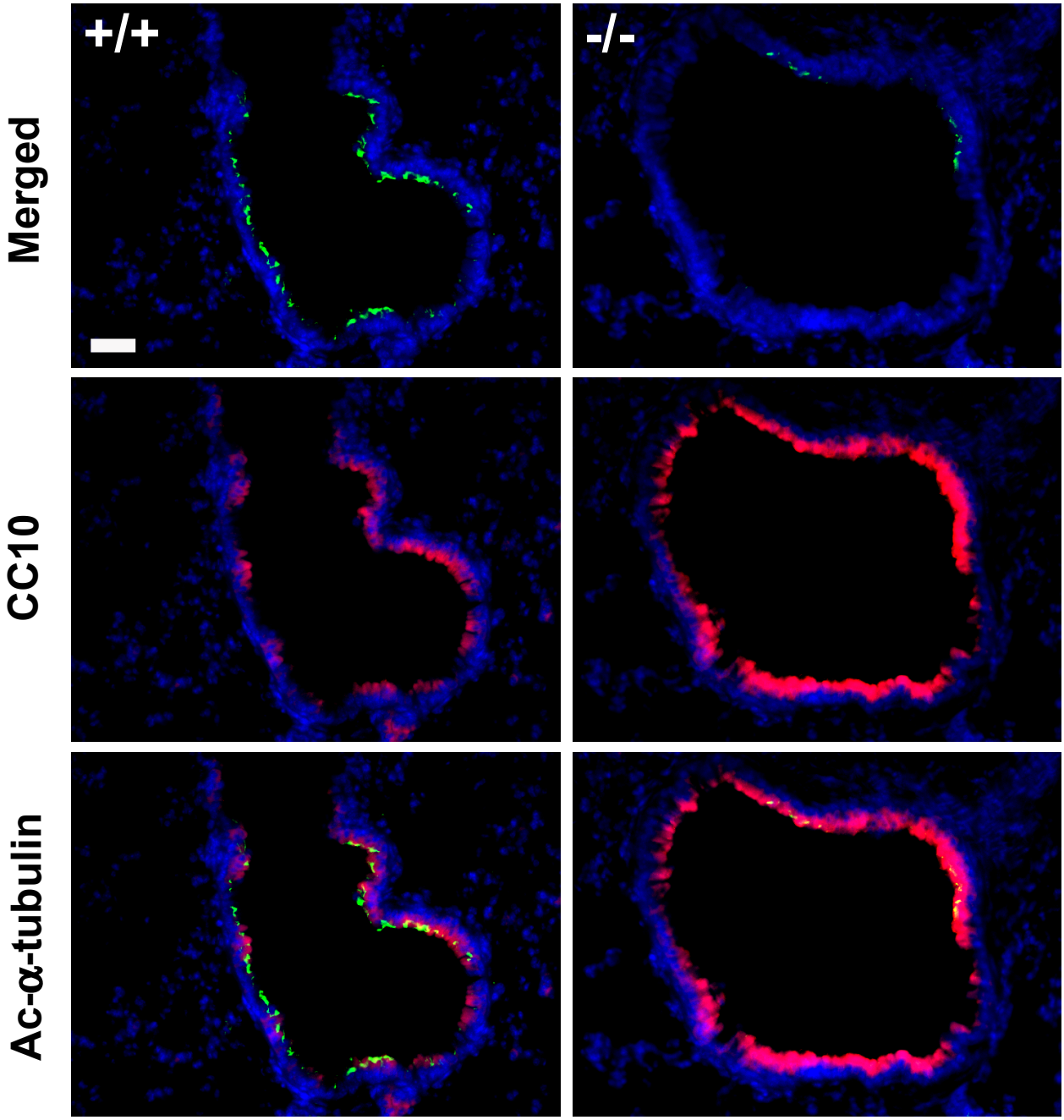

Figure 4-3. Cby null mouse lungs exhibit differentiation defects in airway epithelium. Lungs were harvested from adult WT and KO mice at 1.5 months. Airway sections were double-labeled with antibodies against acetylated alpha-tubulin (green) and CC10 (red) and merged images are shown. Scale = 50μm.

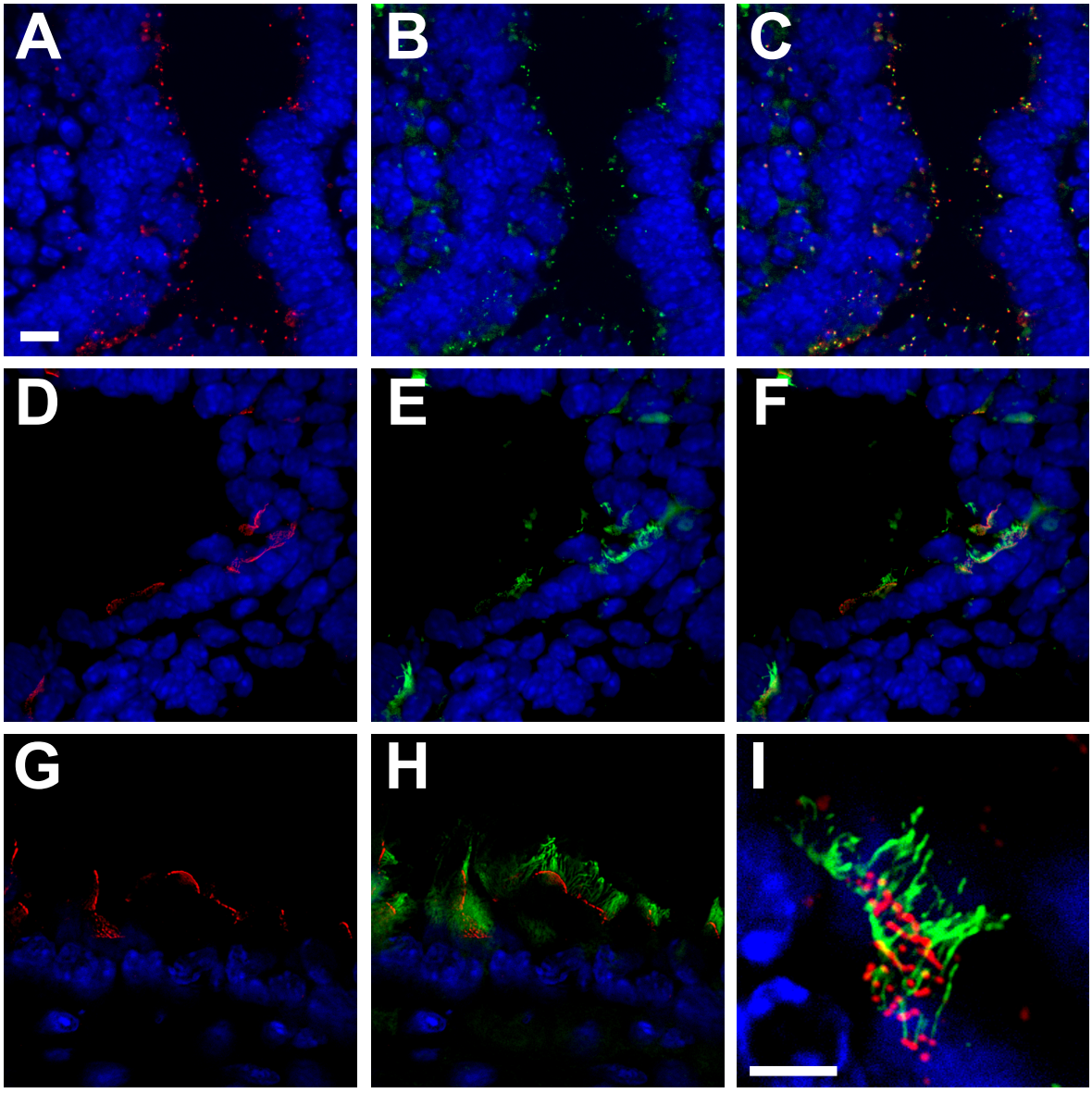

Figure 4-4. Cellular localization of the Cby protein in airway epithelium. Lung sections from embryonic mice at E15.5 (A-C) and E17.5 (D-F) and adult mice (E-G) were double-labeled with antibodies against Cby (red) and acetylated-α-tubulin (green) and merged images are shown (C,F,H,I). Scale: A-H = 5μm, I = 2μm

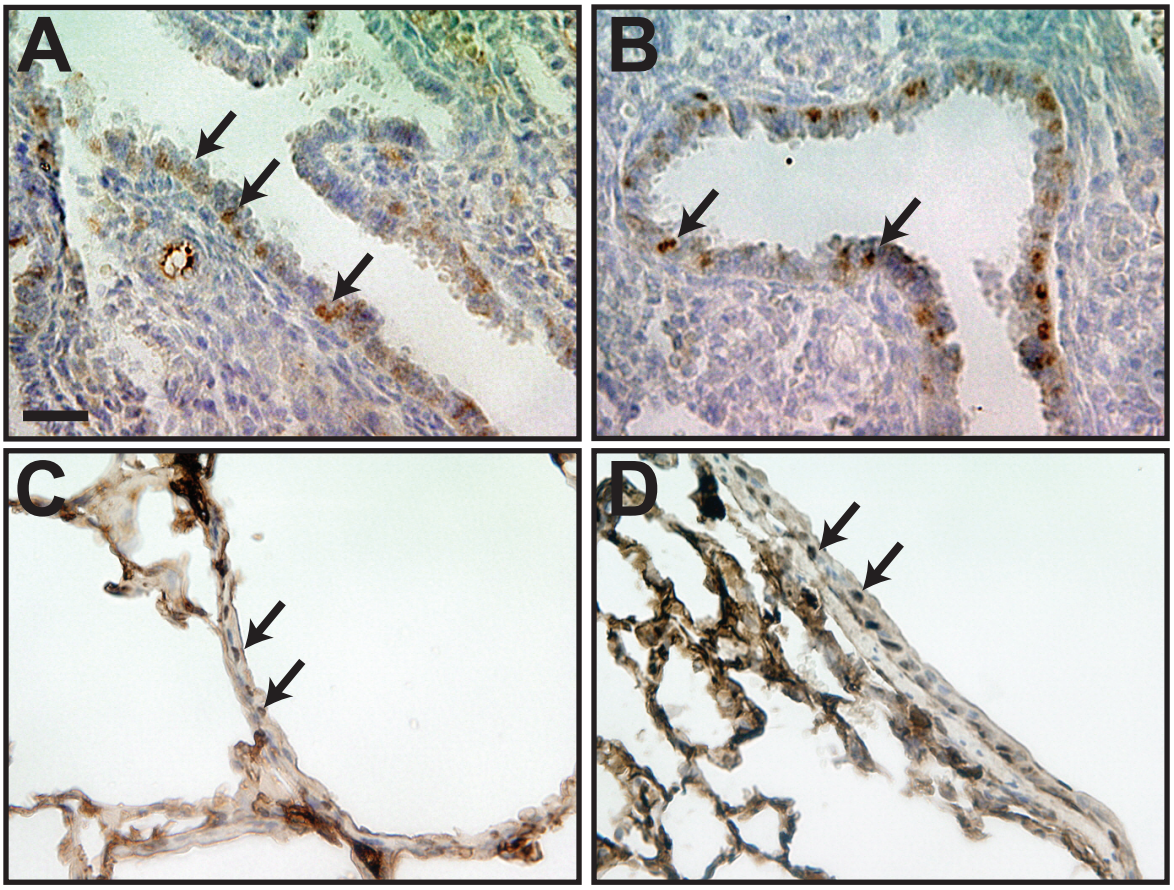

Figure 4-5. Foxj1 is expressed in multiciliated epithelial cells in adult cby+/+ and cby-/- airways. Lungs were harvested from adult cby+/+ (A,C) and cby-/- (B,D) mice. Immunohistochemical staining reveals foxj1-positive cells (brown, arrows). Scale = 50μm.

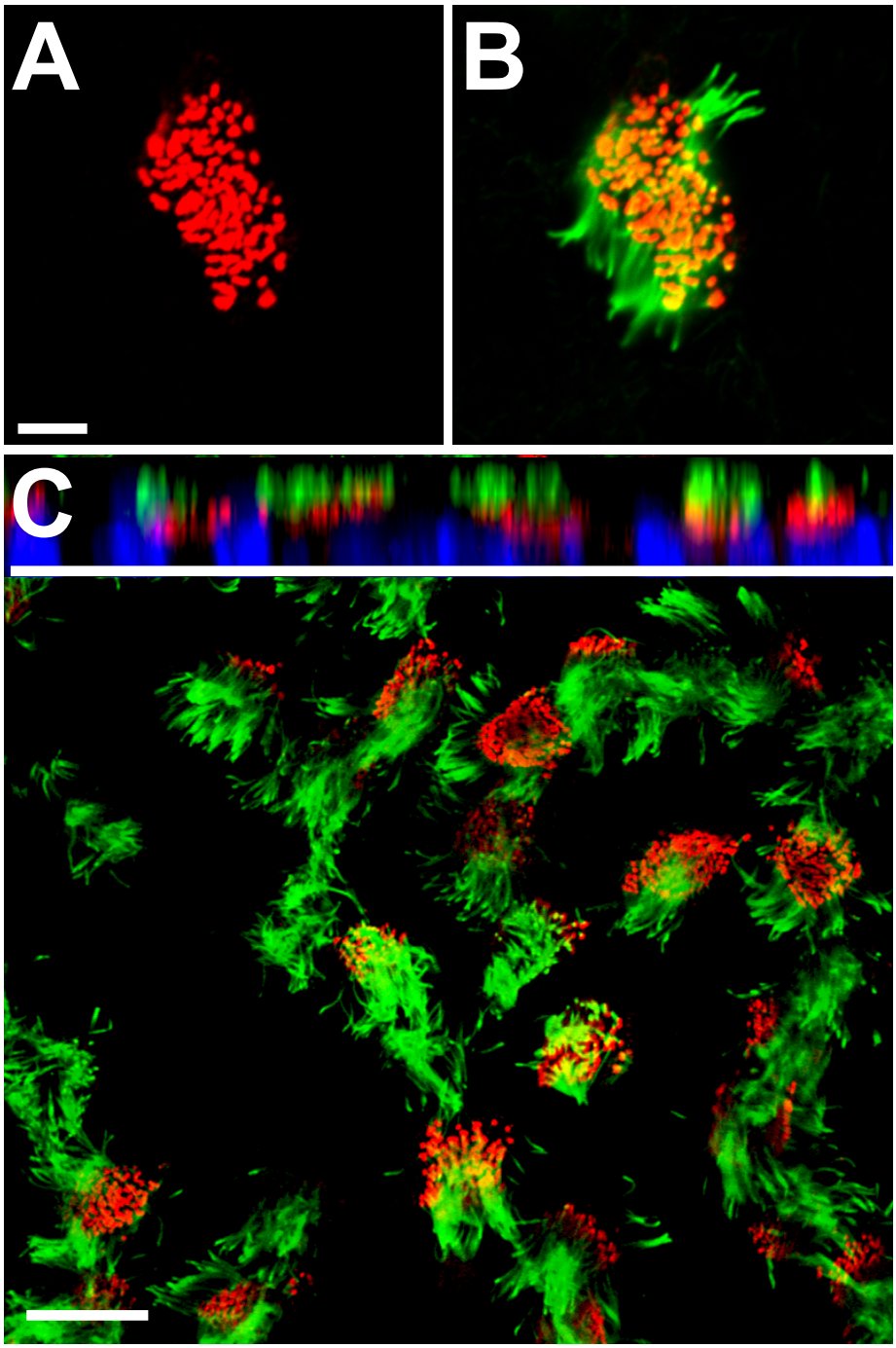

Fig. 4-6. Cby localizes along the motile cilia of airway epithelia in cultured epithelial cells. Confocal immunofluorescence microscopy of cultured mouse airway epithelia with antibodies to cby (red) show that cby localizes to the base of motile cilia, which were identified by antibodies to acetylated α-tubulin in the merged images (B,C,green). Data are stacks of confocal z-series images in the X-Y plane (C) and Z plane (above). Nuclei stained with DAPI are in blue. Scale: A,B = 5μm, C = 20μm

CHAPTER 5: CONCLUSIONS AND FUTURE DIRECTIONS

Summary of thesis findings

Cell development and differentiation in the fetal lung are regulated by mechanical, physiologic, and biochemical factors (Kaplan, 2000). This study has demonstrated that Cby is a complex, multifunctional protein that plays key roles in mediating differentiation of alveolar and airway epithelial cells, maintenance of lung architecture and regulation of pulmonary function. This is accomplished in part through its regulation of the canonical Wnt pathway.

Here, we have demonstrated that Cby is expressed in the developing as well as the adult lung (**FIG. 4-1**) and the loss of the Cby-mediated regulation of the canonical Wnt pathway results in elevated activity (**FIG. 4-2**). BAT-gal reporter mice on the *cby*$^{-/-}$ background exhibited a two-fold elevation of lacZ activity in the lungs during embryogenesis, a trend shown in adult mouse lungs as well, as indicated by the twofold elevation of Wnt/β-catenin target genes axin2 and cyclinD1. Together, these data suggest that the differentiation defect in *cby*$^{-/-}$ mice could be due in part to upregulated β-catenin signaling. Canonical Wnt signaling has been associated with maintenance of stem cell pluripotency, while suppression of Wnt signaling has been linked to promoting differentiation (Nusse, 2008). Because proper lung development is dependent upon precise spatial and temporal regulation of Wnt signaling during embryogenesis, loss of Cby likely results in inappropriate activation of the canonical Wnt pathway and subsequent delays in the developmental cascade mediating lung organogenesis and function (Cohen and Larson, 2008).

Although the precise molecular mechanisms underlying the reduced complexity of *cby*$^{-/-}$ lung parenchyma remain to be elucidated, it is interesting to note that conditional activation of β-catenin specifically in the developing lung epithelium causes airspace enlargement in the postnatal period (Mucenski et al., 2005), implying that impaired alveolarization in *cby*$^{-/-}$ mice is associated with upregulation of β-catenin signaling. This is consistent with previous studies indicating that disruption of Wnt/β-catenin signaling pathway regulation in alveolar and bronchial epithelial cells results in the failure to undergo proper differentiation of the lung epithelium (De Langhe et al., 2005; Mucenski et al., 2003; Shu et al., 2005; Shu et al., 2002).

In addition to Cby's role as an antagonist of the Wnt pathway, this study presents evidence that Cby exists in a cytoplasmic pool residing at the centrosome in a subset of pulmonary epithelial cell types. The centriole is an integral part of the centrosome, which is the major microtubule-organizing center (MTOC) of animal cells. MT triplets of centrioles are highly stable structures and this particular subset of MTs shares with basal bodies and axonemes the acetylation of tubulin(Vinogradova et al., 2005). Using an antibody specific to Cby, we demonstrated coimmunolocalization with the centriolar protein acetylated α-tubulin and observed centrosomal localization in alveolar progenitor cells during development, and in developing and adult bronchial epithelial cells. Microtubules are required for many well characterized functions in eukaryotic cells, establishment and maintenance of cellular morphology and cytoskeletal architecture, cell growth, cell migration and morphogenesis in multicellular organisms (Nogales, 2000). While the role of Cby in alveolar development remains unknown, the defects in lung

architecture and cell structure in *cby*$^{-/-}$ mice may be attributable to its role as a centrosome-associated protein.

During ciliogenesis, centrioles migrate to the apical cell surface and dock with the cell membrane to form basal bodies, from which the cilia extend (Dawe et al., 2007; Sorokin, 1968). This study shows that the Cby protein is located apically in airway epithelial cells in the trachea and in the proximal airways of the lung, localized specifically at the base of the cilia. This is consistent with previous findings that endogenous Cby was detected both at the base of ciliated cells in the nasal epithelium, and in primary cilia in cultured ciliated MDCK2 cells and co-localizes with centrosomal marker γ-tubulin, which is required for basal body assembly (Shang et al., 2005; Voronina et al., 2009), supporting the notion that Cby plays an integral role in ciliogenesis. This is evidenced further by the marked paucity of cilia in the epithelium of the proximal airways of *cby*$^{-/-}$ mouse lungs.

While the mechanism by which the canonical Wnt pathway influences alveologenesis remains poorly understood, there is evidence that ATII differentiation is regulated by mechanotransduction in a Wnt-related manner (Edwards, 2001; Gutierrez et al., 1999; Jaalouk and Lammerding, 2009; Sanchez-Esteban et al., 2001; Torday, 2003). Mechanosensory transduction is described as the cellular process that translates mechanical stimuli into biochemical signals, and its evidence in regulating organ and tissue development is well-established (Hahn and Schwartz, 2009; Torday, 2003; Wang et al., 2009; Wozniak and Chen, 2009). Mediation of the Wnt signaling pathway during alveologenesis has been demonstrated through the parathyroid hormone receptor protein (PTHrP), an evolutionarily conserved, stretch-regulated gene (Daifotis et al., 1992;

Schordan et al., 2004; Torday, 2003; Torday and Rehan, 2002, 2003; Yamamoto et al., 1992). During intrauterine development, epithelial fluid secretion gives rise to a transpulmonary pressure in the potential airways and air spaces which, in turn, upregulates PTHrP signaling and promotes ATII differentiation by downregulating Wnt activity (Sanchez-Esteban et al., 2001; Torday and Rehan, 2006, 2007). Experimental stimulation of this pathway using the Wnt agonist LiCl in lung explants, results in developmentally immature ATII cells while consequently downregulating PTHrP activity. Similarly, *pthrp*$^{-/-}$ mice show similar effects, supporting the notion of ATII sensitivity to Wnt-mediated stretch-induced differentiation (Rubin et al., 2004). In a recent study, Cohen, *et al.*, demonstrated further evidence for stretch-induced regulation of Wnt activity by modulating gene expression of the *cftr* (cystic fibrosis transmembrane conductance regulator), a developmental gene that is responsible for mediating stretch-induced differentiation of the lung and gastrointestinal tract during organogenesis (Cohen and Larson, 2006). Using an intra-amniotic gene therapy procedure, researchers transfected BAT-gal reporter mice with adenoviruses containing a short anti-sense CFTR gene fragment, effectively downregulating stretch and elevating expression of the Wnt reporter (Cohen et al., 2008). This, coupled with studies demonstrating that upregulation of Wnt as well as downregulation of mechanical stretch results in abnormal ATII differentiation, demonstrates a mechanistic link between stretch-induced alveolar development through Wnt pathway modulation (Demayo et al., 2002; Sanchez-Esteban et al., 2001; Torday, 2003). Interestingly, the most pronounced effect on Wnt activity was observed at E16.5, the stage in lung development when PTHrP signaling is upregulated (Burton et al., 1992). These studies provide a possible mechanistic link between the *cby*$^{-}$

$^{-/-}$ phenotype and that of Wnt-mediated stretch-induced alveolar differentiation. In *cby*$^{-/-}$ mice, Wnt/β-catenin activity is elevated during development, with pronounced hyperactivity at E16.5 (Fig. 2-), supporting the notion that the loss of cby could result in inappropriately elevating canonical Wnt pathway activity at a key stage in development, disrupting alveolar maturation in a stretch-dependent manner.

This study has demonstrated that Cby is a multifunctional protein that mediates lung organogenesis both as a regulator of canonical Wnt pathway activity and as a centrosomal protein, likely playing a role in cytoskeletal architecture and ciliogenesis. Recent studies have revealed that a novel role for Cby as a shuttling protein that interacts with β-catenin and 14-3-3 adaptor protein in the nucleus and transports β-catenin to the cytoplasm (Li et al., 2008; Takemaru et al., 2009). Interestingly, Cby bears a functional similarity with other Wnt pathway proteins that also serve dual roles in mediating signaling as well as cytoskeletal maintenance. β-catenin, the main player in the canonical Wnt pathway, shuttles between the nucleus and the cytoplasm where it acts as a cell adhesion molecule as well as a transcriptional co-activator (Brembeck et al., 2006; Gottardi and Gumbiner, 2004; Kam and Quaranta, 2009). APC, too, is a component of the destruction complex and a β-catenin binding partner, which also acts as a microtubule-associated protein and regulates microtubule assembly (Akhmanova and Hoogenraad, 2005). In addition, 14-3-3 has been demonstrated as a key component in mediating ciliogenesis and intraciliary transport by targeting specific proteins to the centrosome (Fan et al., 2004; Molla-Herman et al., 2008; Ostrowski et al., 2002). Further studies, however, are needed to elucidate a potential role Cby may have in mediating

ciliogenesis as well as in the maintenance of cell morphology and differentiation through its association with cytoskeletal components.

Future directions

Although this study has provided a characterization of the role for cby in lung organogenesis and the development of pulmonary respiratory epithelial cells, there remains a number of unanswered questions. For instance, the precise cellular localization of cby in the lung parenchyma has yet to be determined. Immunolocalization studies demonstrate cby localization in the cytoplasm of what appear to be alveolar progenitor cells, likely ATII cells, but further studies could be performed to elucidate its exact location. Isolation of primary ATII cells from $cby^{+/+}$ and $cby^{-/-}$ mice would allow for more precise immunolocalization than tissue-based immunofluorescence has allowed. Cell culture examination has successfully revealed cytoplasmic as well as nuclear cby localization (Li et al., 2008; Li et al., 2007; Mofunanya et al., 2009), suggesting this as a means to more easily localize cby by immunostaining. Furthermore, cell culture allows for greater versatility in manipulating Wnt pathway components, including *cby* expression using overexpression and knockdown studies, to interpret the mechanism involved in alveolar differentiation. In situ hybridization studies could also be performed in tissues to examine localization of *cby* mRNA to determine its nuclear localization which, presently, has only been demonstrated *in vitro*.

The lung is constantly subjected to injury by pathogens and toxins, and requires rapid repair of its epithelial surfaces for proper maintenance of pulmonary homeostasis. Though the adult lung is not mitotically active, several subsets of epithelial cells have

been shown to have proliferative activity in response to injury, including basal cells, Clara cells and pulmonary neuroendocrine cells (PNECs) lining the respiratory epithelium (Kim et al., 2002; McElroy and Kasper, 2004; Park et al., 2006a; Reynolds et al., 2000). These cells repopulate the airway epithelium and further differentiate into terminally differentiated cell types (Levitsky, 2003; Stripp et al., 1995). Park *et al.* (2006) demonstrated that ciliated cells, believed to be terminally differentiated cell types, undergo morphological changes and play a role in regeneration in response to naphthalene-induced injury (Park et al., 2006a).

The Wnt/β-catenin signaling pathway has been implicated in the fibroproliferative response to acute lung injury (Douglas et al., 2006) More importantly, the β-catenin-responsive reporter in BAT-Gal mice is activated in proliferating Clara cells in response to lung injury upon naphthalene treatment (Nusse, 2006). Recent studies have linked elevated Wnt/β-catenin activity with the expansion of bronchial progenitor cells and repair of the airway epithelium (Reynolds et al., 2008; Zhang et al., 2008). In light of these studies and the observed maturation defects in the lung of *cby*$^{-/-}$ mice and resulting abundance of undifferentiated cell types it would be interesting to examine the lung injury response of *cby*$^{-/-}$ mice.

Further examination of the role of cby in ciliary function is also required. While the association of cby with mono- and multiciliated cells has been demonstrated, there remains the obvious potential association with Dvl as it relates to basal body colocalization and a potential function in docking. In both cases, loss of the protein results in defects in apical localization (though more pronounced and consistent in Dvl knockouts). It may be useful to consider a potential role in the non-canonical Wnt

pathway as well. Conditional knockout and overexpression of pathway components in established cell lines (e.g., MDCK2) could enable examination of mechanism and resulting phenotypes in these instances. Furthermore, the role of other developmental pathways, such as the sonic hedgehog pathway (Shh) has been well-characterized in the development of lung epithelial cells as well as ciliogenesis (Bellusci et al., 1997; Bellusci et al., 1996; Breunig et al., 2008; Cortellino et al., 2009; Han et al., 2008; Kiprilov et al., 2008; Kumar et al., 2005; Pepicelli et al., 1998; Quinlan et al., 2008; Spassky and Aguilar, 2008; Stewart et al., 2003; Urase et al., 1996). It would be interesting to examine the potential role for cby interaction in other pathways such as Shh.

This study revealed a powerful and versatile model for examining primary mouse tracheal epithelial cells in culture (You et al., 2002). Using this method of isolating multiciliated cells, it is possible to further examine the role of cby in ciliogenesis and function in multiciliated cells, which themselves have a developmental program, structure and function distinctly different from their monociliated counterparts (Dawe et al., 2007; Toskala et al., 2005; You et al., 2004; Yu et al., 2008). These cells are viable for periods of up to 8 months and are readily manipulated for gene expression studies, having a tranfection efficiency of approximately 60% using lentiviral transfection (Huang et al., 2003; You et al., 2004). Therefore, it is possible to perform overexpression and knockdown studies of various Wnt pathway components, as well as other components related to shuttling and basal body docking (e.g., 14-3-3), insertion of cby mutants (e.g., mutants deficient in nuclear import/export) and expression studies examining cby expression levels during ciliogenesis. Further immunolocalization studies can be conducted, tracing cby during various stages of epithelial cell differentiation.

In light of the prevalence of pulmonary and ciliopathic disorders, it is crucial to further understand the molecular mechanisms underlying lung development and diseases. Cby is a potent repressor of β-catenin and has been clearly demonstrated to have functional biological importance. Exploring functions of Cby and Wnt/β-catenin signaling in lung development and homeostasis may eventually provide a foundation to develop novel therapeutic strategies for treating pulmonary disorders. Clearly, further examination is required characterize the complex and diverse roles of Cby in lung development and function, and contribute to better understanding of the complicated processes underlying lung morphogenesis and diseases.

REFERENCES

Akhmanova, A., and Hoogenraad, C.C. (2005). Microtubule plus-end-tracking proteins: mechanisms and functions. Curr Opin Cell Biol *17*, 47-54.

Baritussio, A., Pettenazzo, A., Benevento, M., Alberti, A., and Gamba, P. (1992). Surfactant protein C is recycled from the alveoli to the lamellar bodies. The American journal of physiology *263*, L607-611.

Barker, N., and Clevers, H. (2006). Mining the Wnt pathway for cancer therapeutics. Nat Rev Drug Discov *5*, 997-1014.

Beers, M.F., Wali, A., Eckenhoff, M.F., Feinstein, S.I., Fisher, J.H., and Fisher, A.B. (1992). An antibody with specificity for surfactant protein C precursors: identification of pro-SP-C in rat lung. American journal of respiratory cell and molecular biology *7*, 368-378.

Bellusci, S., Furuta, Y., Rush, M.G., Henderson, R., Winnier, G., and Hogan, B.L. (1997). Involvement of Sonic hedgehog (Shh) in mouse embryonic lung growth and morphogenesis. Development *124*, 53-63.

Bellusci, S., Henderson, R., Winnier, G., Oikawa, T., and Hogan, B.L. (1996). Evidence from normal expression and targeted misexpression that bone morphogenetic protein (Bmp-4) plays a role in mouse embryonic lung morphogenesis. Development *122*, 1693-1702.

Bhaskaran, M., Kolliputi, N., Wang, Y., Gou, D., Chintagari, N.R., and Liu, L. (2007). Trans-differentiation of alveolar epithelial type II cells to type I cells involves autocrine signaling by transforming growth factor beta 1 through the Smad pathway. J Biol Chem *282*, 3968-3976.

Brembeck, F.H., Rosario, M., and Birchmeier, W. (2006). Balancing cell adhesion and Wnt signaling, the key role of beta-catenin. Curr Opin Genet Dev *16*, 51-59.

Breunig, J.J., Sarkisian, M.R., Arellano, J.I., Morozov, Y.M., Ayoub, A.E., Sojitra, S., Wang, B., Flavell, R.A., Rakic, P., and Town, T. (2008). Primary cilia regulate hippocampal neurogenesis by mediating sonic hedgehog signaling. Proceedings of the National Academy of Sciences of the United States of America *105*, 13127-13132.

Brody, J.S., and Williams, M.C. (1992). Pulmonary alveolar epithelial cell differentiation. Annual review of physiology *54*, 351-371.

Brody, S.L., Hackett, B.P., and White, R.A. (1997). Structural characterization of the mouse Hfh4 gene, a developmentally regulated forkhead family member. Genomics *45*, 509-518.

Broeckaert, F., Clippe, A., Knoops, B., Hermans, C., and Bernard, A. (2000). Clara cell secretory protein (CC16): features as a peripheral lung biomarker. Ann N Y Acad Sci *923*, 68-77.

Broussard, D., Larson, J.E., Cohen, J.C., and Lundblad, L.K. (2006). Developmental changes in respiratory mechanics in the neonatal rat. Exp Lung Res *32*, 263-273.

Burton, P.B., Moniz, C., Quirke, P., Malik, A., Bui, T.D., Juppner, H., Segre, G.V., and Knight, D.E. (1992). Parathyroid hormone-related peptide: expression in fetal and neonatal development. J Pathol *167*, 291-296.

Cardoso, W.V. (2000). Lung morphogenesis revisited: old facts, current ideas. Dev Dyn *219*, 121-130.

Cardoso, W.V., and Lu, J. (2006). Regulation of early lung morphogenesis: questions, facts and controversies. Development *133*, 1611-1624.

Chilosi, M., Poletti, V., Zamo, A., Lestani, M., Montagna, L., Piccoli, P., Pedron, S., Bertaso, M., Scarpa, A., Murer, B*., et al.* (2003). Aberrant Wnt/beta-catenin pathway activation in idiopathic pulmonary fibrosis. Am J Pathol *162*, 1495-1502.

Chinoy, M.R. (2003). Lung growth and development. Front Biosci *8*, d392-415.

Chuang, P.T., and McMahon, A.P. (2003). Branching morphogenesis of the lung: new molecular insights into an old problem. Trends Cell Biol *13*, 86-91.

Clevers, H. (2006). Wnt/beta-catenin signaling in development and disease. Cell *127*, 469-480.

Cohen, J.C., and Larson, J.E. (2006). Cystic fibrosis transmembrane conductance regulator (CFTR) dependent cytoskeletal tension during lung organogenesis. Dev Dyn *235*, 2736-2748.

Cohen, J.C., and Larson, J.E. (2008). The Peter Pan paradigm. Theor Biol Med Model *5*, 1.

Cohen, J.C., Larson, J.E., Killeen, E., Love, D., and Takemaru, K. (2008). CFTR and Wnt/beta-catenin signaling in lung development. BMC Dev Biol *8*, 70.

Cohen, J.C., Lundblad, L.K., Bates, J.H., Levitzky, M., and Larson, J.E. (2004). The "Goldilocks effect" in cystic fibrosis: identification of a lung phenotype in the cftr knockout and heterozygous mouse. BMC genetics *5*, 21.

Cohen, J.C., Morrow, S.L., Cork, R.J., Delcarpio, J.B., and Larson, J.E. (1998). Molecular pathophysiology of cystic fibrosis based on the rescued knockout mouse model. Mol Genet Metab *64*, 108-118.

Cortellino, S., Wang, C., Wang, B., Bassi, M.R., Caretti, E., Champeval, D., Calmont, A., Jarnik, M., Burch, J., Zaret, K.S., *et al.* (2009). Defective ciliogenesis, embryonic lethality and severe impairment of the Sonic Hedgehog pathway caused by inactivation of the mouse complex A intraflagellar transport gene Ift122/Wdr10, partially overlapping with the DNA repair gene Med1/Mbd4. Developmental biology *325*, 225-237.

Daifotis, A.G., Weir, E.C., Dreyer, B.E., and Broadus, A.E. (1992). Stretch-induced parathyroid hormone-related peptide gene expression in the rat uterus. J Biol Chem *267*, 23455-23458.

Dawe, H.R., Farr, H., and Gull, K. (2007). Centriole/basal body morphogenesis and migration during ciliogenesis in animal cells. J Cell Sci *120*, 7-15.

De Langhe, S.P., and Reynolds, S.D. (2008). Wnt signaling in lung organogenesis. Organogenesis *4*, 100-108.

De Langhe, S.P., Sala, F.G., Del Moral, P.M., Fairbanks, T.J., Yamada, K.M., Warburton, D., Burns, R.C., and Bellusci, S. (2005). Dickkopf-1 (DKK1) reveals that fibronectin is a major target of Wnt signaling in branching morphogenesis of the mouse embryonic lung. Developmental biology *277*, 316-331.

Dean, C.H., Miller, L.A., Smith, A.N., Dufort, D., Lang, R.A., and Niswander, L.A. (2005). Canonical Wnt signaling negatively regulates branching morphogenesis of the lung and lacrimal gland. Developmental biology *286*, 270-286.

Demayo, F., Minoo, P., Plopper, C.G., Schuger, L., Shannon, J., and Torday, J.S. (2002). Mesenchymal-epithelial interactions in lung development and repair: are modeling and remodeling the same process? American journal of physiology *283*, L510-517.

Douglas, I.S., Diaz del Valle, F., Winn, R.A., and Voelkel, N.F. (2006). Beta-catenin in the fibroproliferative response to acute lung injury. American journal of respiratory cell and molecular biology *34*, 274-285.

Echelard, Y., Vassileva, G., and McMahon, A.P. (1994). Cis-acting regulatory sequences governing Wnt-1 expression in the developing mouse CNS. Development *120*, 2213-2224.

Edwards, Y.S. (2001). Stretch stimulation: its effects on alveolar type II cell function in the lung. Comp Biochem Physiol A Mol Integr Physiol *129*, 245-260.

Evans, M.J., Cabral, L.J., Stephens, R.J., and Freeman, G. (1975). Transformation of alveolar type 2 cells to type 1 cells following exposure to NO2. Exp Mol Pathol *22*, 142-150.

Evans, M.J., Shami, S.G., Cabral-Anderson, L.J., and Dekker, N.P. (1986). Role of nonciliated cells in renewal of the bronchial epithelium of rats exposed to NO2. Am J Pathol *123*, 126-133.

Fan, S., Hurd, T.W., Liu, C.J., Straight, S.W., Weimbs, T., Hurd, E.A., Domino, S.E., and Margolis, B. (2004). Polarity proteins control ciliogenesis via kinesin motor interactions. Curr Biol *14*, 1451-1461.

Fredberg, J.J., and Stamenovic, D. (1989). On the imperfect elasticity of lung tissue. J Appl Physiol *67*, 2408-2419.

Germino, G.G. (2005). Linking cilia to Wnts. Nat Genet *37*, 455-457.

Gibson, U.E., Heid, C.A., and Williams, P.M. (1996). A novel method for real time quantitative RT-PCR. Genome Res *6*, 995-1001.

Gomes, R.F., Shen, X., Ramchandani, R., Tepper, R.S., and Bates, J.H. (2000). Comparative respiratory system mechanics in rodents. J Appl Physiol *89*, 908-916.

Gottardi, C.J., and Gumbiner, B.M. (2004). Distinct molecular forms of beta-catenin are targeted to adhesive or transcriptional complexes. J Cell Biol *167*, 339-349.

Greaves, S. (2003). Small changes in Wnt signalling. Nature cell biology *5*, 387.

Groenman, F., Unger, S., and Post, M. (2005). The molecular basis for abnormal human lung development. Biol Neonate *87*, 164-177.

Gutierrez, J.A., Ertsey, R., Scavo, L.M., Collins, E., and Dobbs, L.G. (1999). Mechanical distention modulates alveolar epithelial cell phenotypic expression by transcriptional regulation. American journal of respiratory cell and molecular biology *21*, 223-229.

Hahn, C., and Schwartz, M.A. (2009). Mechanotransduction in vascular physiology and atherogenesis. Nat Rev Mol Cell Biol *10*, 53-62.

Han, Y.G., Spassky, N., Romaguera-Ros, M., Garcia-Verdugo, J.M., Aguilar, A., Schneider-Maunoury, S., and Alvarez-Buylla, A. (2008). Hedgehog signaling and primary cilia are required for the formation of adult neural stem cells. Nat Neurosci *11*, 277-284.

Hantos, Z., Daroczy, B., Suki, B., Nagy, S., and Fredberg, J.J. (1992). Input impedance and peripheral inhomogeneity of dog lungs. J Appl Physiol *72*, 168-178.

Hong, K.U., Reynolds, S.D., Giangreco, A., Hurley, C.M., and Stripp, B.R. (2001). Clara cell secretory protein-expressing cells of the airway neuroepithelial body microenvironment include a label-retaining subset and are critical for epithelial renewal after progenitor cell depletion. American journal of respiratory cell and molecular biology *24*, 671-681.

Hong, K.U., Reynolds, S.D., Watkins, S., Fuchs, E., and Stripp, B.R. (2004a). Basal cells are a multipotent progenitor capable of renewing the bronchial epithelium. Am J Pathol *164*, 577-588.

Hong, K.U., Reynolds, S.D., Watkins, S., Fuchs, E., and Stripp, B.R. (2004b). In vivo differentiation potential of tracheal basal cells: evidence for multipotent and unipotent subpopulations. American journal of physiology *286*, L643-649.

Huang, T., You, Y., Spoor, M.S., Richer, E.J., Kudva, V.V., Paige, R.C., Seiler, M.P., Liebler, J.M., Zabner, J., Plopper, C.G.*, et al.* (2003). Foxj1 is required for apical localization of ezrin in airway epithelial cells. J Cell Sci *116*, 4935-4945.

Irvin, C.G., and Bates, J.H. (2003). Measuring the lung function in the mouse: the challenge of size. Respir Res *4*, 4.

Jaalouk, D.E., and Lammerding, J. (2009). Mechanotransduction gone awry. Nat Rev Mol Cell Biol *10*, 63-73.

Jho, E.H., Zhang, T., Domon, C., Joo, C.K., Freund, J.N., and Costantini, F. (2002). Wnt/beta-catenin/Tcf signaling induces the transcription of Axin2, a negative regulator of the signaling pathway. Molecular and cellular biology *22*, 1172-1183.

Kam, Y., and Quaranta, V. (2009). Cadherin-bound beta-catenin feeds into the Wnt pathway upon adherens junctions dissociation: evidence for an intersection between beta-catenin pools. PLoS ONE *4*, e4580.

Kaplan, F. (2000). Molecular determinants of fetal lung organogenesis. Mol Genet Metab *71*, 321-341.

Kim, C.F., Jackson, E.L., Woolfenden, A.E., Lawrence, S., Babar, I., Vogel, S., Crowley, D., Bronson, R.T., and Jacks, T. (2005). Identification of bronchioalveolar stem cells in normal lung and lung cancer. Cell *121*, 823-835.

Kim, K., Lu, Z., and Hay, E.D. (2002). Direct evidence for a role of beta-catenin/LEF-1 signaling pathway in induction of EMT. Cell Biol Int *26*, 463-476.

Kiprilov, E.N., Awan, A., Desprat, R., Velho, M., Clement, C.A., Byskov, A.G., Andersen, C.Y., Satir, P., Bouhassira, E.E., Christensen, S.T.*, et al.* (2008). Human embryonic stem cells in culture possess primary cilia with hedgehog signaling machinery. J Cell Biol *180*, 897-904.

Kumar, V.H., Lakshminrusimha, S., El Abiad, M.T., Chess, P.R., and Ryan, R.M. (2005). Growth factors in lung development. Adv Clin Chem *40*, 261-316.

Levitsky, M.G. (2003). Pulmonary Physiology, 6th edn (McGraw-Hill).

Li, C., Li, A., Li, M., Xing, Y., Chen, H., Hu, L., Tiozzo, C., Anderson, S., Taketo, M.M., and Minoo, P. (2009). Stabilized beta-catenin in lung epithelial cells changes cell fate and leads to tracheal & bronchial polyposis. Developmental biology.

Li, F.Q., Mofunanya, A., Harris, K., and Takemaru, K. (2008). Chibby cooperates with 14-3-3 to regulate beta-catenin subcellular distribution and signaling activity. J Cell Biol *181*, 1141-1154.

Li, F.Q., Singh, A.M., Mofunanya, A., Love, D., Terada, N., Moon, R.T., and Takemaru, K. (2007). Chibby promotes adipocyte differentiation through inhibition of beta-catenin signaling. Molecular and cellular biology *27*, 4347-4354.

Liu, C., Ikegami, M., Stahlman, M.T., Dey, C.R., and Whitsett, J.A. (2003). Inhibition of alveolarization and altered pulmonary mechanics in mice expressing GATA-6. American journal of physiology *285*, L1246-1254.

Liu, X., Driskell, R.R., and Engelhardt, J.F. (2006). Stem cells in the lung. Methods Enzymol *419*, 285-321.

Livak, K.J., and Schmittgen, T.D. (2001). Analysis of relative gene expression data using real-time quantitative PCR and the 2(-Delta Delta C(T)) Method. Methods *25*, 402-408.

Ludwig, M.S., Robatto, F.M., Simard, S., Stamenovic, D., and Fredberg, J.J. (1992). Lung tissue resistance during contractile stimulation: structural damping decomposition. J Appl Physiol *72*, 1332-1337.

Lutchen, K.R., Hantos, Z., Petak, F., Adamicza, A., and Suki, B. (1996). Airway inhomogeneities contribute to apparent lung tissue mechanics during constriction. J Appl Physiol *80*, 1841-1849.

Maretto, S., Cordenonsi, M., Dupont, S., Braghetta, P., Broccoli, V., Hassan, A.B., Volpin, D., Bressan, G.M., and Piccolo, S. (2003). Mapping Wnt/beta-catenin signaling during mouse development and in colorectal tumors. Proceedings of the National Academy of Sciences of the United States of America *100*, 3299-3304.

McElroy, M.C., and Kasper, M. (2004). The use of alveolar epithelial type I cell-selective markers to investigate lung injury and repair. Eur Respir J *24*, 664-673.

Mofunanya, A., Li, F.Q., Hsieh, J.C., and Takemaru, K. (2009). Chibby forms a homodimer through a heptad repeat of leucine residues in its C-terminal coiled-coil motif. BMC Mol Biol *10*, 41.

Molla-Herman, A., Boularan, C., Ghossoub, R., Scott, M.G., Burtey, A., Zarka, M., Saunier, S., Concordet, J.P., Marullo, S., and Benmerah, A. (2008). Targeting of beta-arrestin2 to the centrosome and primary cilium: role in cell proliferation control. PLoS ONE *3*, e3728.

Moon, R.T., Kohn, A.D., De Ferrari, G.V., and Kaykas, A. (2004). WNT and beta-catenin signalling: diseases and therapies. Nat Rev Genet *5*, 691-701.

Morrisey, E.E. (2003). Wnt signaling and pulmonary fibrosis. Am J Pathol *162*, 1393-1397.

Mucenski, M.L., Nation, J.M., Thitoff, A.R., Besnard, V., Xu, Y., Wert, S.E., Harada, N., Taketo, M.M., Stahlman, M.T., and Whitsett, J.A. (2005). Beta-catenin regulates differentiation of respiratory epithelial cells in vivo. American journal of physiology *289*, L971-979.

Mucenski, M.L., Wert, S.E., Nation, J.M., Loudy, D.E., Huelsken, J., Birchmeier, W., Morrisey, E.E., and Whitsett, J.A. (2003). beta-Catenin is required for specification of proximal/distal cell fate during lung morphogenesis. J Biol Chem *278*, 40231-40238.

Nelson, W.J., and Nusse, R. (2004). Convergence of Wnt, beta-catenin, and cadherin pathways. Science *303*, 1483-1487.

Nogales, E. (2000). Structural insights into microtubule function. Annu Rev Biochem *69*, 277-302.

Nusse, R. (2006). Wnt Proteins as Cell Fate Determinants. Paper presented at: Wnt and beta-Catenin Signaling in Development and Disease (Snowbird, UT).

Nusse, R. (2008). Wnt signaling and stem cell control. Cell Res *18*, 523-527.

Okubo, T., and Hogan, B.L. (2004). Hyperactive Wnt signaling changes the developmental potential of embryonic lung endoderm. J Biol *3*, 11.

Ostrowski, L.E., Blackburn, K., Radde, K.M., Moyer, M.B., Schlatzer, D.M., Moseley, A., and Boucher, R.C. (2002). A proteomic analysis of human cilia: identification of novel components. Mol Cell Proteomics *1*, 451-465.

Park, K.S., Wells, J.M., Zorn, A.M., Wert, S.E., Laubach, V.E., Fernandez, L.G., and Whitsett, J.A. (2006a). Transdifferentiation of ciliated cells during repair of the respiratory epithelium. American journal of respiratory cell and molecular biology *34*, 151-157.

Park, K.S., Wells, J.M., Zorn, A.M., Wert, S.E., and Whitsett, J.A. (2006b). Sox17 influences the differentiation of respiratory epithelial cells. Developmental biology *294*, 192-202.

Park, T.J., Mitchell, B.J., Abitua, P.B., Kintner, C., and Wallingford, J.B. (2008). Dishevelled controls apical docking and planar polarization of basal bodies in ciliated epithelial cells. Nat Genet *40*, 871-879.

Pepicelli, C.V., Lewis, P.M., and McMahon, A.P. (1998). Sonic hedgehog regulates branching morphogenesis in the mammalian lung. Curr Biol *8*, 1083-1086.

Piperno, G., LeDizet, M., and Chang, X.J. (1987). Microtubules containing acetylated alpha-tubulin in mammalian cells in culture. J Cell Biol *104*, 289-302.

Pongracz, J.E., and Stockley, R.A. (2006). Wnt signalling in lung development and diseases. Respir Res *7*, 15.

Quinlan, R.J., Tobin, J.L., and Beales, P.L. (2008). Modeling ciliopathies: Primary cilia in development and disease. Curr Top Dev Biol *84*, 249-310.

Rawlins, E.L., and Hogan, B.L. (2006). Epithelial stem cells of the lung: privileged few or opportunities for many? Development *133*, 2455-2465.

Reynolds, S.D., Hong, K.U., Giangreco, A., Mango, G.W., Guron, C., Morimoto, Y., and Stripp, B.R. (2000). Conditional clara cell ablation reveals a self-renewing progenitor function of pulmonary neuroendocrine cells. American journal of physiology *278*, L1256-1263.

Reynolds, S.D., Zemke, A.C., Giangreco, A., Brockway, B.L., Teisanu, R.M., Drake, J.A., Mariani, T., Di, P.Y., Taketo, M.M., and Stripp, B.R. (2008). Conditional stabilization of beta-catenin expands the pool of lung stem cells. Stem Cells *26*, 1337-1346.

Ross, A.J., Dailey, L.A., Brighton, L.E., and Devlin, R.B. (2007). Transcriptional profiling of mucociliary differentiation in human airway epithelial cells. American journal of respiratory cell and molecular biology *37*, 169-185.

Rowe, S.M., Miller, S., and Sorscher, E.J. (2005). Cystic fibrosis. N Engl J Med *352*, 1992-2001.

Rubin, L.P., Kovacs, C.S., De Paepe, M.E., Tsai, S.W., Torday, J.S., and Kronenberg, H.M. (2004). Arrested pulmonary alveolar cytodifferentiation and defective surfactant synthesis in mice missing the gene for parathyroid hormone-related protein. Dev Dyn *230*, 278-289.

Sakai, H., Ingenito, E.P., Mora, R., Abbay, S., Cavalcante, F.S., Lutchen, K.R., and Suki, B. (2001). Hysteresivity of the lung and tissue strip in the normal rat: effects of heterogeneities. J Appl Physiol *91*, 737-747.

Salazar, E., and Knowles, J.H. (1964). An Analysis of Pressure-Volume Characteristics of the Lungs. J Appl Physiol *19*, 97-104.

Sanchez-Esteban, J., Cicchiello, L.A., Wang, Y., Tsai, S.W., Williams, L.K., Torday, J.S., and Rubin, L.P. (2001). Mechanical stretch promotes alveolar epithelial type II cell differentiation. J Appl Physiol *91*, 589-595.

Schordan, E., Welsch, S., Rothhut, S., Lambert, A., Barthelmebs, M., Helwig, J.J., and Massfelder, T. (2004). Role of parathyroid hormone-related protein in the regulation of stretch-induced renal vascular smooth muscle cell proliferation. J Am Soc Nephrol *15*, 3016-3025.

Selman, M., and Pardo, A. (2006). Role of epithelial cells in idiopathic pulmonary fibrosis: from innocent targets to serial killers. Proc Am Thorac Soc *3*, 364-372.

Shang, Y., Tsao, C.C., and Gorovsky, M.A. (2005). Mutational analyses reveal a novel function of the nucleotide-binding domain of gamma-tubulin in the regulation of basal body biogenesis. J Cell Biol *171*, 1035-1044.

Shtutman, M., Zhurinsky, J., Simcha, I., Albanese, C., D'Amico, M., Pestell, R., and Ben-Ze'ev, A. (1999). The cyclin D1 gene is a target of the beta-catenin/LEF-1 pathway. Proceedings of the National Academy of Sciences of the United States of America *96*, 5522-5527.

Shu, W., Guttentag, S., Wang, Z., Andl, T., Ballard, P., Lu, M.M., Piccolo, S., Birchmeier, W., Whitsett, J.A., Millar, S.E.*, et al.* (2005). Wnt/beta-catenin signaling acts upstream of N-myc, BMP4, and FGF signaling to regulate proximal-distal patterning in the lung. Developmental biology *283*, 226-239.

Shu, W., Jiang, Y.Q., Lu, M.M., and Morrisey, E.E. (2002). Wnt7b regulates mesenchymal proliferation and vascular development in the lung. Development *129*, 4831-4842.

Simons, M., Gloy, J., Ganner, A., Bullerkotte, A., Bashkurov, M., Kronig, C., Schermer, B., Benzing, T., Cabello, O.A., Jenny, A.*, et al.* (2005). Inversin, the gene product

mutated in nephronophthisis type II, functions as a molecular switch between Wnt signaling pathways. Nat Genet *37*, 537-543.

Singh, A.M., Li, F.Q., Hamazaki, T., Kasahara, H., Takemaru, K., and Terada, N. (2007). Chibby, an antagonist of the Wnt/beta-catenin pathway, facilitates cardiomyocyte differentiation of murine embryonic stem cells. Circulation *115*, 617-626.

Sorokin, S.P. (1968). Reconstructions of centriole formation and ciliogenesis in mammalian lungs. J Cell Sci *3*, 207-230.

Spassky, N., and Aguilar, A. (2008). [Shh regulates neurogenesis through primary cilia]. Med Sci (Paris) *24*, 790-791.

Steffen, W., Fajer, E.A., and Linck, R.W. (1994). Centrosomal components immunologically related to tektins from ciliary and flagellar microtubules. J Cell Sci *107 (Pt 8)*, 2095-2105.

Stewart, G.A., Hoyne, G.F., Ahmad, S.A., Jarman, E., Wallace, W.A., Harrison, D.J., Haslett, C., Lamb, J.R., and Howie, S.E. (2003). Expression of the developmental Sonic hedgehog (Shh) signalling pathway is up-regulated in chronic lung fibrosis and the Shh receptor patched 1 is present in circulating T lymphocytes. J Pathol *199*, 488-495.

Stripp, B.R., Maxson, K., Mera, R., and Singh, G. (1995). Plasticity of airway cell proliferation and gene expression after acute naphthalene injury. The American journal of physiology *269*, L791-799.

Takemaru, K., Fischer, V., and Li, F.Q. (2009). Fine-tuning of nuclear-catenin by Chibby and 14-3-3. Cell Cycle *8*, 210-213.

Takemaru, K., Yamaguchi, S., Lee, Y.S., Zhang, Y., Carthew, R.W., and Moon, R.T. (2003). Chibby, a nuclear beta-catenin-associated antagonist of the Wnt/Wingless pathway. Nature *422*, 905-909.

Tomioka, S., Bates, J.H., and Irvin, C.G. (2002). Airway and tissue mechanics in a murine model of asthma: alveolar capsule vs. forced oscillations. J Appl Physiol *93*, 263-270.

Torday, J.S. (2003). Parathyroid hormone-related protein is a gravisensor in lung and bone cell biology. Adv Space Res *32*, 1569-1576.

Torday, J.S., and Rehan, V.K. (2002). Stretch-stimulated surfactant synthesis is coordinated by the paracrine actions of PTHrP and leptin. American journal of physiology *283*, L130-135.

Torday, J.S., and Rehan, V.K. (2003). Mechanotransduction determines the structure and function of lung and bone: a theoretical model for the pathophysiology of chronic disease. Cell Biochem Biophys *37*, 235-246.

Torday, J.S., and Rehan, V.K. (2006). Up-regulation of fetal rat lung parathyroid hormone-related protein gene regulatory network down-regulates the Sonic Hedgehog/Wnt/betacatenin gene regulatory network. Pediatr Res *60*, 382-388.

Torday, J.S., and Rehan, V.K. (2007). The evolutionary continuum from lung development to homeostasis and repair. American journal of physiology *292*, L608-611.

Toskala, E., Smiley-Jewell, S.M., Wong, V.J., King, D., and Plopper, C.G. (2005). Temporal and spatial distribution of ciliogenesis in the tracheobronchial airways of mice. American journal of physiology *289*, L454-459.

Urase, K., Mukasa, T., Igarashi, H., Ishii, Y., Yasugi, S., Momoi, M.Y., and Momoi, T. (1996). Spatial expression of Sonic hedgehog in the lung epithelium during branching morphogenesis. Biochem Biophys Res Commun *225*, 161-166.

van Tuyl, M., Liu, J., Groenman, F., Ridsdale, R., Han, R.N., Venkatesh, V., Tibboel, D., and Post, M. (2006). Iroquois genes influence proximo-distal morphogenesis during rat lung development. American journal of physiology *290*, L777-L789.

Van Winkle, L.S., Buckpitt, A.R., Nishio, S.J., Isaac, J.M., and Plopper, C.G. (1995). Cellular response in naphthalene-induced Clara cell injury and bronchiolar epithelial repair in mice. The American journal of physiology *269*, L800-818.

Vinogradova, T.M., Balashova, E.E., Smirnov, V.N., and Bystrevskaya, V.B. (2005). Detection of the centriole tyr- or acet-tubulin changes in endothelial cells treated with thrombin using microscopic immunocytochemistry. Cell Motil Cytoskeleton *62*, 1-12.

Vladar, E.K., and Axelrod, J.D. (2008). Dishevelled links basal body docking and orientation in ciliated epithelial cells. Trends Cell Biol *18*, 517-520.

Voronina, V.A., Takemaru, K.I., Treuting, P., Love, D., Grubb, B.R., Hajjar, A.M., Adams, A., Li, F.Q., and Moon, R.T. (2009). Inactivation of Chibby affects function of motile airway cilia. J Cell Biol.

Wade, K.C., Guttentag, S.H., Gonzales, L.W., Maschhoff, K.L., Gonzales, J., Kolla, V., Singhal, S., and Ballard, P.L. (2006). Gene Induction during Differentiation of Human Pulmonary Type II Cells In Vitro. American journal of respiratory cell and molecular biology *34*, pp. 727-737.

Wang, N., Tytell, J.D., and Ingber, D.E. (2009). Mechanotransduction at a distance: mechanically coupling the extracellular matrix with the nucleus. Nat Rev Mol Cell Biol *10*, 75-82.

Warburton, D., Bellusci, S., De Langhe, S., Del Moral, P.M., Fleury, V., Mailleux, A., Tefft, D., Unbekandt, M., Wang, K., and Shi, W. (2005). Molecular mechanisms of early lung specification and branching morphogenesis. Pediatr Res *57*, 26R-37R.

Warburton, D., Schwarz, M., Tefft, D., Flores-Delgado, G., Anderson, K.D., and Cardoso, W.V. (2000). The molecular basis of lung morphogenesis. Mech Dev *92*, 55-81.

Williams, M.C. (2003). Alveolar type I cells: molecular phenotype and development. Annual review of physiology *65*, 669-695.

Winer, J., Jung, C.K., Shackel, I., and Williams, P.M. (1999). Development and validation of real-time quantitative reverse transcriptase-polymerase chain reaction for monitoring gene expression in cardiac myocytes in vitro. Anal Biochem *270*, 41-49.

Wozniak, M.A., and Chen, C.S. (2009). Mechanotransduction in development: a growing role for contractility. Nat Rev Mol Cell Biol *10*, 34-43.

Yamamoto, M., Harm, S.C., Grasser, W.A., and Thiede, M.A. (1992). Parathyroid hormone-related protein in the rat urinary bladder: a smooth muscle relaxant produced locally in response to mechanical stretch. Proceedings of the National Academy of Sciences of the United States of America *89*, 5326-5330.

You, Y., Huang, T., Richer, E.J., Schmidt, J.E., Zabner, J., Borok, Z., and Brody, S.L. (2004). Role of f-box factor foxj1 in differentiation of ciliated airway epithelial cells. American journal of physiology *286*, L650-657.

You, Y., Richer, E.J., Huang, T., and Brody, S.L. (2002). Growth and differentiation of mouse tracheal epithelial cells: selection of a proliferative population. American journal of physiology *283*, L1315-1321.

Young, B., Lowe, J.S., Stevens, A., and Heath, J.W. (2006). Wheater's Functional Histology: A Text and Colour Atlas, 5th edn (Churchill Livingstone).

Yu, X., Ng, C.P., Habacher, H., and Roy, S. (2008). Foxj1 transcription factors are master regulators of the motile ciliogenic program. Nat Genet *40*, 1445-1453.

Zhang, Y., Goss, A.M., Cohen, E.D., Kadzik, R., Lepore, J.J., Muthukumaraswamy, K., Yang, J., DeMayo, F.J., Whitsett, J.A., Parmacek, M.S.*, et al.* (2008). A Gata6-Wnt pathway required for epithelial stem cell development and airway regeneration. Nat Genet *40*, 862-870.

Zhou, L., Lim, L., Costa, R.H., and Whitsett, J.A. (1996). Thyroid transcription factor-1, hepatocyte nuclear factor-3beta, surfactant protein B, C, and Clara cell secretory protein in developing mouse lung. J Histochem Cytochem *44*, 1183-1193.

Zhurinsky, J., Shtutman, M., and Ben-Ze'ev, A. (2000). Differential mechanisms of LEF/TCF family-dependent transcriptional activation by beta-catenin and plakoglobin. Molecular and cellular biology *20*, 4238-4252.